CHAPTER-5

BEHAVIOUR OF CONTAINMENT STRUCTURES AGAINST DIFFERENT AIRCRAFTS

5.1 GENERAL

The safety assessment of important structures like reactor containment wall against deliberate or accidental crash of commercial and fighter aircraft has drawn significant attention throughout the world. The structural design of the upcoming reactor buildings has been revised by many countries keeping in view the threats of aircraft crash. Most of the NPP containment has two different walls, one is inner and other is outer. The inner wall is made up of prestressed concrete and it is provided to control the emission of radioactive radiation. The outer wall made up of RCC and it is provided for safety against possible external threat. In some countries, reinforced concrete wall with steel liner is constructed which is provided at the inner face of wall.

In present research only outer containment wall has been considered to get the response under impact load due to aircraft crash. Some hypothetical simple structures and some actual NPP containment walls are taken into consideration. The hypothetical structures are PCC flat plate, RCC plat plate and RCC cylindrical wall whereas the actual NPP containments are BWR mark-III, CMR, FBR and TMIR containment. Many researchers tried to predict the response of BWR containment wall for impact load but no one studied on CMR, FBR and TMIR containment. The BWR containment wall has been

taken only for the validation of results. Various type of aircrafts is considered to apply the impact load and these aircrafts are Boeing 707-320, Boeing 767-400, Phantom F4 and Airbus A320. As the Boeing 707-320 aircraft is the bench mark of Boeing group, several studies have been done with this aircraft. The containment wall is simulated under the impact of Boeing 707-320 aircraft to compare the results with existing literatures.

In this chapter, deformation, stress and damage analysis of hypothetical structure as well as real NPP containment walls under different aircrafts have been studied. The most damage prone NPP containment wall among CMR, FBR, BWR and TMIR under the impact of Boeing 707-320 aircraft has also been investigated. To find the most devasting aircraft, most damage prone NPP containment wall and most vulnerable location in containment wall, several analyses are simulated. The deformation behaviour of TMIR containment has also been performed for various parameters i.e., wall thickness, reinforcement ratio, curvature of containment, impact velocities, impact angles and the effect of stain rate.

It is observed that the most vulnerable location is not the mid height of cylindrical portion of the containment which is different form available literatures. It is also found that the Boeing 747-400 has the most damaging potential and the CMR is more affected NPP containment. The strain rate of the material has been found to play important role on the behaviour of containment under high impact load. It is also observed that the thickness of NPP wall, % of steel reinforcement in wall, radius of curvature of containment, impact angle and velocity of aircraft affects the deformation response.

5.2 ANALYSIS OF PCC PLATE

In the present study, a flat PCC plate has been taken to know the structural behaviour under aircraft crash. The impact location for the Boeing 707- 320 aircraft and Phantom F4 has been impacted at the mid height of the plate structure (20 m from the base).

5.2.1 Impact of Boeing 707-320 on PCC plate

The impact analysis is performed up to 0.3472sec and the of deformation, stress, acceleration and damage analysis are obtained using ABAQUS/Explicit scheme. Three different paths are considered which has been shown in Fig. 5.1. The average area method is used to apply the impact through the reaction force time curve. The maximum stress in concrete is observed at time 0.2084 sec and the value of stress is 9MPa which is shown in Fig. 5.2 and at the same time the deformation is 12.4mm which has been shown in Fig. 5.3. It is clearly observed that the damages in concrete started at time 0.2257sec (Fig. 5.4) and at the end of analysis, the damages are maximum at time 0.3472sec (Fig. 5.5). Here the damages are due the tensile cracking not due to compression cracking. It is also observed that the deformation is global before damage starts but when the damaging started, the deformation is local and the value of deformation is also large, Fig. 5.3. Just after impact, the damage was initiated at point of loading. The impact load is applied in the structure by the force time history curve (Riera, 1968). The time duration of reaction force time curve is small. At the end of time, it is observed that the damage is observed at the fixed end of the plate and it is due to the fixed end moments and reactions. The

deformation along different path has been shown in Fig. 5.6, Fig. 5.7 and Fig. 5.8. From three plots it is concluded that the deformations are increasing with increasing time and after some time, the deformations are decreasing (it is due to the variation in force time history curve). It is also found that the deformation is maximum at the inner face of the plate compare to outer face of the plate (Fig. 5.8). The stress in different path has been plotted and shown in Fig. 5.9-5.11. From all three stress plots, it is seen that stress is increasing with increasing time and after some time the stress is decreasing because of variation in reaction force time curve.

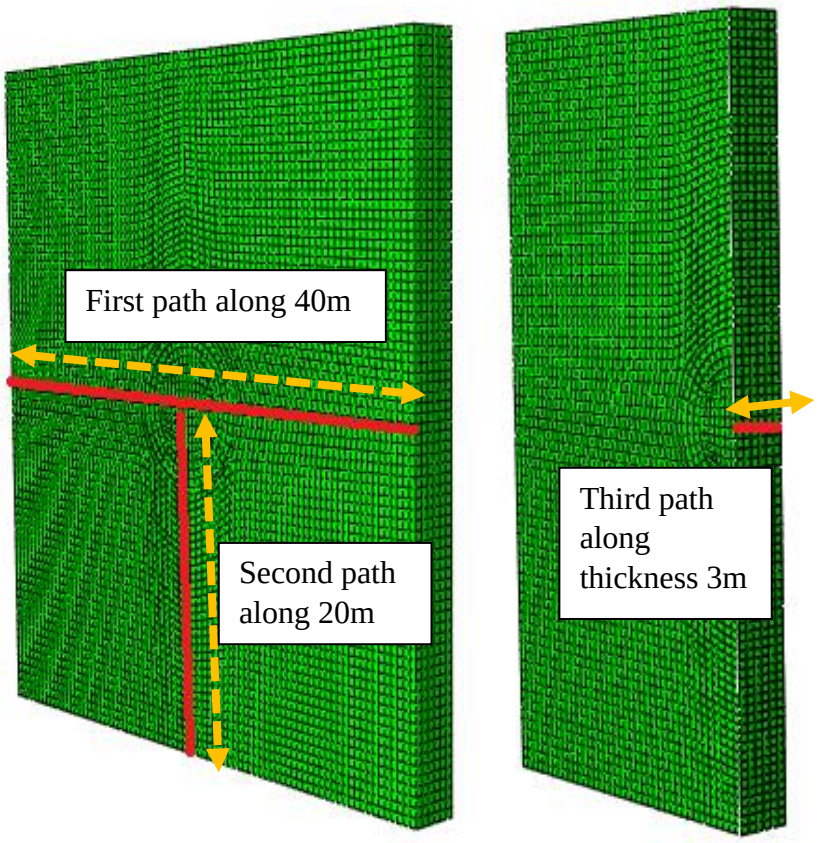

Fig. 5.1 The different path along 40m, 20m, 3m

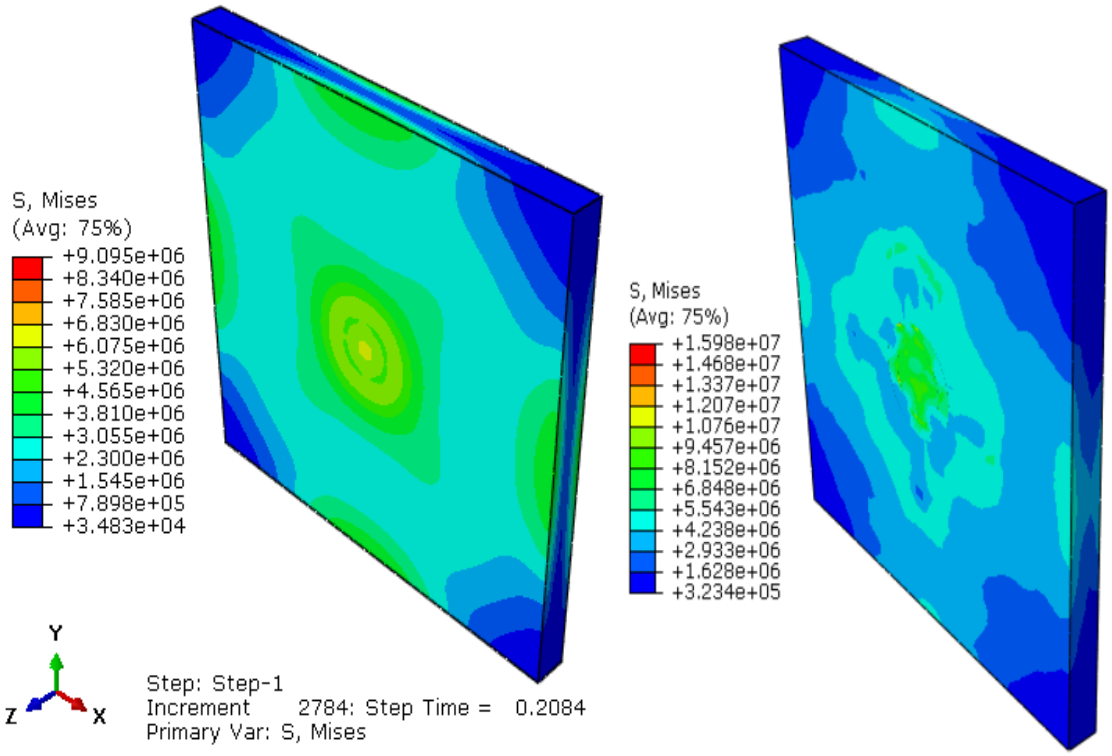

Fig. 5.2 Stress profile in concrete at 0.2084sec and 0.3472sec

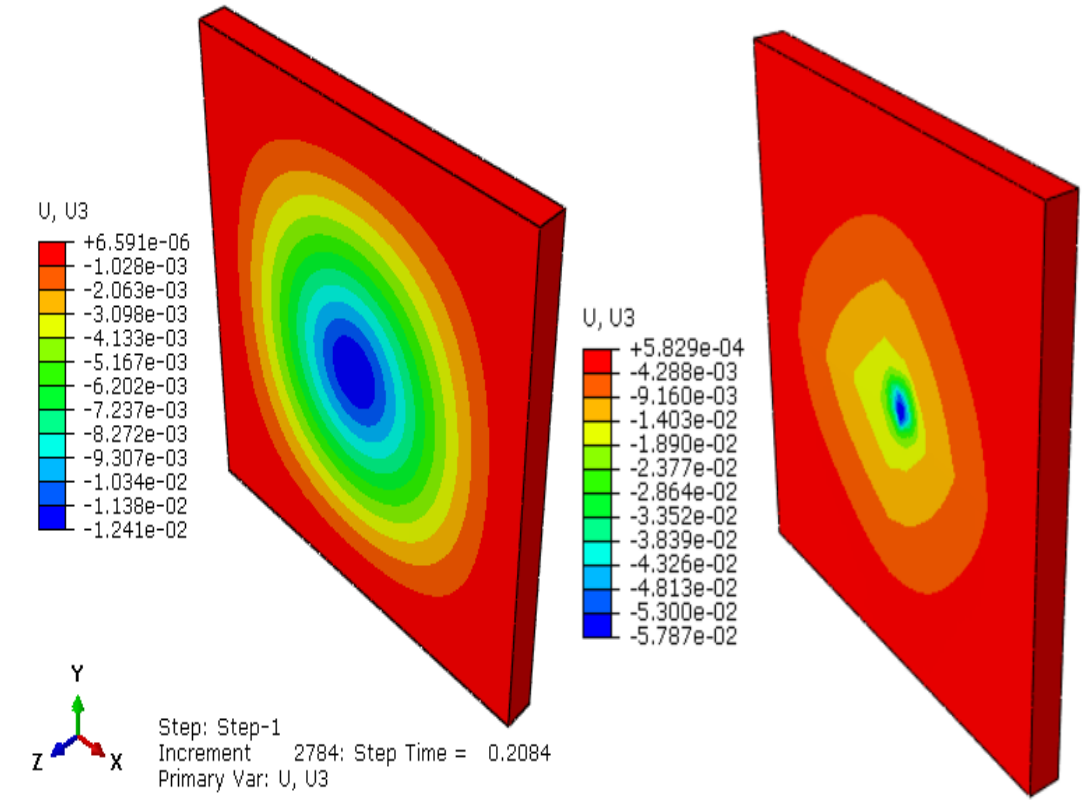

Fig. 5.3 Deformation profile in concrete at 0.2084sec and 0.3472sec

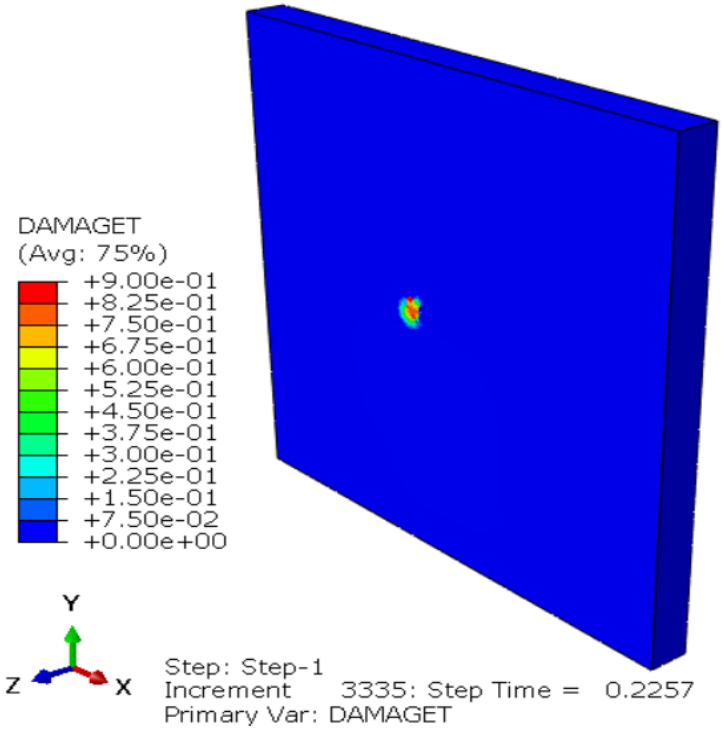

Fig. 5.4 Damages profile in concrete at 0.2257sec

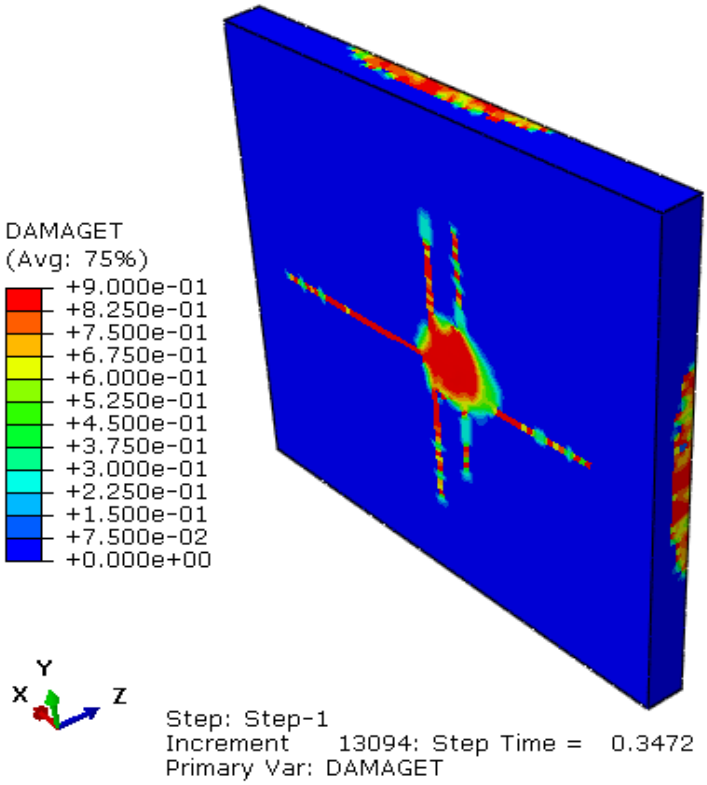

Fig. 5.5 Damages profile in concrete at 0.3472sec

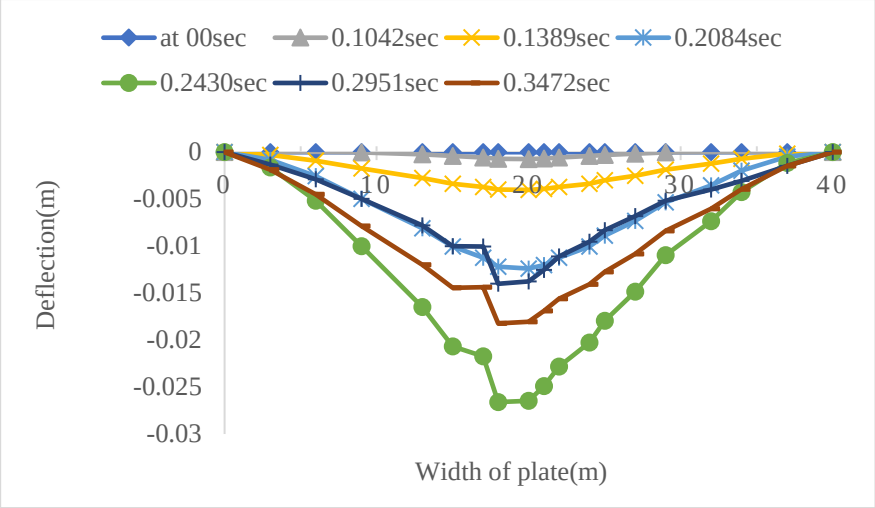

Fig. 5.6 Deformation in concrete along first path

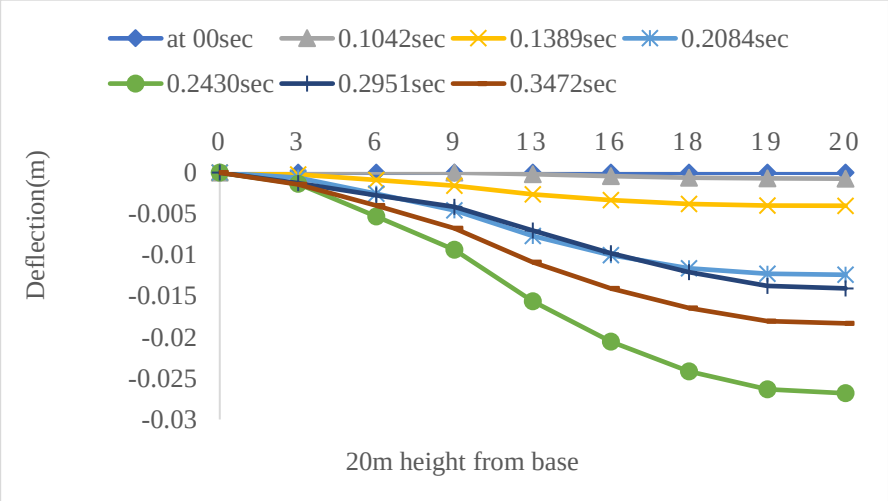

Fig. 5.7 Deformation in concrete along second path

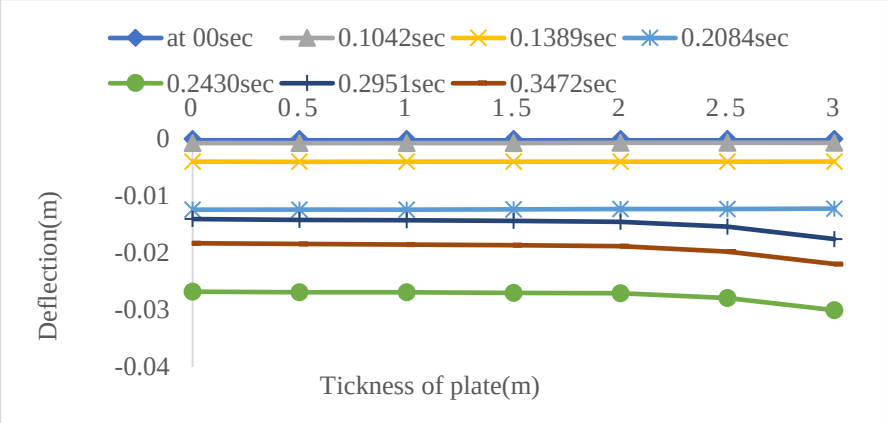

Fig. 5.8 Deformation in concrete along third path

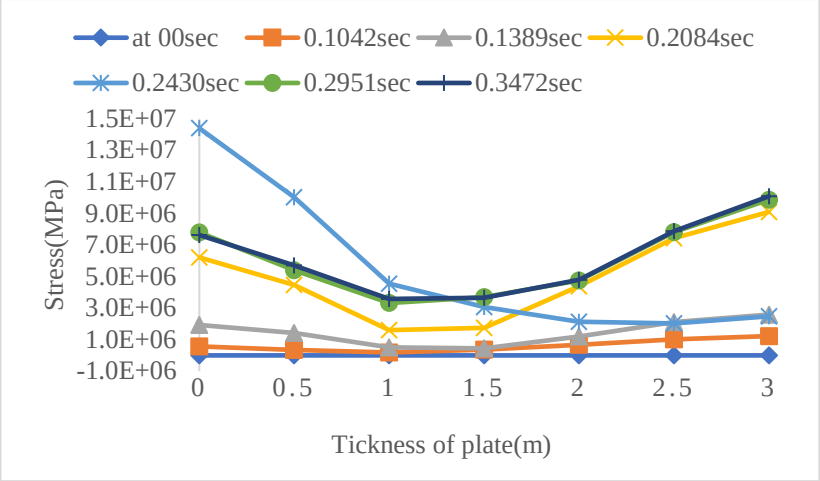

Fig. 5.9 Stress in concrete along third path

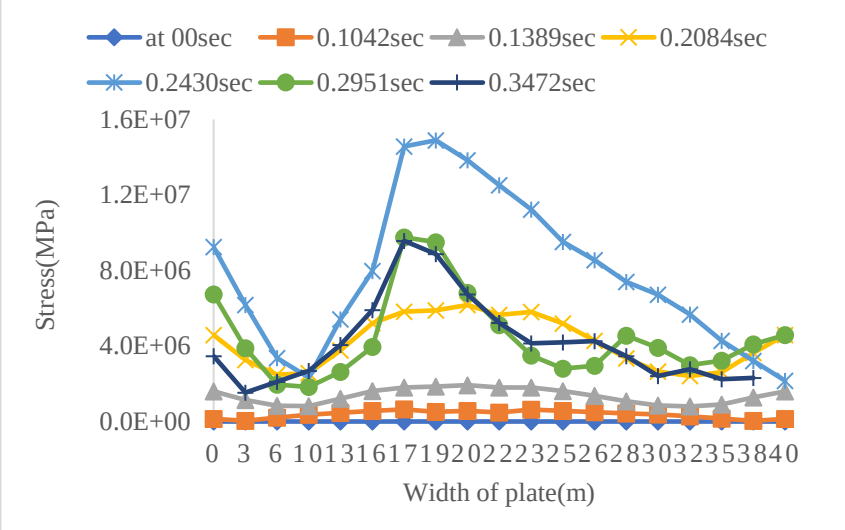

Fig. 5.10 Stress in concrete along first path

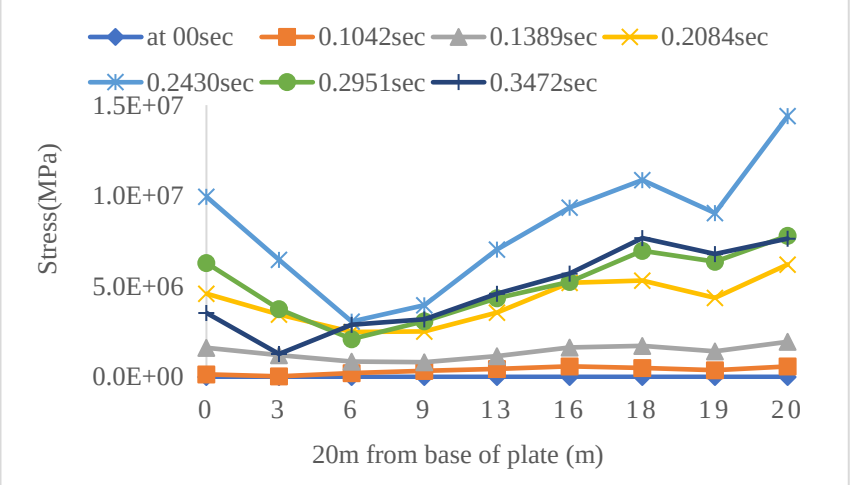

Fig. 5.11 Stress in concrete along second path

5.2.2 Impact of Phantom F4 on PCC plate

In this case also the average area approach is used for applying the load through reaction force time curve. The Explicit impact analysis has been performed up to 0.08sec and the deformation, stress and damage analysis are carried out. The maximum stress of 8.33MPa in concrete is observed at time 0.032sec which is shown in Fig. 5.12 and at the same time the deformation of 6.6mm is noticed which has been shown in Fig. 5.13. It is clearly found that the damages in concrete start at time 0.036sec (Fig. 5.14) and at the end of analysis (at time 0.08sec), the damages are maximum (Fig. 5.15). Here the damages are due the tensile cracking not due to compression cracking. It is also observed that before damaging the deformation behaviour is global but when the damage starts, the deformation is local and the value of deformation is also large. The deformation value are 6.6 mm and 253 mm at time 0.034sec and at 0.08sec respectively, Fig. 5.13. At the starting time, the damage is only at the middle of the plate but at the end the, the damage is observed at the fixed end of the plate and it is due to the fixed end moments and support reactions. The deformation along different path has been shown in Fig. 5.16, 5.17, 5.18. From three plots it is observed that the deformations are increasing with increasing time (it is due to the variation in force time history curve). The deformation is maximum at the inner face of the plate compare to outer face of the plate (Fig. 5.18). The stress in different path is plotted and shown in Fig. 5.19,5.20,5.21. From all three stress plots it is also observed that stress is increasing with increasing time and after some time the stress was decreasing.

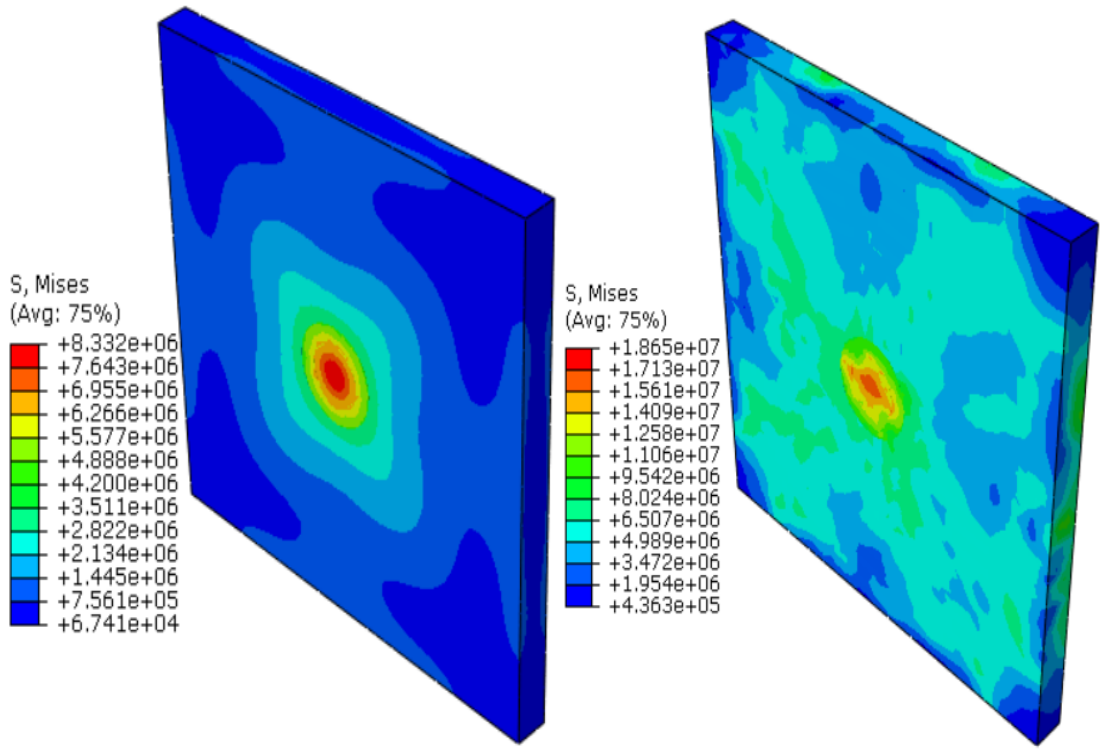

Fig. 5.12 Stress profile in concrete at 0.032sec and at 0.08sec

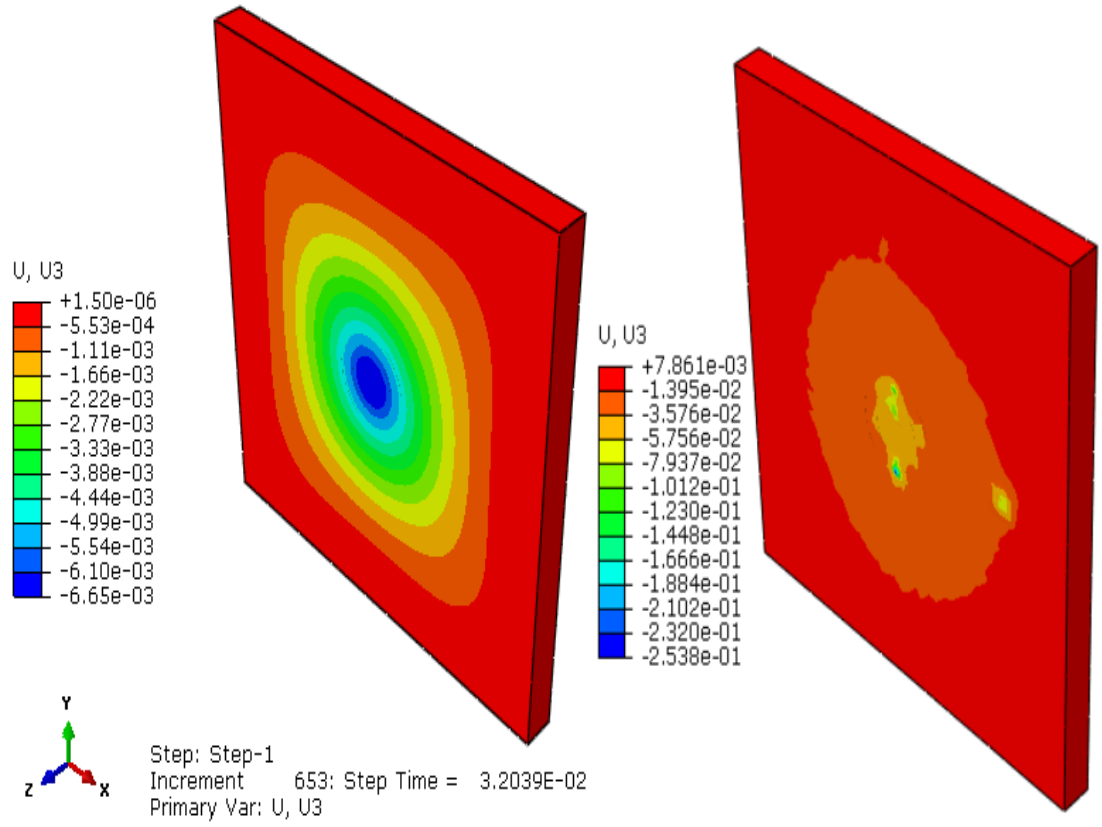

Fig. 5.13 Deformation profile in concrete at 0.032sec and at 0.08sec

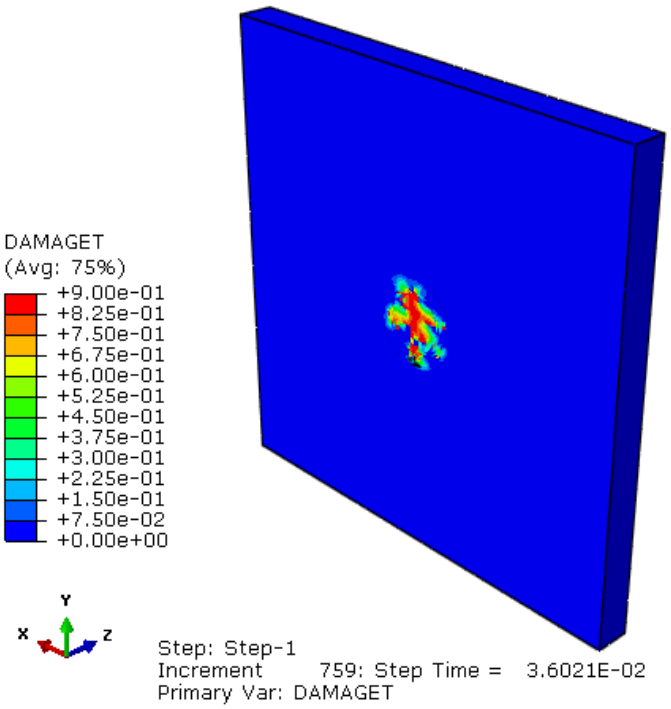

Fig. 5.14 Damages profile in concrete at 0.036sec

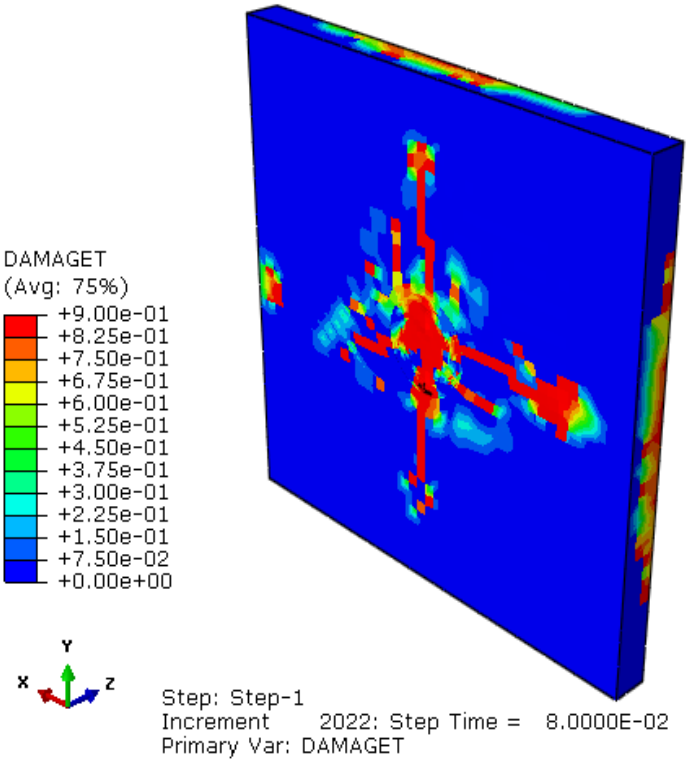

Fig. 5.15 Damages profile in concrete at 0.08sec

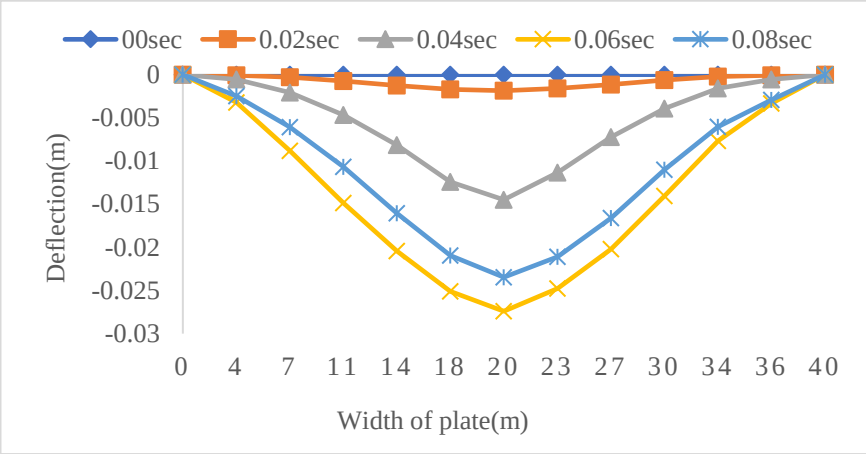

Fig. 5.16 Deformation in concrete along first path

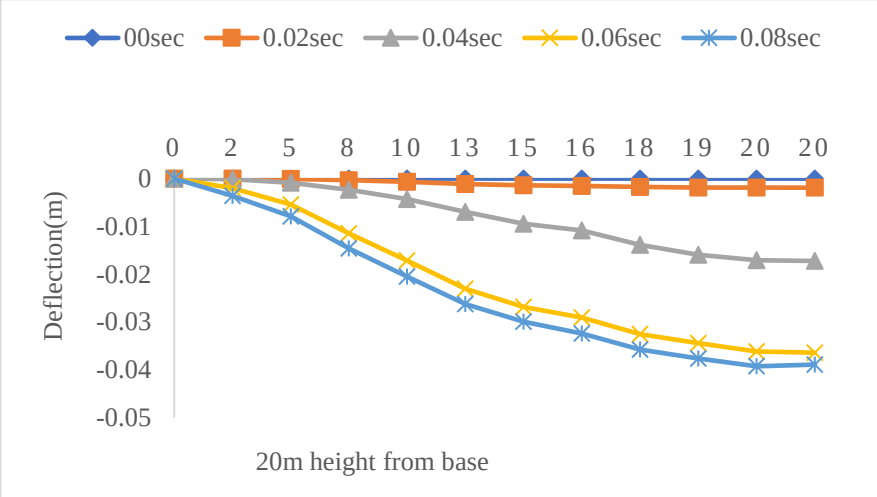

Fig. 5.17 Deformation in concrete along second path

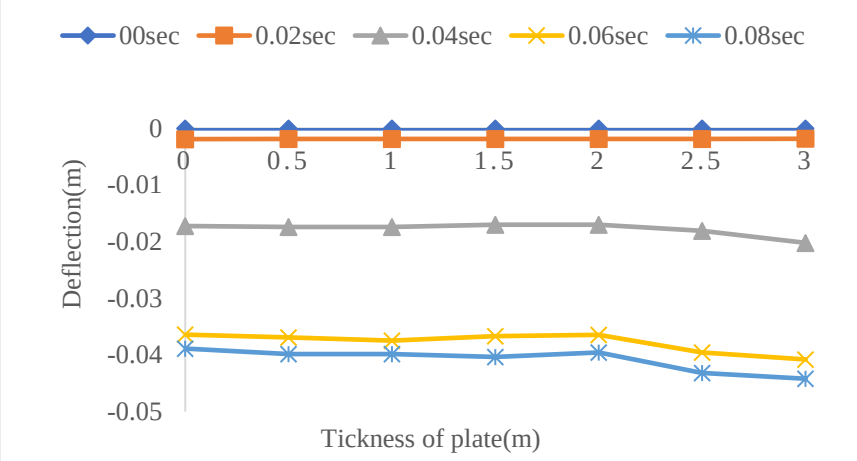

Fig. 5.18 Deformation in concrete along third path

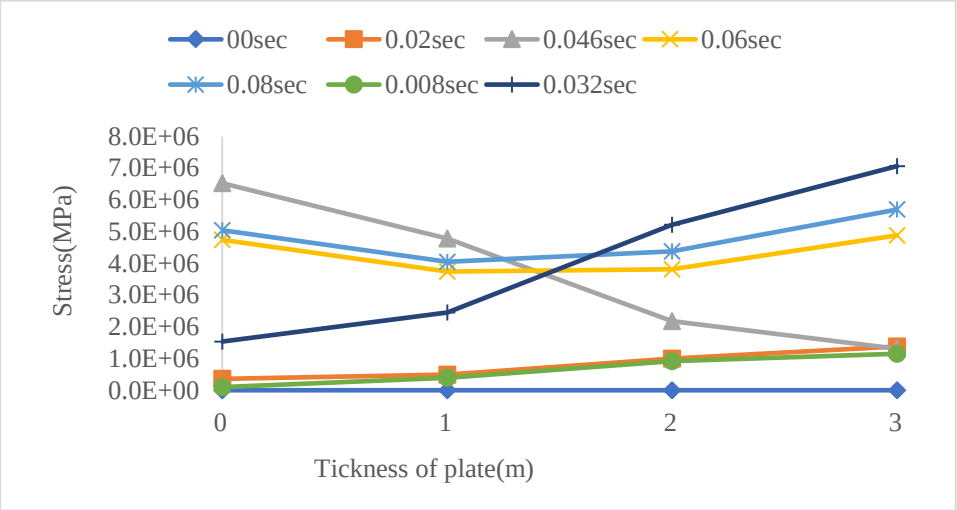

Fig. 5.19 Stress in concrete along third path

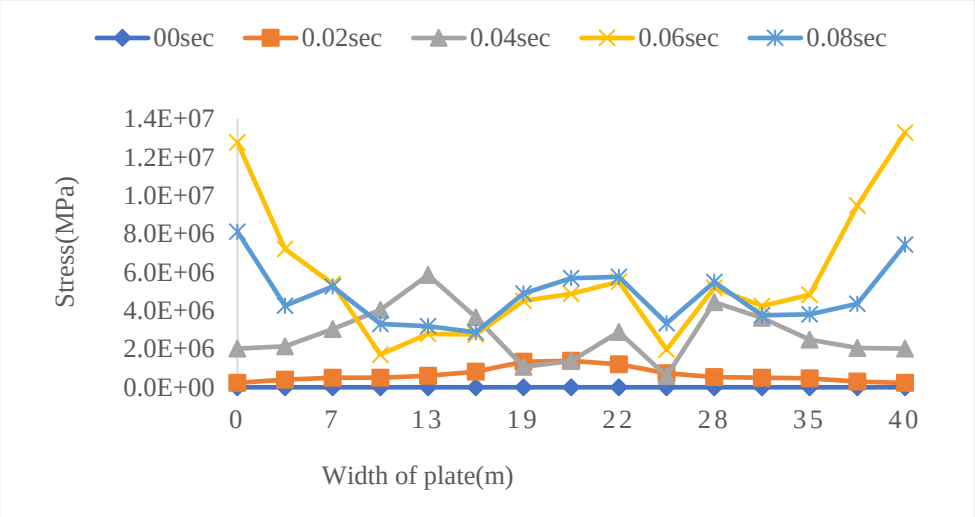

Fig. 5.20 Stress in concrete along first path

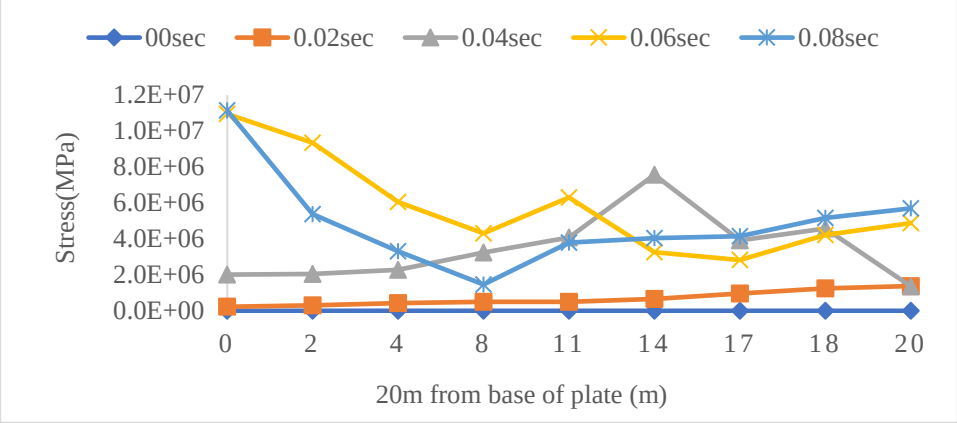

Fig. 5.21 Stress in concrete along second path

In this study, an attempt is made to find out the PCC plate behaviour for two different aircraft crash using finite element code. In the first case an impact analysis is performed for the force-time history of Boeing 707-320 aircraft and in the second case an impact analysis is performed on the same model for Phantom F4 aircraft crash. The following observations are drawn from the analysis:

- From the impact analysis it is clearly observed that the maximum deformation was 57.8 mm for Boeing 707-320 and 253 mm for Phantom F4 aircraft.
- The deformation in front elements is less than the rear elements of plate structure.
- The tensile cracking in concrete plate starts from 0.2257sec for Boeing 707-320 and from 0.034 sec for Phantom F4. That means it occurred after when the aircraft wings come in contact with target structure.
- Finally, it is concluded that the aircraft Boeing 707-320 has less damaging potential than Phantom F4 fighter jet for the PCC plate.

5.3 Analysis of RCC plate

The average area method is used to apply the impact load to get the response of RCC plate under Boeing 707-320 aircraft crash. The impact analysis is performed up to 0.34sec using ABAQUS/Explicit scheme. The deformation, stress and damage are investigated throughout the analysis. The maximum deformation of 1.88m and stress of 26.7 MPa in concrete is observed at time 0.34sec which is shown in Fig. 5.22 and Fig. 5.24. Similarly, the maximum deformation of 1.6 m and stress of 492 MPa in steel reinforcement is observed at time 0.34sec which is shown in Fig. 5.23 and Fig. 5.24. The deformation value is much higher in concrete because of concrete get damaged. It is clearly observed that the damages in concrete start at time 0.16sec (Fig. 5.25) and at the

end of analysis, the damages are maximum at time 0.3472sec (Fig. 5.25). Here the damages are due the tensile cracking as well as compression cracking. It was also observed that before damaging the deformation was global but when the damaging starts, the deformation is local and the value of deformation is also large. At the starting time, the damage is only at the middle of the plate but at the end the, the damage is noticed at the fixed end of the plate and it is due to the fixed end moments and support reactions. A path along the width of plate at height 30 m has been considered to plot deformation, stress and damage variation, Fig. 5.26. The deformation along path A has been shown in Fig. 5.27. From deformation plot it has been found that the deformations are increasing with increasing time and at the end the deformations are maximum (it is due to the damage variation). The stress along path A is plotted and shown in Fig. 5.28. From the stress plot it is also observed that stress pattern is totally different before and after 0.16 sec because the tension damages are started after 0.16sec. Fig. 2.29 is showing the damages variation with time along path A.

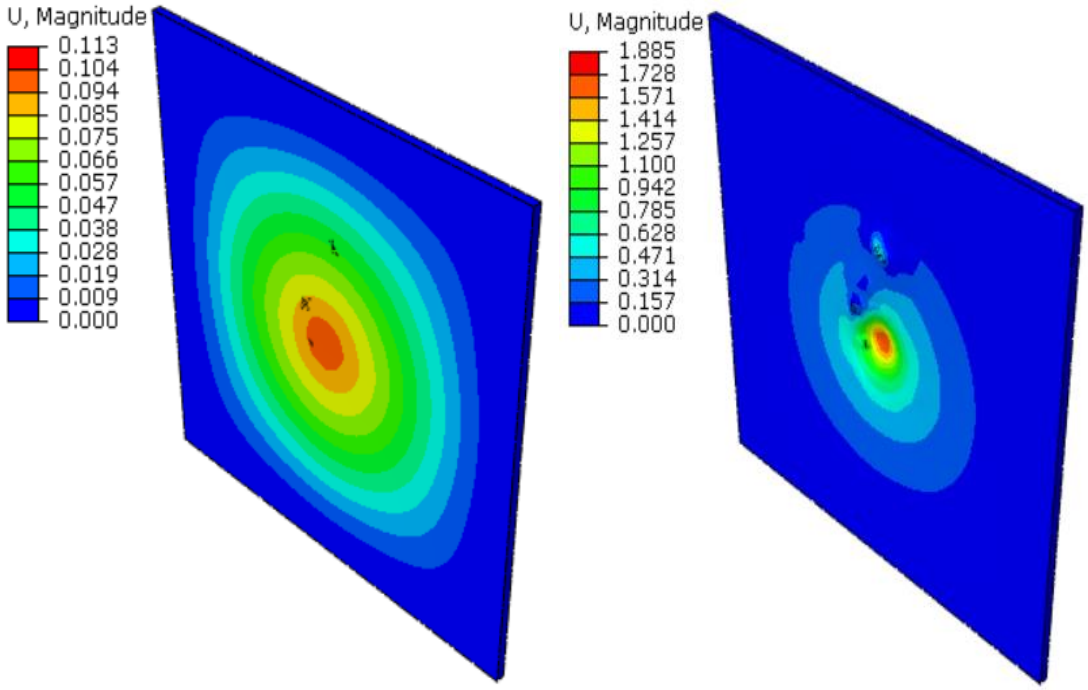

Fig. 5.22 Deformation profile in concrete at 0.16 sec and at 0.34 sec

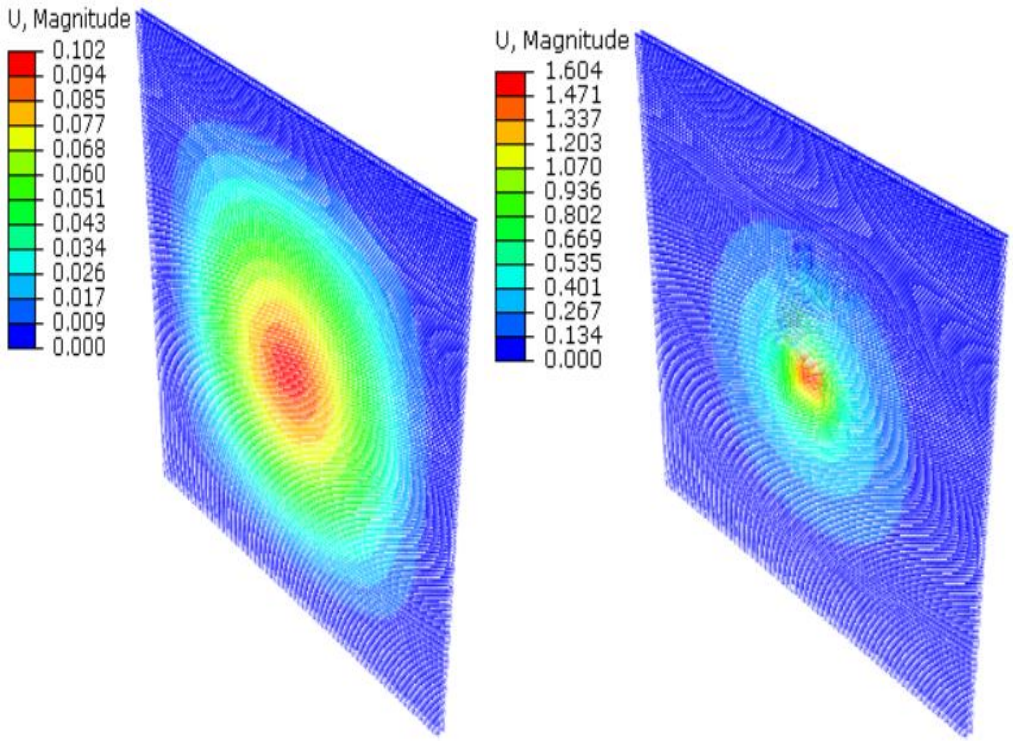

Fig. 5.23 Deformation in reinforcement steel at 0.16 sec and at 0.34 sec

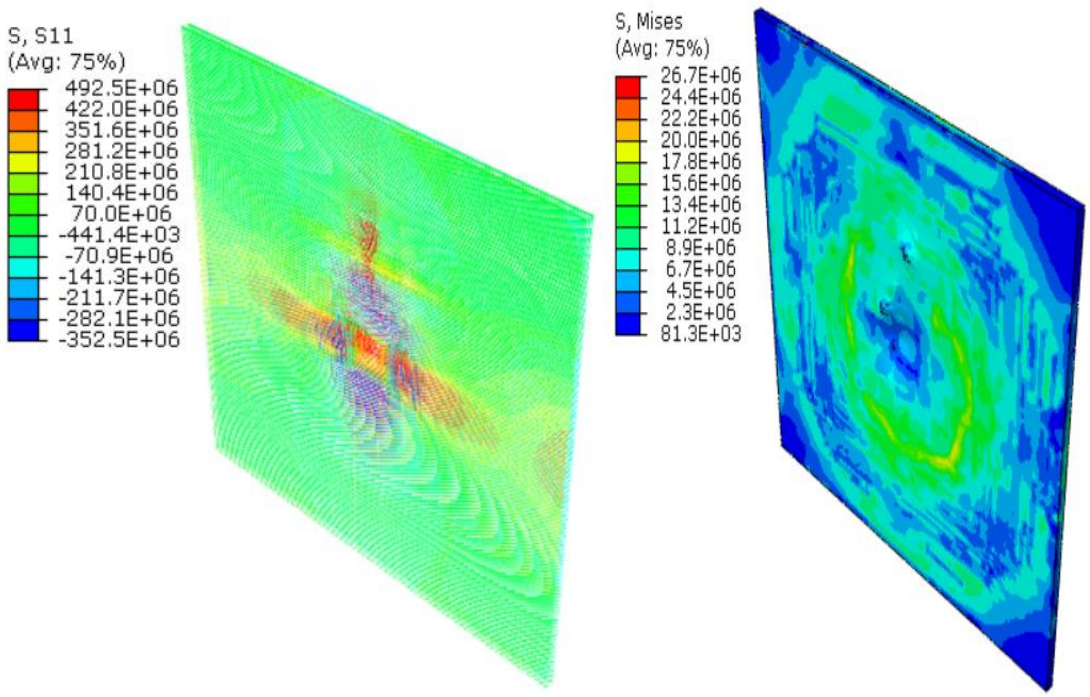

Fig. 5.24 Stress profile in reinforcement steel at 0.34 sec and in concrete at 0.34 sec

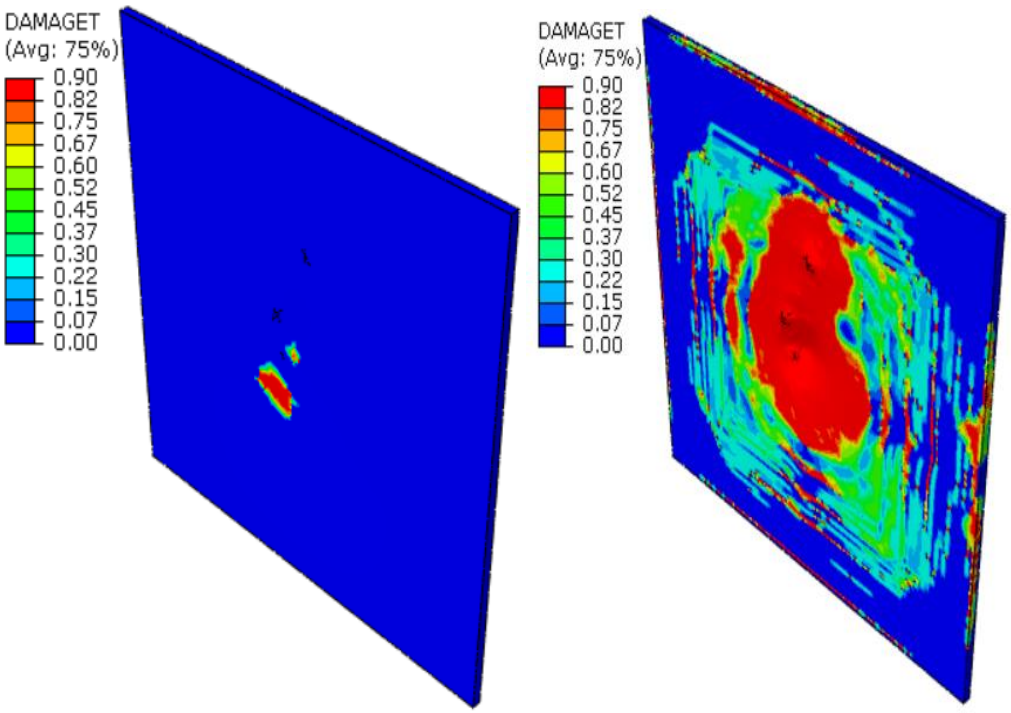

Fig. 5.25 Tension damage profile in concrete at 0.16 sec and at 0.34 sec

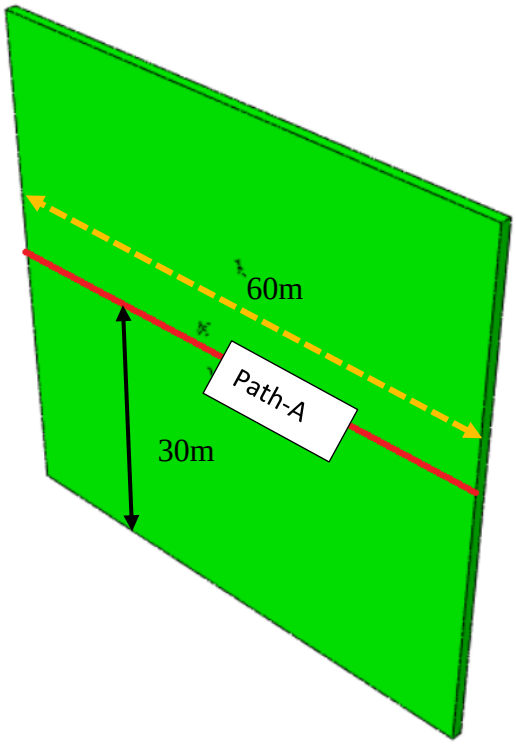

Fig. 5.26 Path A in concrete body for plotting results

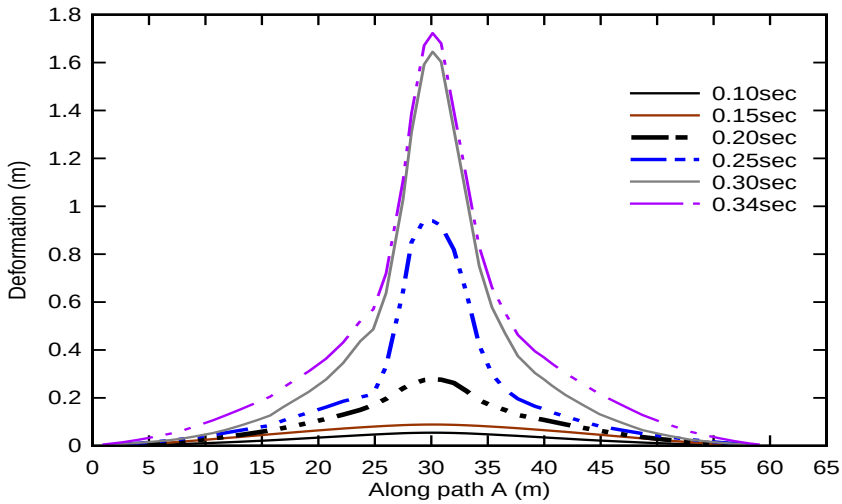

Fig. 5.27 Deformation in concrete body along path A

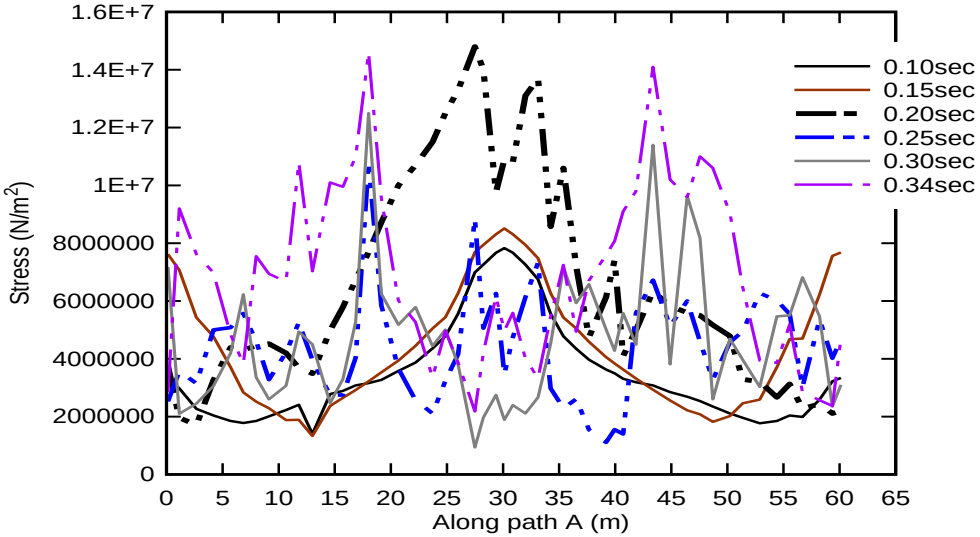

Fig. 5.28 Stress in concrete body along path A

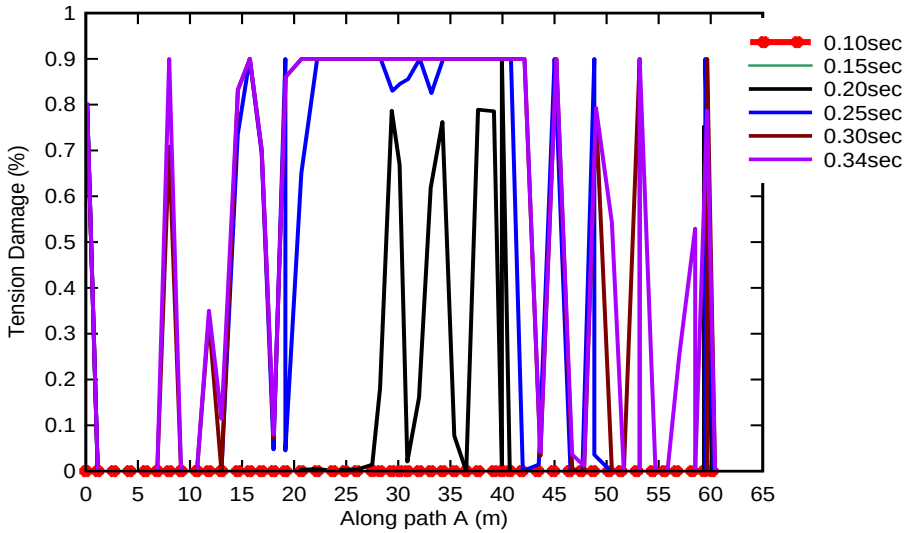

Fig. 5.29 Tension damages in concrete body along path A

5.4 Analysis of RCC cylindrical wall

The dimension of the hypothetical RCC model is kept similar to BWR mark-III containment wall but here fixed support has been used in place of circular dome roof. The impact location for the Boeing 707-320 aircraft is considered at mid-high structure (23 m from base) in the present study. The results are validated with the existing literatures.

The average area approach is used to apply the load via the reaction force time curve. The impact analysis is performed up to 0.34sec using ABAQUS/Explicit scheme. The deformation, stress, reaction, plastic strain and damage are investigated throughout the analysis. The maximum stress of 34.6 MPa in concrete body at time 0.2344sec and 265 MPa in steel reinforcement bar at time 0.2517sec is found which has been shown in Fig. 5.30 and 5.31. The maximum deformation of 84.9 mm in concrete body at time 0.2517sec and 70.7 mm in steel reinforcement bar at same time is found which has been shown in Fig. 5.32 and 5.33. The deformation contours for concrete and steel reinforcement have been shown in Fig. 5.34 and 5.35 respectively and from these contours it is observed that the deformations are decreased from previous value. At time 0.3472 sec, it is clearly observed that the damages in concrete starts at time 0.1736sec (Fig. 5.36) and at the end of analysis, the damages are maximum at time 0.3472sec (Fig. 5.37). Here the damages are due the tensile cracking not due to compression cracking. It is also observed that before damaging the deformation is global but when the damage starts, the deformation is local and the value of deformation is also large. At the starting time, the damage is only at the middle of the model but at the end the, the damage is observed at the fixed end of the model and it is due to the fixed end moments and

reactions. For the reactions plotting, the four locations have been taken from the base of containment shown in Fig. 5.38. Fig. 5.39 is showing the reaction variation of different elements at different location with time. Here three different paths are taken into consideration to plot the results. The deformation along different path has been shown in Fig. 5.41-5.43. From three plots it is observed that the deformations are increasing with increasing time and after some time the deformations are decreasing (it is due to the variation in force time history curve). The deformation is maximum in concrete body than steel reinforcement bar (comparing the results from Fig. 5.32 and 5.33). The stress in different paths is also plotted and shown in Fig. 5.44-5.47. From all four stress plots it is also observed that stress is increasing with increasing time and after some time the stress is decreasing. The Boeing 707-320 does not give the global damage to RCC cylindrical containment but it gives some local concrete damages and the maximum damages are found at the impact region (Fig. 4.48). When the damages are produced in concrete after that time the plastic strain generated in concrete and its value is increased with increase in time (Fig. 5.49). In the previous literature (Iqbal et al., 2012) noticed the maximum deformation in BWR containment wall was 66.9mm but here the deformation value is slightly higher (84 mm) because the impact location is different for both the cases.

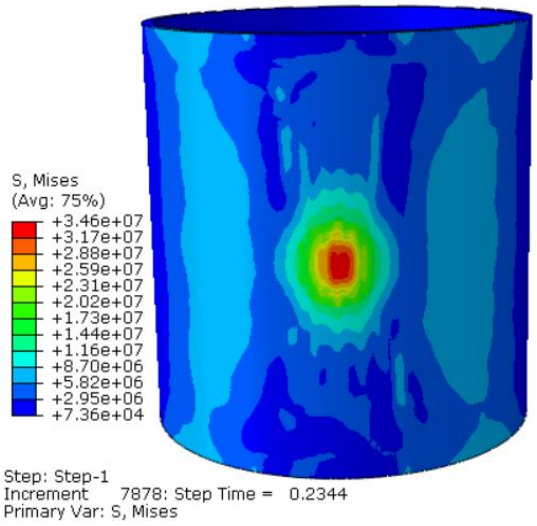

Fig. 5.30 Stress profile in concrete at 0.2344sec

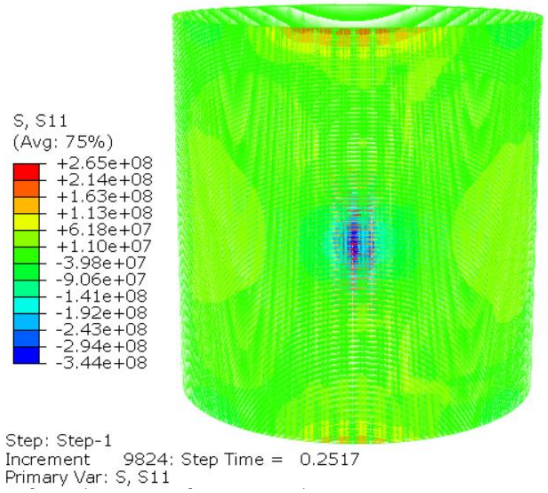

Fig. 5.31 Stress profile in steel bar at 0.2517sec

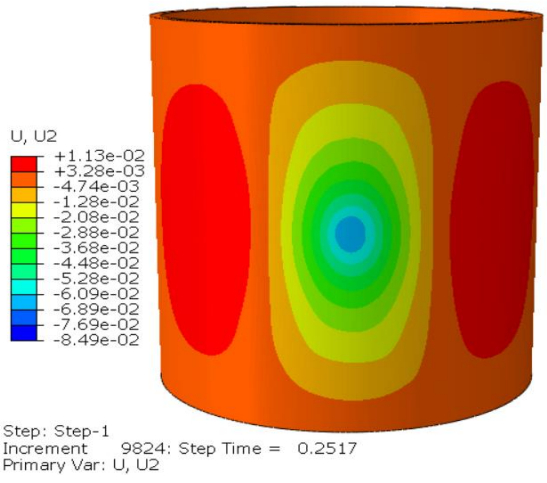

Fig. 5.32 Deformation profile in concrete at 0.2517sec

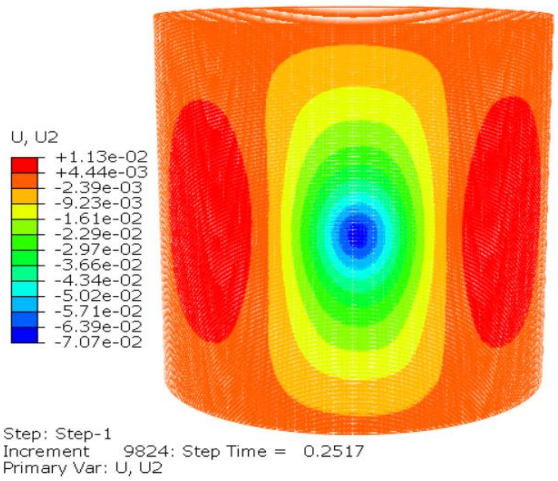

Fig. 5.33 Deformation profile in steel at 0.2517sec

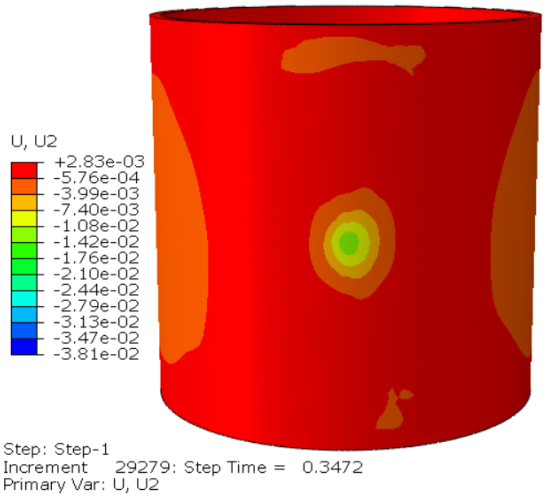

Fig. 5.34 Deformation profile in concrete at 0.3472sec

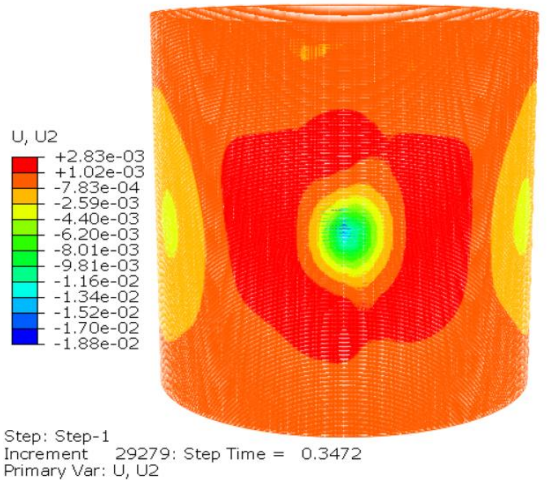

Fig. 5.35 Deformation profile in steel at 0.3472sec

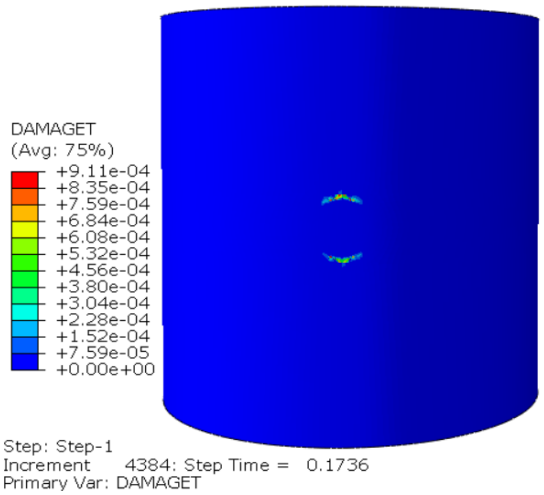

Fig. 5.36 Damages profile in concrete at 0.1736sec

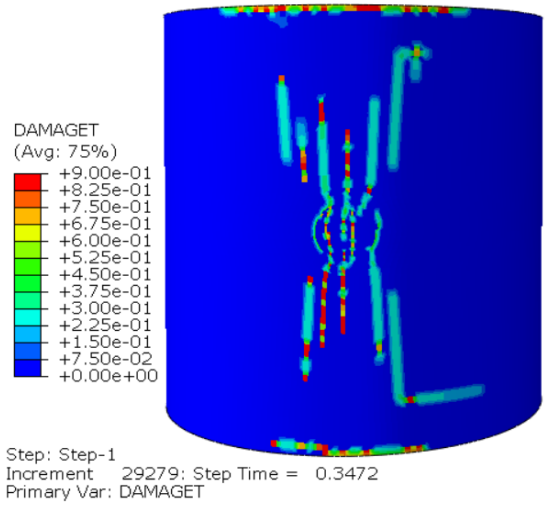

Fig. 5.37 Damages profile in concrete at 0.3472sec

9

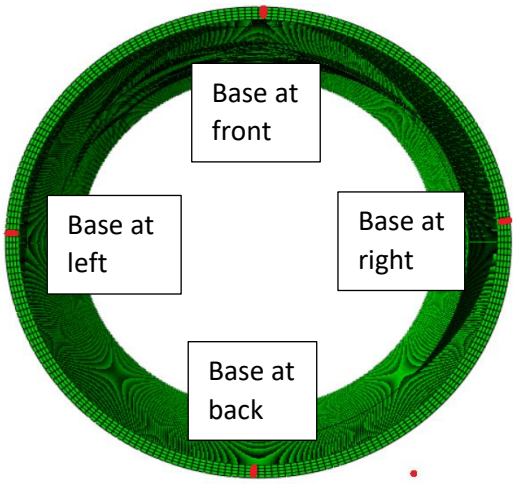

Fig. 5.38 Four locations for reaction calculation

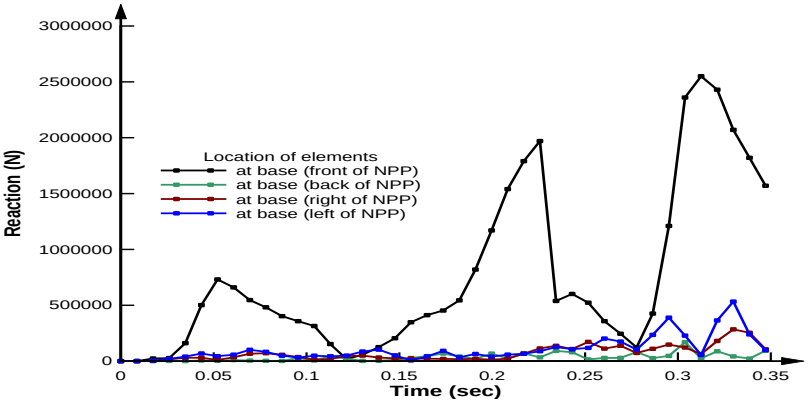

Fig. 5.39 Reactions at base of NPP with different locations

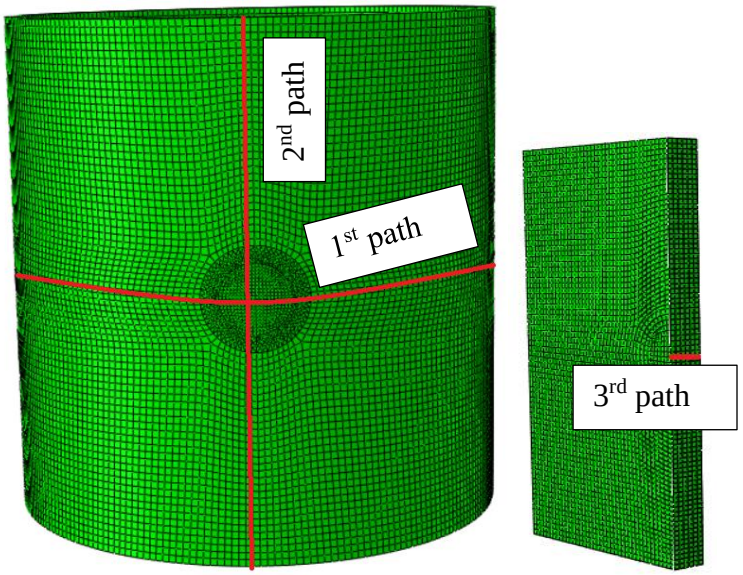

Fig. 5.40 The different paths in the cylindrical containment

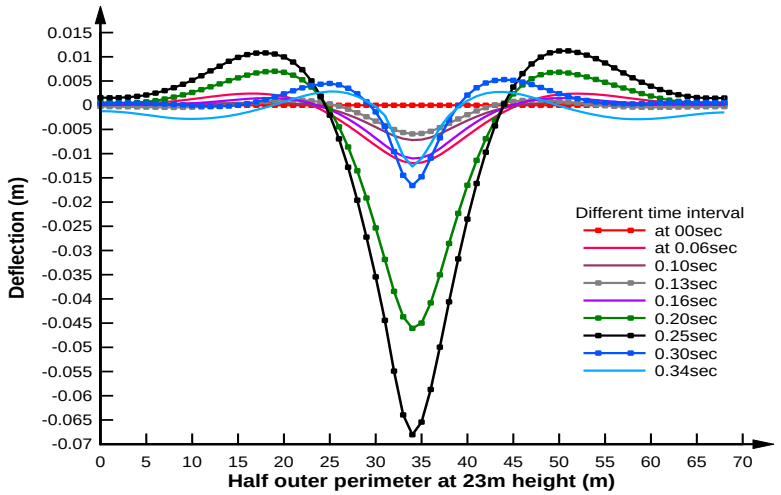

Fig. 5.41 Deformation in concrete along first path (outer face)

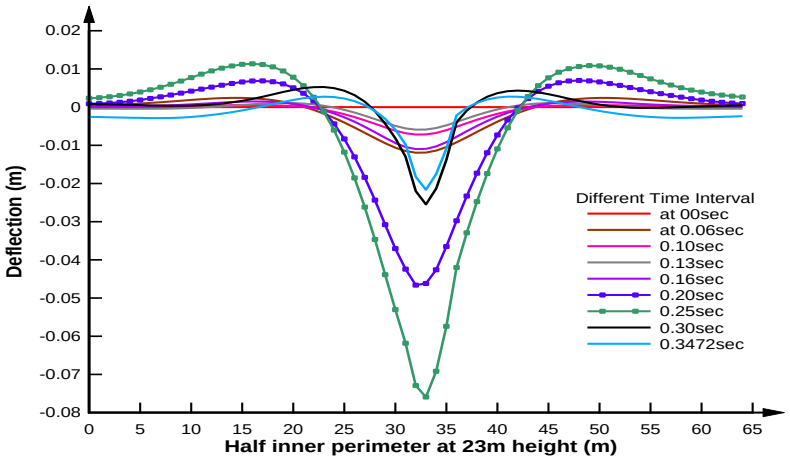

Fig. 5.42 Deformation in concrete along first path (inner face)

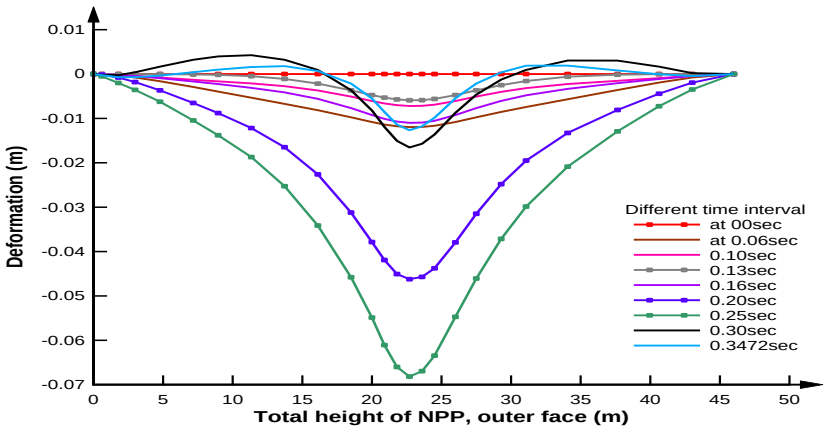

Fig. 5.43 Deformation in concrete along second path

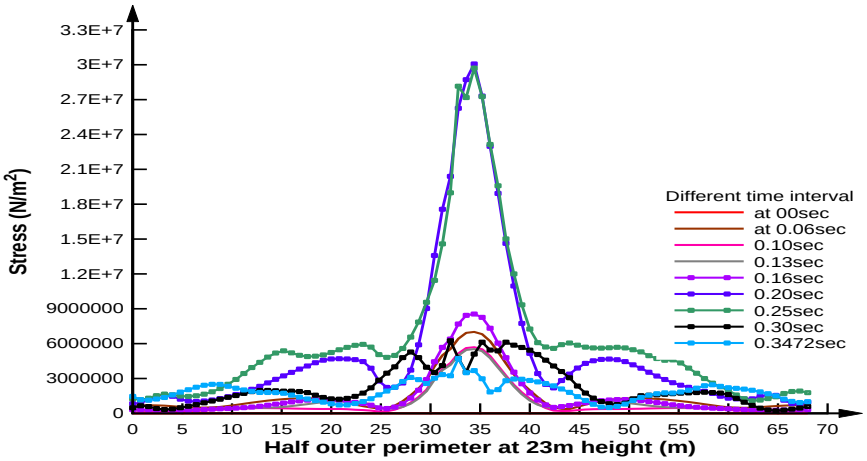

Fig. 5.44 Stress in concrete along first path (outer face)

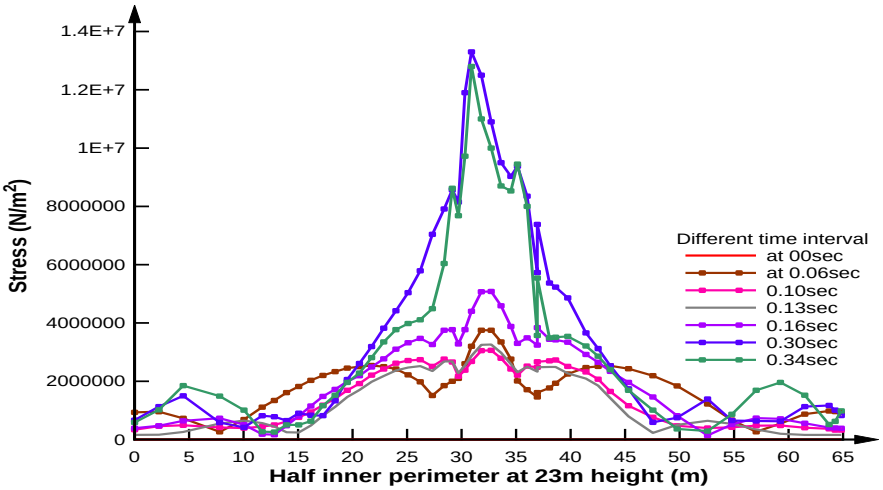

Fig. 5.45 Stress in concrete along first path (inner face)

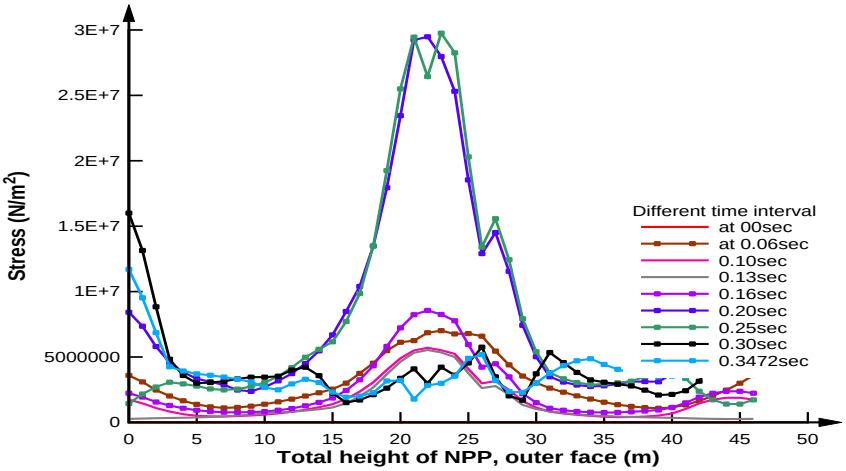

Fig. 5.46 Stress in concrete along 2nd path (outer face)

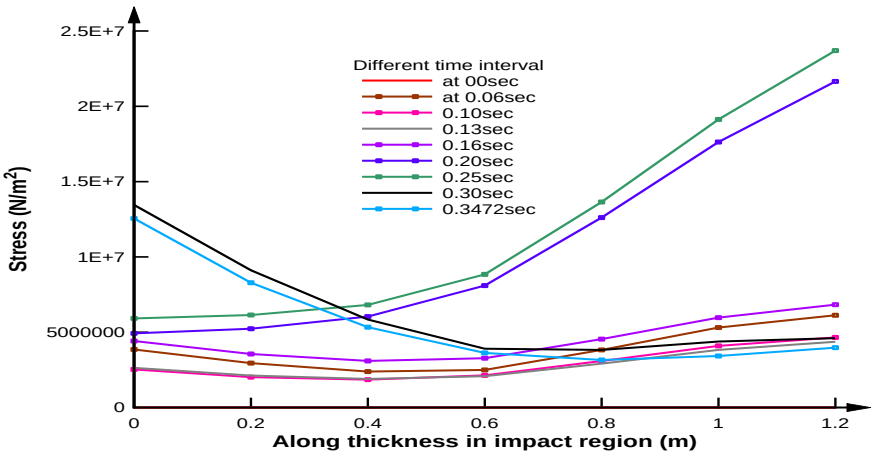

Fig. 5.47 Stress in concrete along third path

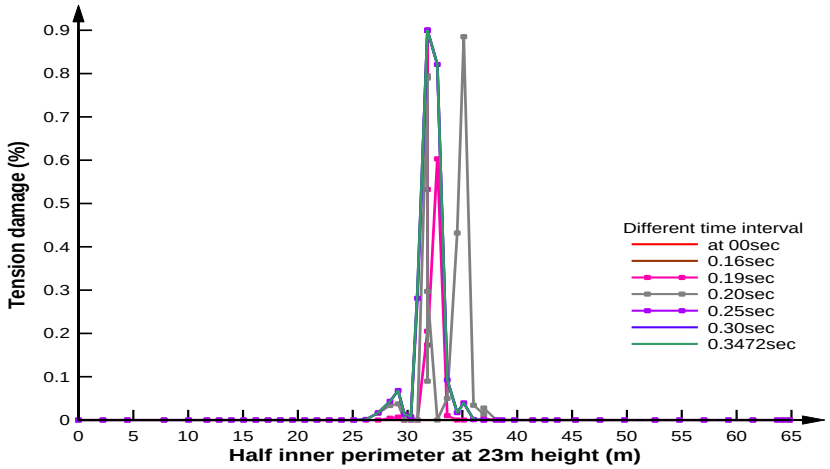

Fig. 5.48 Tension Damage (TD) in concrete along first path (inner face)

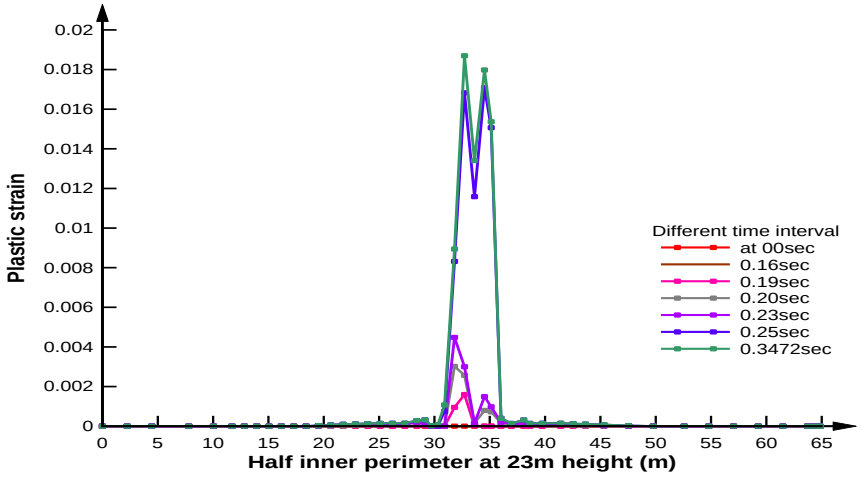

Fig. 5.49 Plastic strain in concrete along first path (inner face)

In this present study, an attempt is made to find out the behavior of RCC cylindrical wall for Boeing 707-320 aircraft crash using finite element code. Here the model is same as BWR-III type but this model is without top dome or slab. The fixed conditions are applied on the upper face of the model in place of dome. The following conclusions arecdrawn from the analysis:

- From the impact analysis it is clearly observed that the maximum deformation is 84 mm for concrete and 70 mm for reinforcement steel bar.
- The maximum deformation occurs neither in initial time nor in end time. It occurs at 0.2517sec for steel as well as concrete (it is due to the variation in force time history curve)
- The maximum stress in concrete and steel is observed 13 MPa and 344 MPa at time 0.1736 and 0.2517sec respectively.
- The tensile cracking in concrete starts from 0.1736sec for Boeing 707-320 and the value of damages increase with time. The Maximum damage occur at rear face of containment.
- Finally, it can be concluded that the aircraft Boeing 707-320 does no give the global threat to RCC cylindrical containment wall.

5.5 ANALYSIS OF THREE MILE ISLAND REACTOR (TMIR) CONTAINMENT WALL

Now a real nuclear containment wall (TMIR) is analysed against the impact of Boeing 707-320 aircraft to get complete behaviour. Two nodal paths and some nodes were chosen for plotting the results of stress and deformation. The path A is in the longitudinal direction (along height) whereas path B is in circumferential direction (along

periphery) of the containment, 5.50. The selected paths are at the inner face of model. Fig. 5.51 highlight the elements chosen at the outer face of the containment wall to plot stress and deformation curves. The selected nodes are 7939, 154, 21, 3776, 28045 and 47348 which are in the concrete body. The deformation contours in concrete body, steel reinforcement and inner steel liner at different time interval have been shown in Fig. 5.52, 5.53 and 5.54 respectively. Similarly, the stress contours in concrete body, steel reinforcement and inner steel liner have been shown in Fig. 5.55, 5.56 and 5.57 respectively. The selective time intervals are 0.00, 0.03, 0.10, 0.20, 0.25 and 0.34sec. The deformation contours at time 0.27sec for U, U1, U2 and U3 (U means deformation in magnitude, U1, U2 and U3 deformation in X, Y, Z direction) is shown in Fig. 5.58. The stress contours in different direction (S11, S22, S33, S12, S13, S23) at time 0.27 sec is shown in Fig. 5.59. In this study the direction of loading is assumed to be the Z direction. The deformation and stress variation along path A and path B is plotted with different time interval, Fig. 5.60-5.63. The stress variation along the thickness at the centre impact location has been shown in Fig. 5.64. The deformation and stress in different direction for the selective nodes have been drawn in Fig. 5.65 and 5.66. The peak deflection has been found to be 14 mm at 0.24 seconds (Fig. 5.60). The deformation is found to be highest at the impact location, it decreases as the distance from the impact location increases at longitudinal as well as circumferential axis (Fig. 5.60 and Fig. 5.61). The positive sign shows the outward and the negative sign inward deformation. The stress in the direction of loading is symbolled as S33. The positive sign indicates tension while the negative sign indicates compression. At the outer face of containment both concrete and reinforcement are found to be under compression at the location of impact. The maximum stress in concrete is found to be of the 7.3 MPa while in steel 60 MPa and in steel liner 65 MPa at the impact location (Fig. 5.55, 5.56, 5.57). At the inner face, both

the concrete and reinforcement are found to be under tension at the impact region (Fig. 5.64). From Fig. 5.65 and 5.66, it can be concluded that the deformation and stress are maximum near the impact location (at element 21).

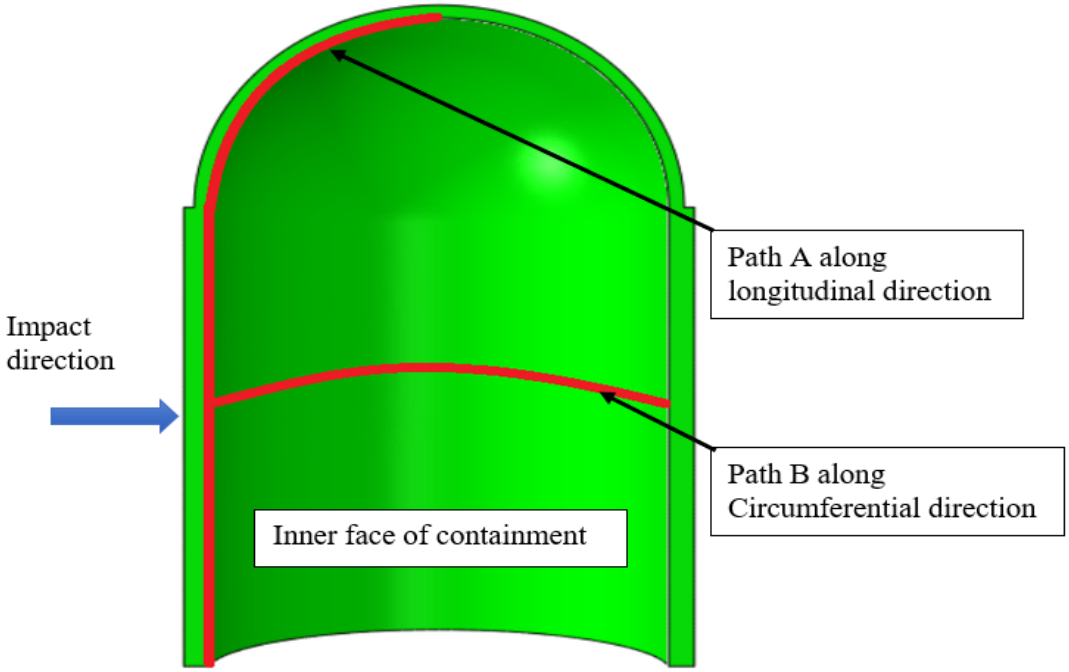

Fig. 5.50 Path-A and Path-B in concrete body for plotting results

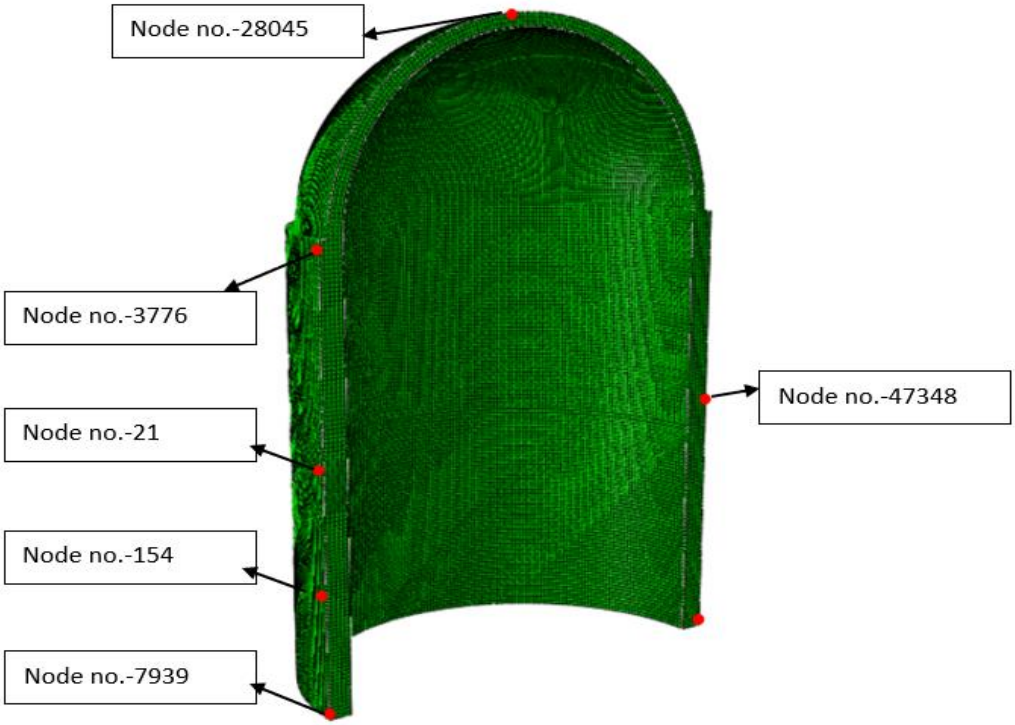

Fig. 5.51 Some selective nodes in concrete and steel reinforcement bar

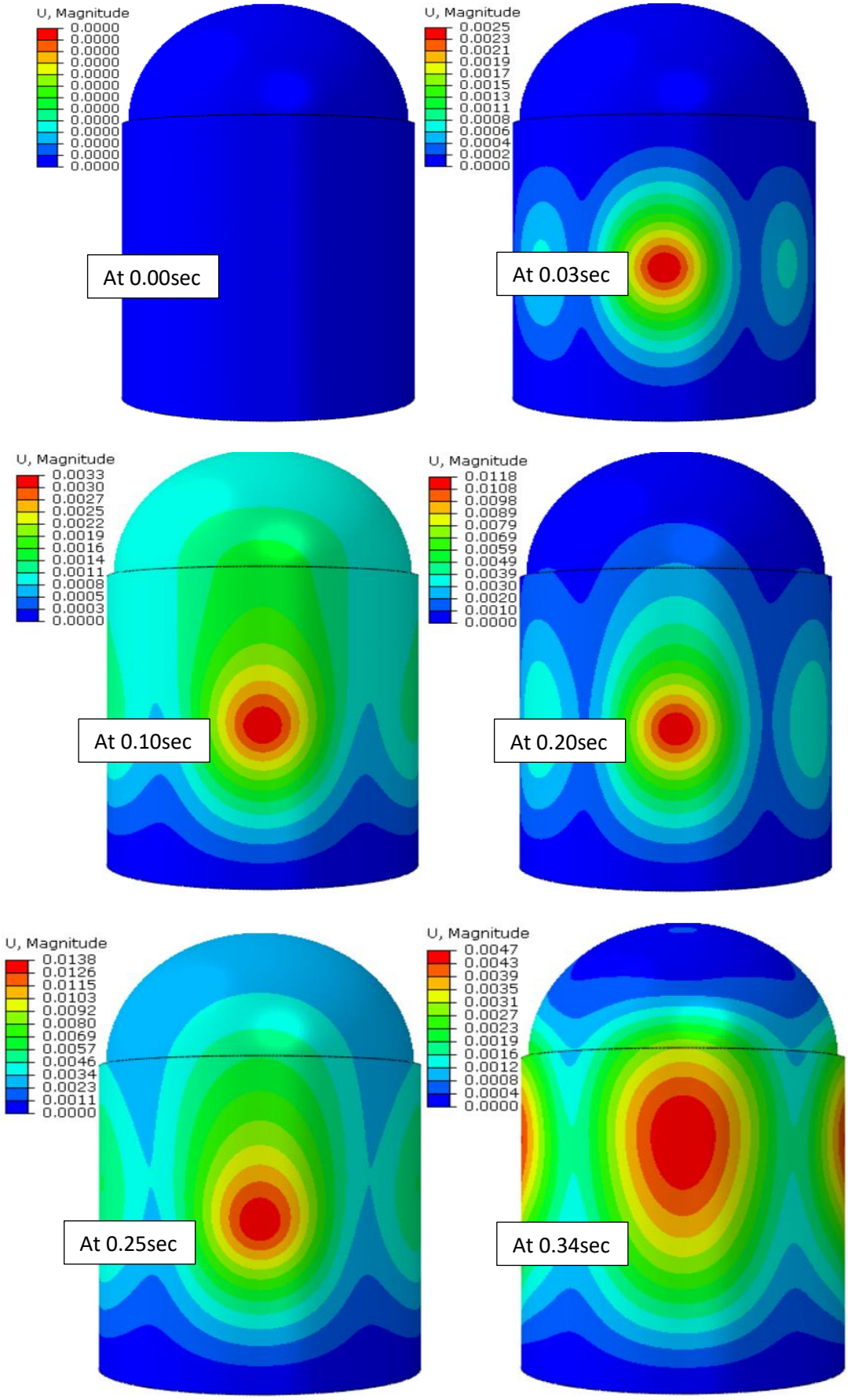

Fig. 5.52 Deformation contour in concrete at different time interval

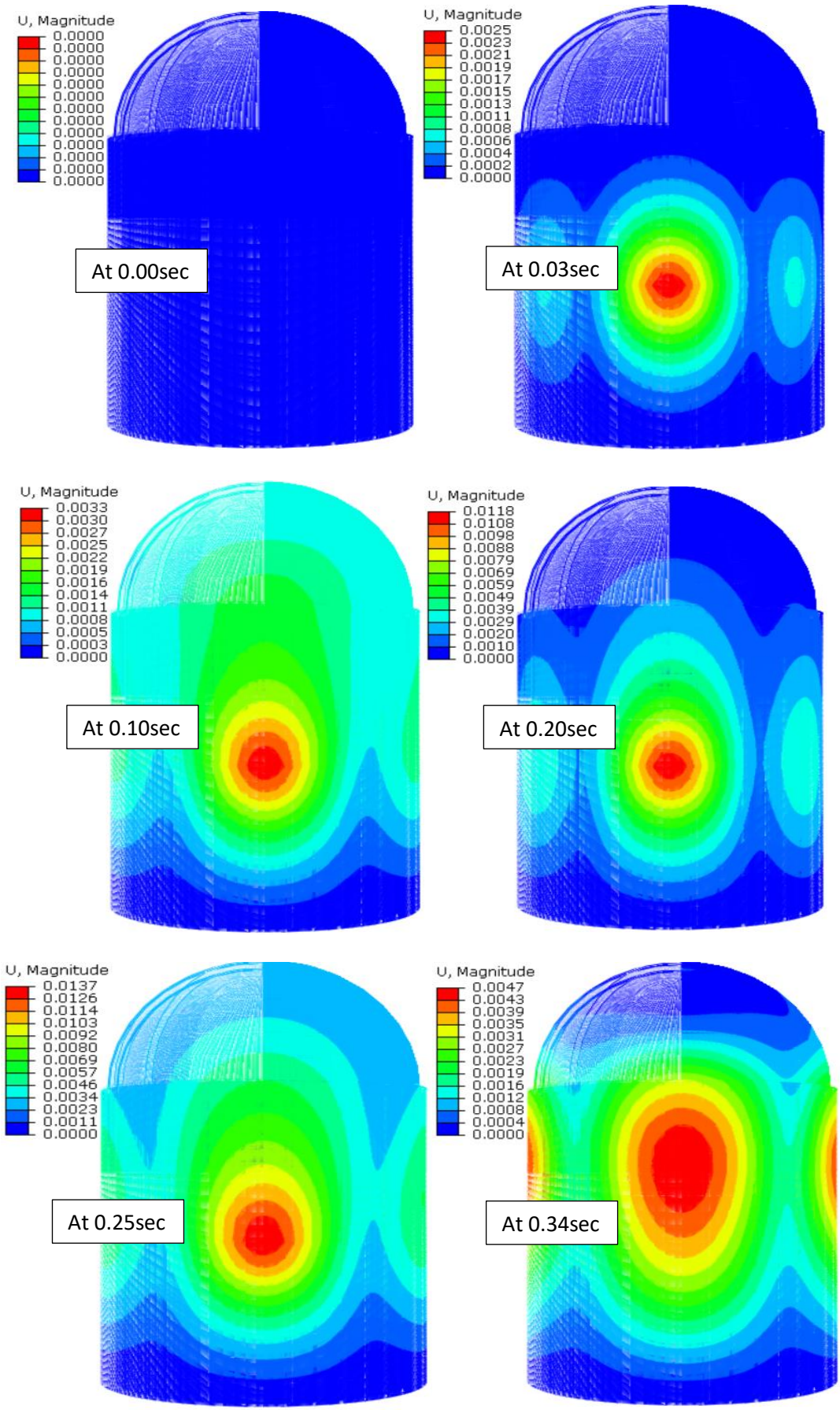

Fig. 5.53 Deformation contour in steel reinforcement bar at different time interval

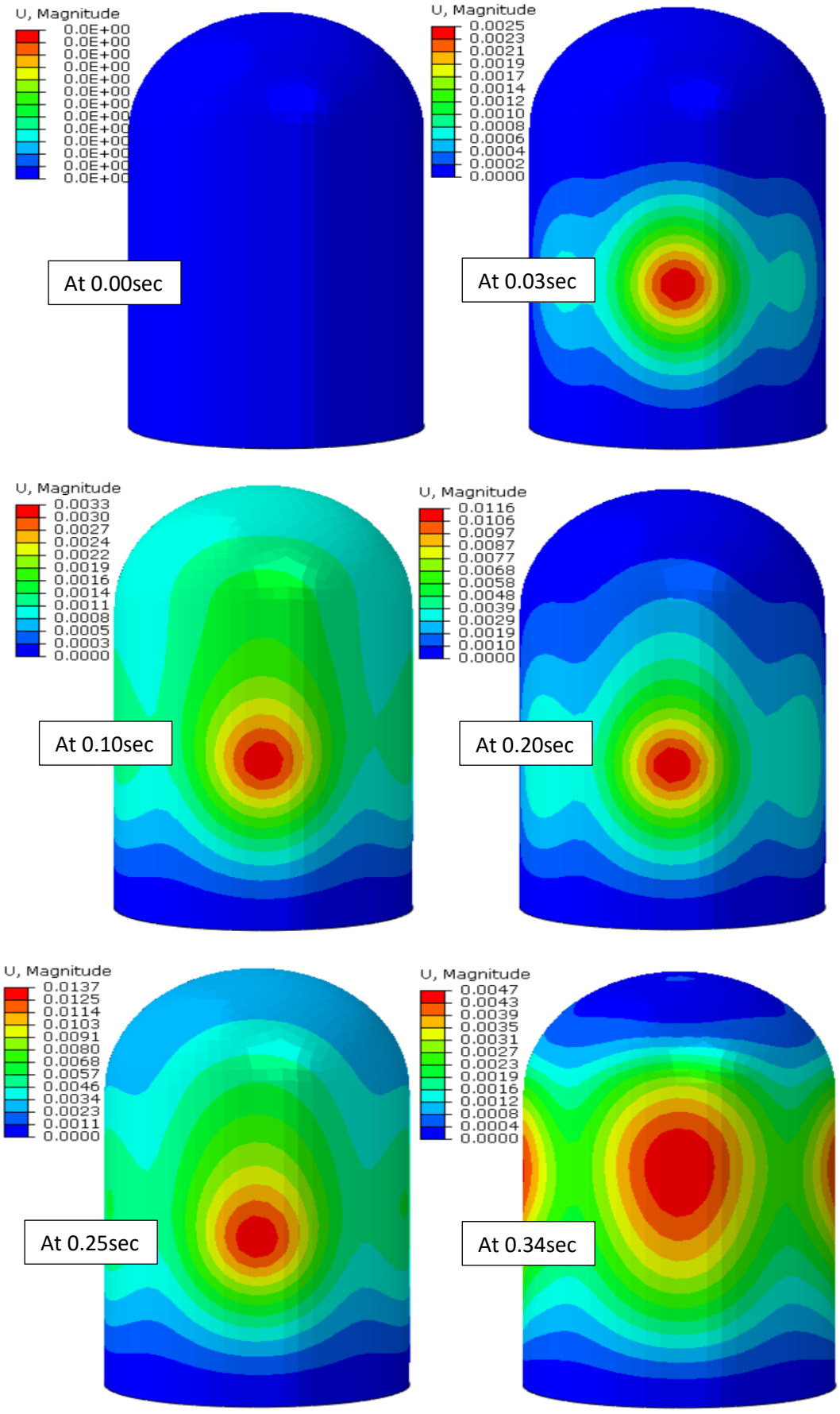

Fig. 5.54 Deformation contour in steel liner at different time interval

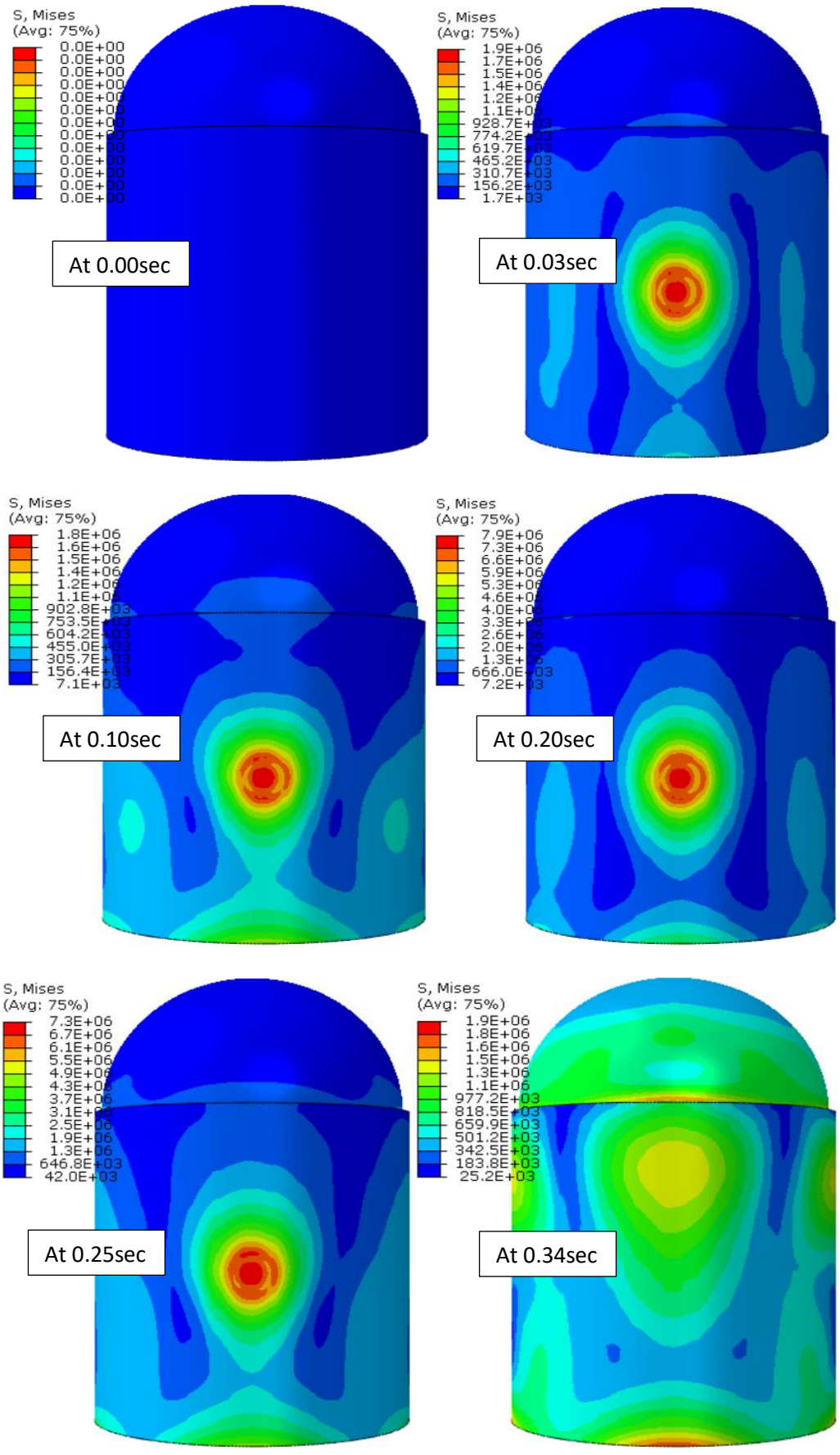

Fig. 5.55 Stress contour in concrete at different time interval

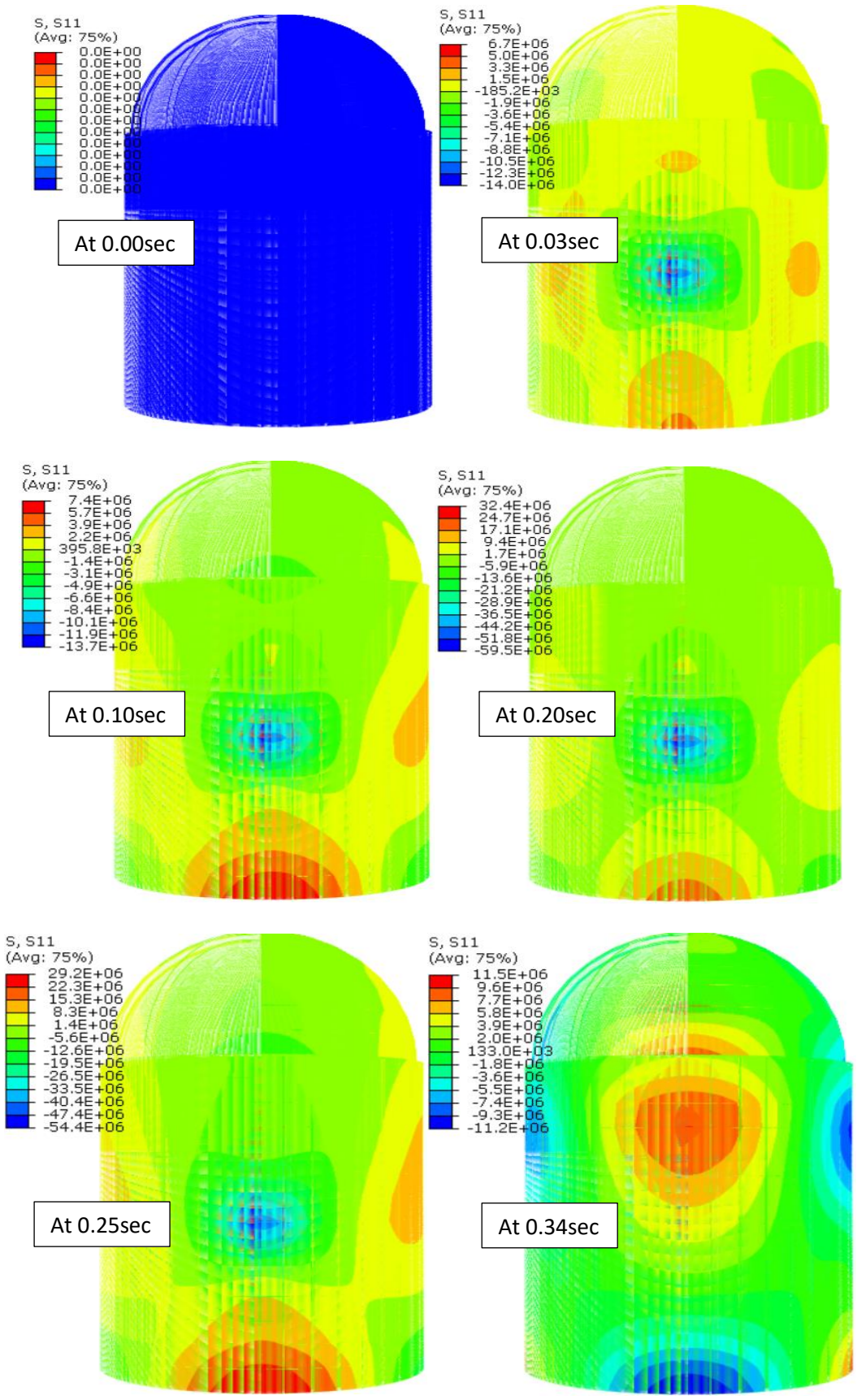

Fig. 5.56 Stress contour in steel reinforcement bar at different time interval

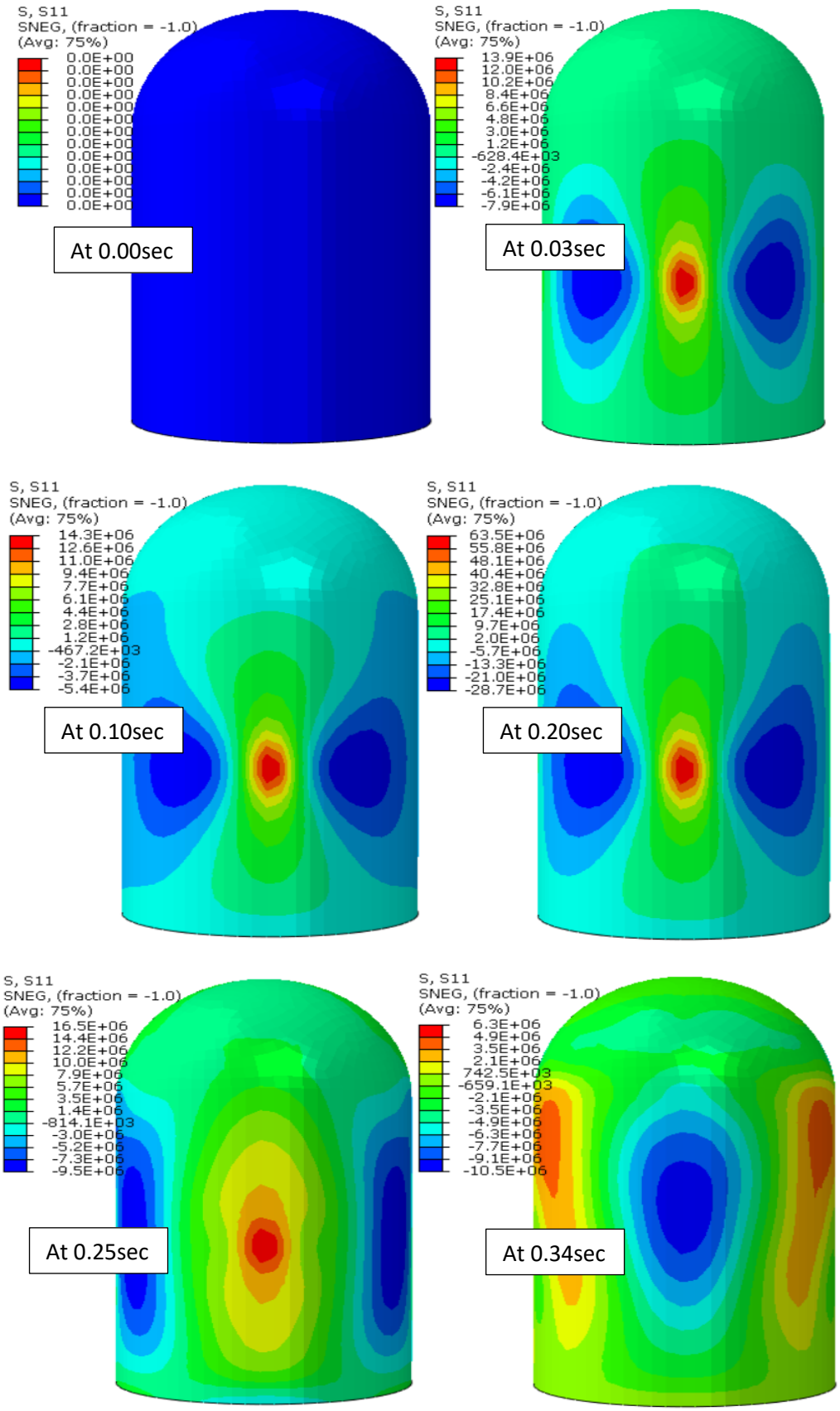

Fig. 5.57 Stress contour in steel liner at different time interval

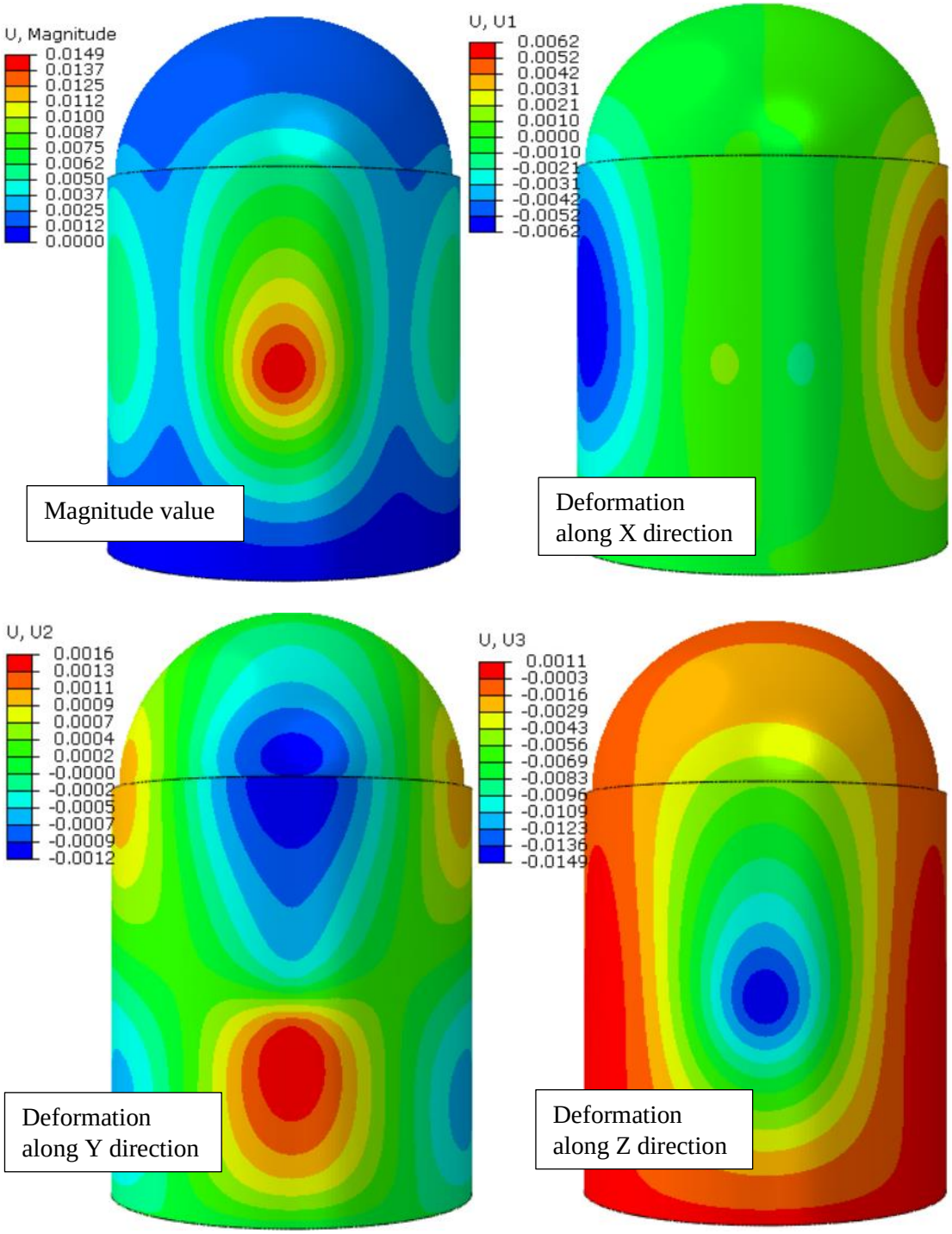

Fig. 5.58 Deformation profile in concrete body at time 0.27sec

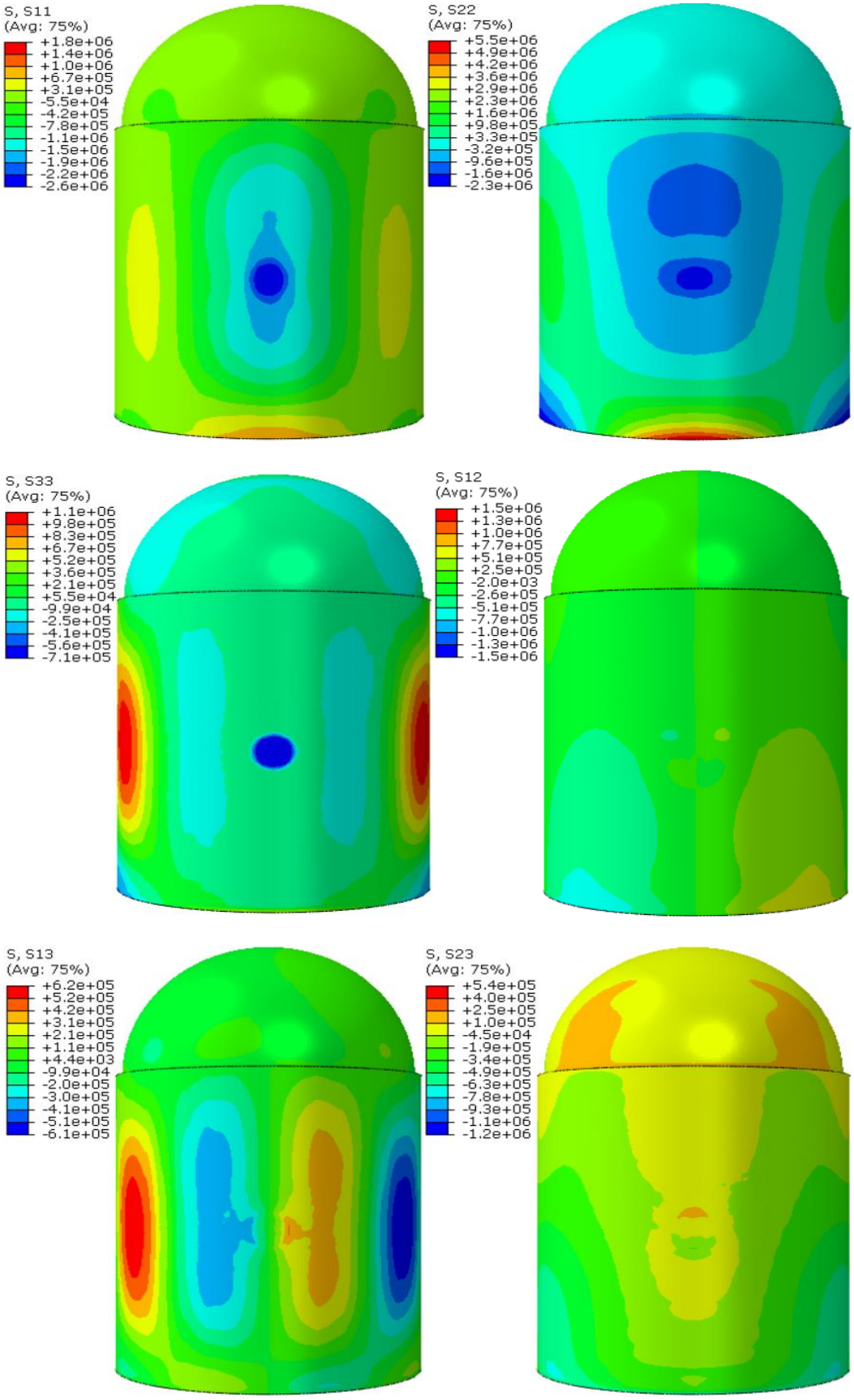

Fig. 5.59 The different stress profile in concrete at time 0.27sec

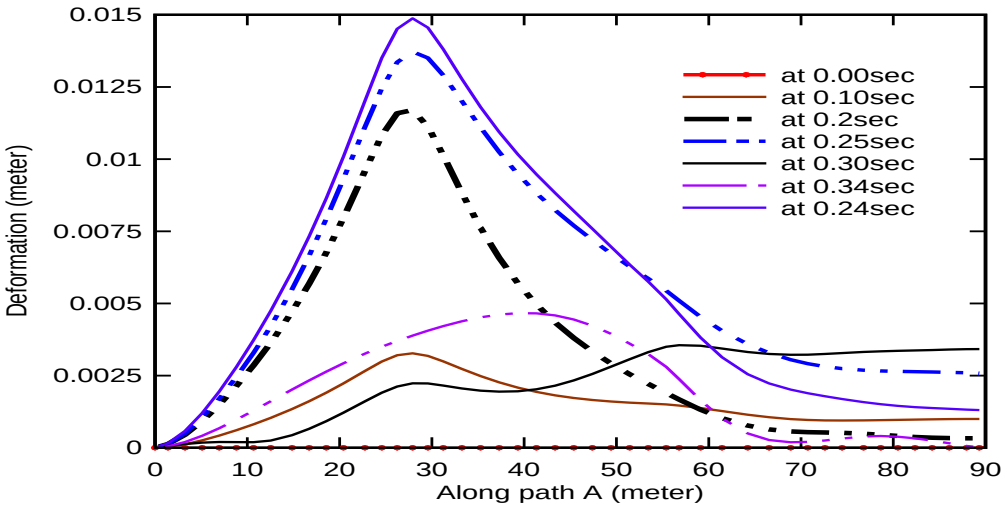

Fig. 5.60 Deformation in concrete along Path A (along longitudinal direction)

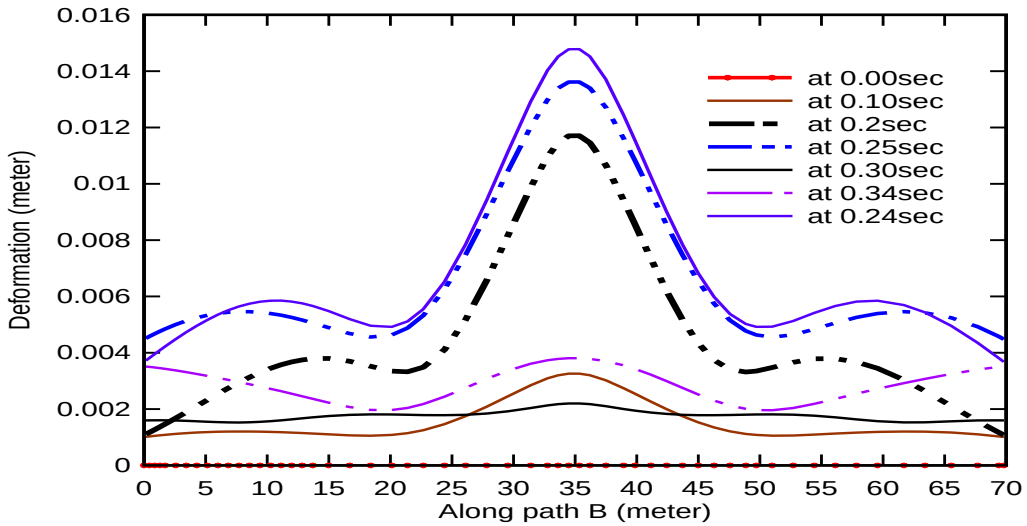

Fig. 5.61 Deformation in concrete along Path B (along Circumferential direction)

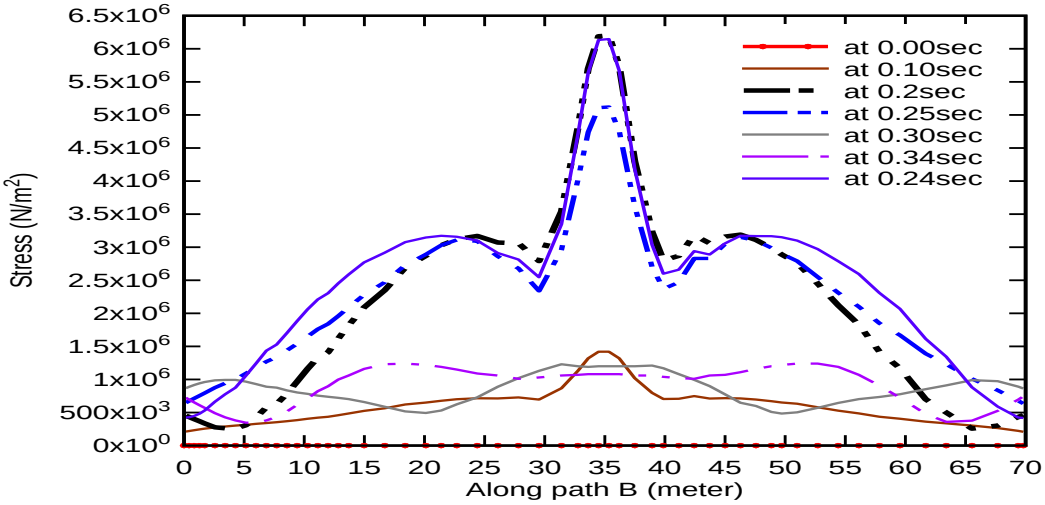

Fig. 5.62 Stress in concrete along Path A (along longitudinal direction)

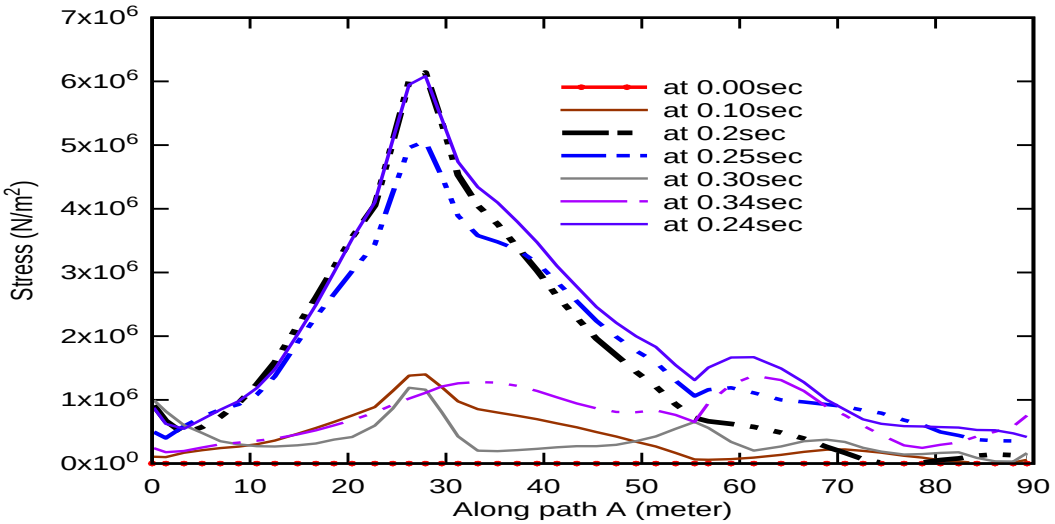

Fig. 5.63 Stress in concrete along Path B (along Circumferential direction)

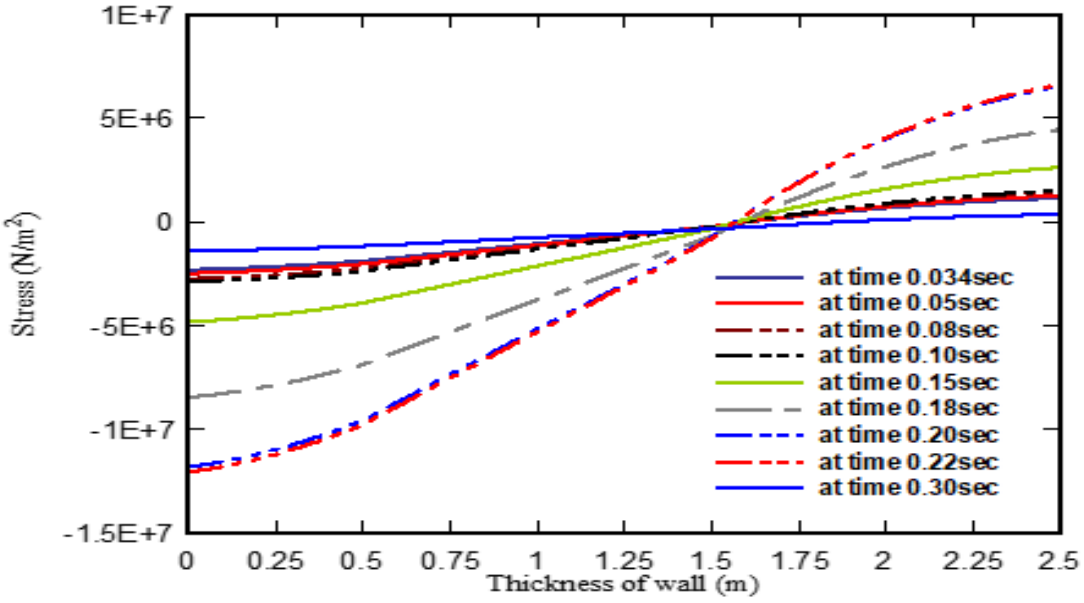

Fig. 5.64 Stress variation along the thickness of TMIR wall

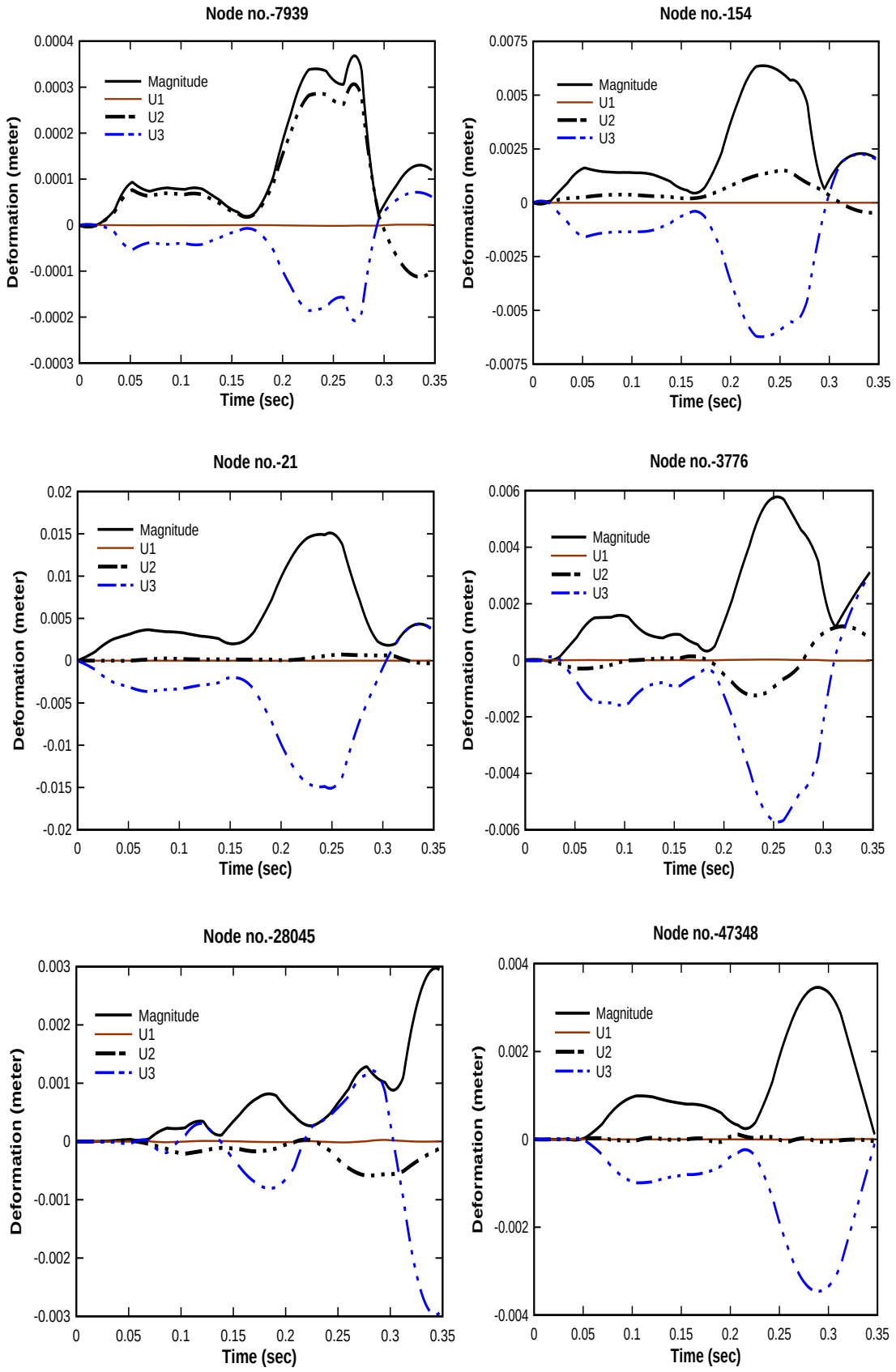

Fig. 5.65 Deformation in concrete body at some selected nodes

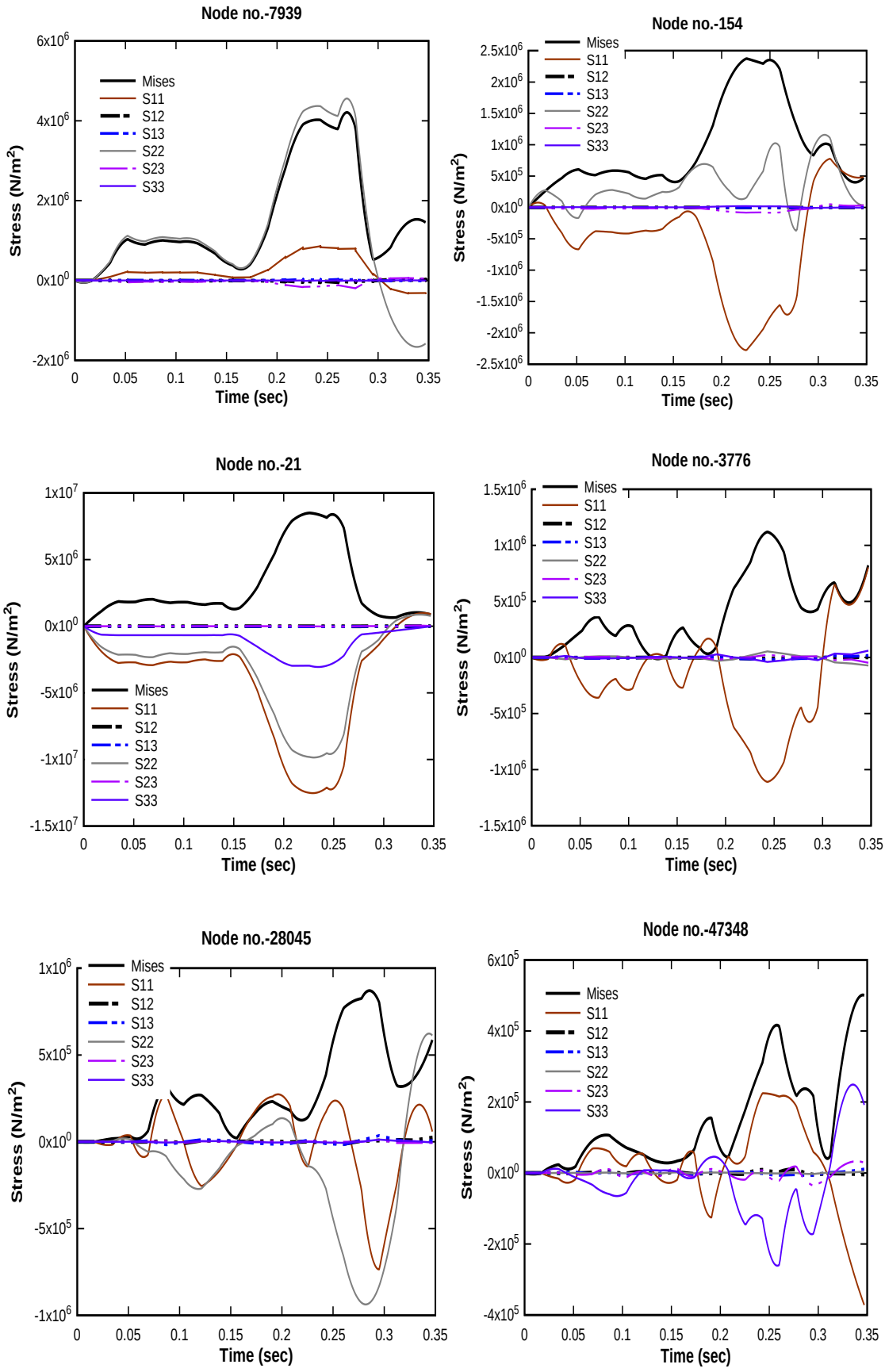

Fig. 5.66 Stress in concrete body at some selected nodes

5.6 MOST DAMAGED PRONE NPP REACTOR CONTAINMENT

Total four types of real NPP containment wall have been taken into consideration to get the damage prone nuclear containment wall. In the present study, the location of impact for all the reactors are considered at mid-height from the base of containment structure. The Boeing 707-320 aircraft has taken to apply the impact load on NPPs wall. This height has been taken because maximum deformation, stress and damages are observed in this location so it is the most vulnerable location of NPP structure. The average area approach is used to apply the load via the force time history curve. The Explicit impact analysis has been performed for simulation of model. The deformations, stress, plastic strain and damages are calculated in the model under the impact of Boeing 707-320 aircraft. The deformation contours of concrete, steel reinforcement and inner steel liner for every NPP wall are shown in Fig. 5.67-5.70. Thereafter the stress contours of concrete, steel reinforcement and inner steel liner are shown in Fig. 5.71-5.74. The maximum deformation of 2.1m in concrete, 1.533m in steel rebars and 1.879m in steel liner are observed in CMR containment wall among all reactors (Fig. 5.68). The minimum deformation of 0.015m in concrete, 0.015m in steel rebars and 0.015m in steel liner are observed in TMIR for the same aircraft impact (Fig. 5.70). The maximum stress of 49 MPa in concrete, 622 MPa in steel rebars and 988 MPa in steel liner are found in CMR among all reactors (Fig. 5.72). The minimum stress of 9 MPa in concrete, 37 MPa in steel rebars and 63 MPa in steel liner are noticed in TMIR among all reactors (Fig. 5.74). As the maximum stress in concrete, reinforcement and steel liner in CMR containment wall is much higher than the permissible limit, it is considered every material is damaged locally. So, the most damage prone reactor is CMR. The maximum area of tension damage occurs in concrete of CMR which has been shown in Fig. 5.75. Here two

paths are considered to show the deformation and stress variation with time i.e., path A and path B. The deformation and stress variation along path A and path B for all NPPs containment wall are plotted (Fig. 5.76-5.78). The path A is along the circumferential direction (along half periphery) whereas path B is along longitudinal direction (along height). As the base of containment is fixed so deformation is zero but some deformation is found in the junction between cylinder and dome (Fig. 5.77). When the deformation variation of a single element in impact location has been plotted for every NPP containment wall, it is also observed the CMR has maximum deformation (Fig. 5.79). From Fig. 5.80, it may be concluded that the tension damage starts in structural elements at different time because every containment has different thickness and dimension. The tension damage starts at 0.18 sec in CMR, 0.2 sec in FBC and 0.22 sec in BWR (Fig. 5.80). The stress variation curve for TMIR through path-A is not zigzag but all the curves are zigzag because TMIR has no damage and the reason is more thickness of reactor (Fig. 5.78).

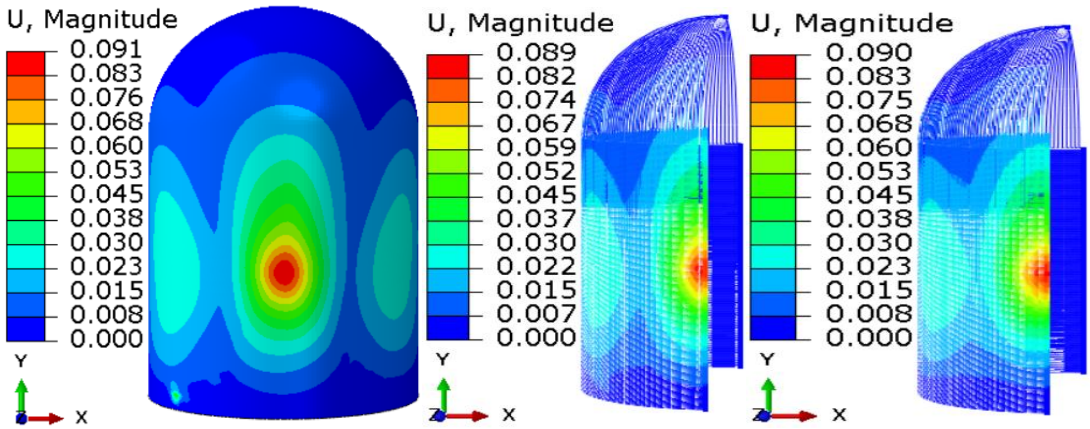

Fig. 5.67 Maximum deformation in BWR Mark-III containment (a) concrete (b) inner steel rebars (c) outer steel rebars

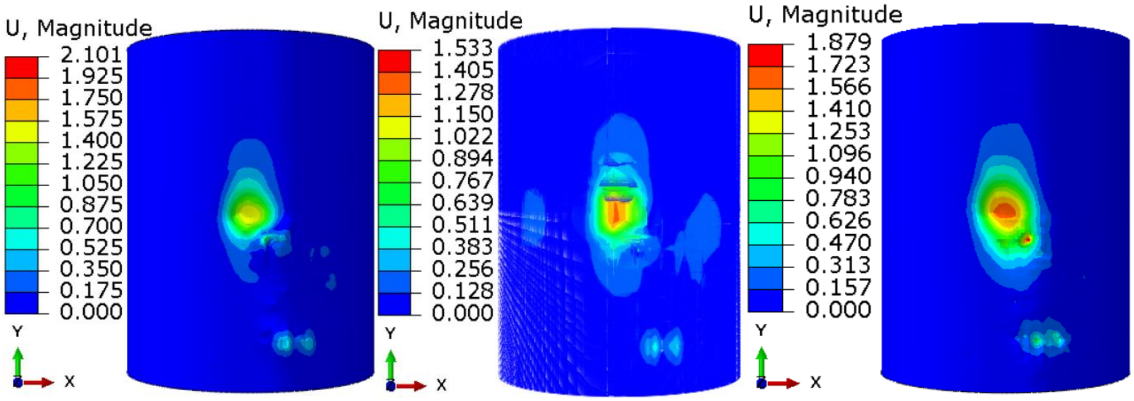

Fig. 5.68 Maximum deformation in CMR containment (a) concrete (b) steel rebars (c) inner steel liner

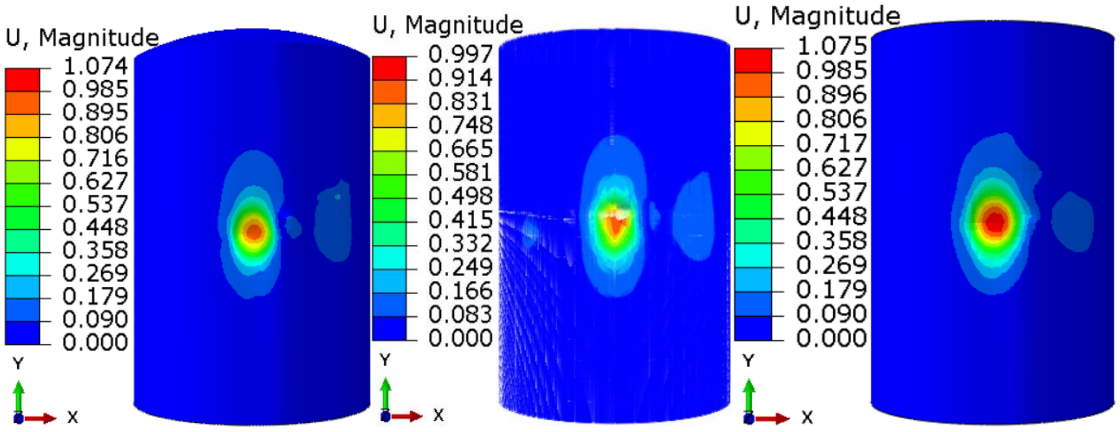

Fig. 5.69 Maximum deformation in FBR containment (a) concrete (b) steel rebars (c) inner steel liner

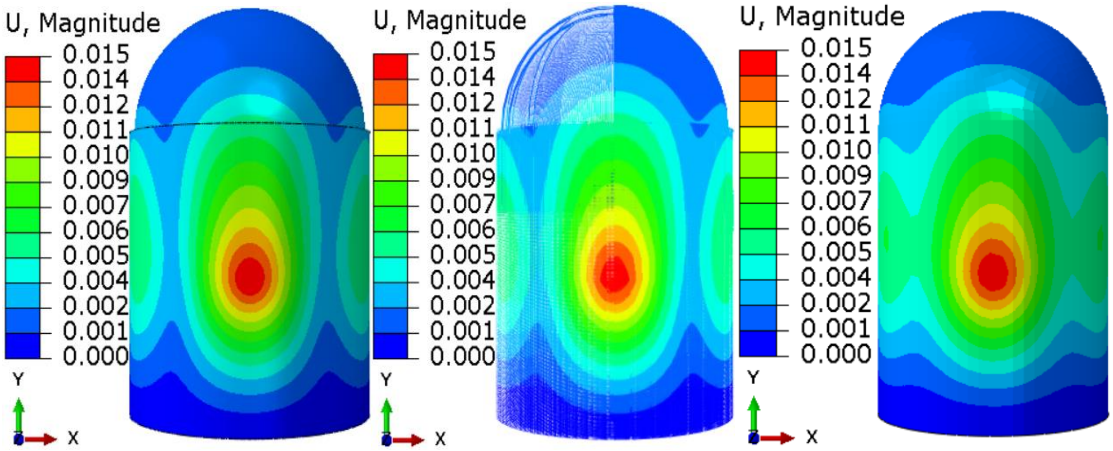

Fig. 5.70 Maximum deformation in TMIR containment (a) concrete (b) steel rebars (c) inner steel liner

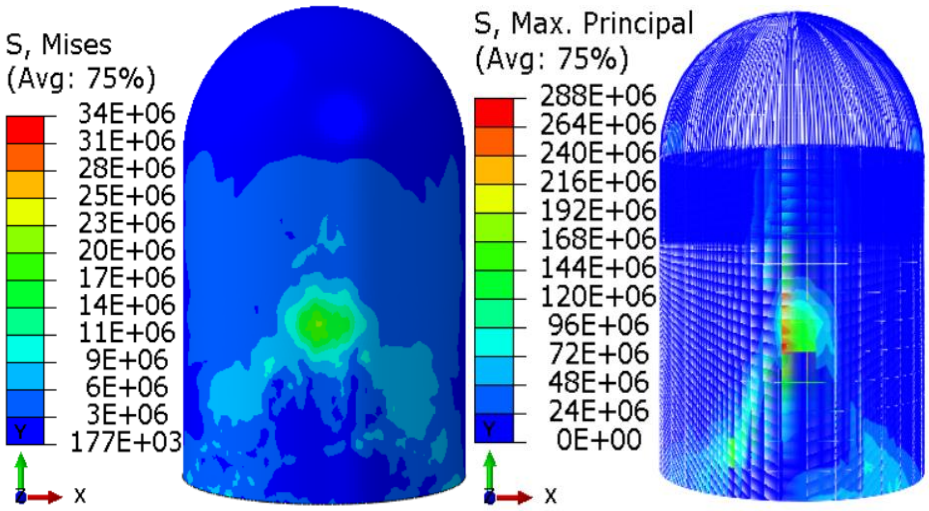

Fig. 5.71 Maximum stress in BWR Mark-III containment (a) concrete (b) steel rebars

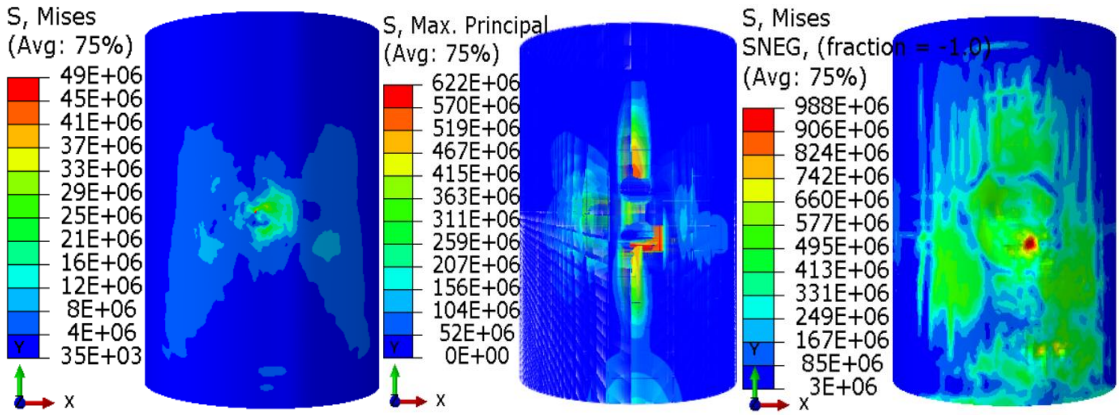

Fig. 5.72 Maximum stress in CMR containment (a) concrete (b) steel rebars (c) inner steel liner

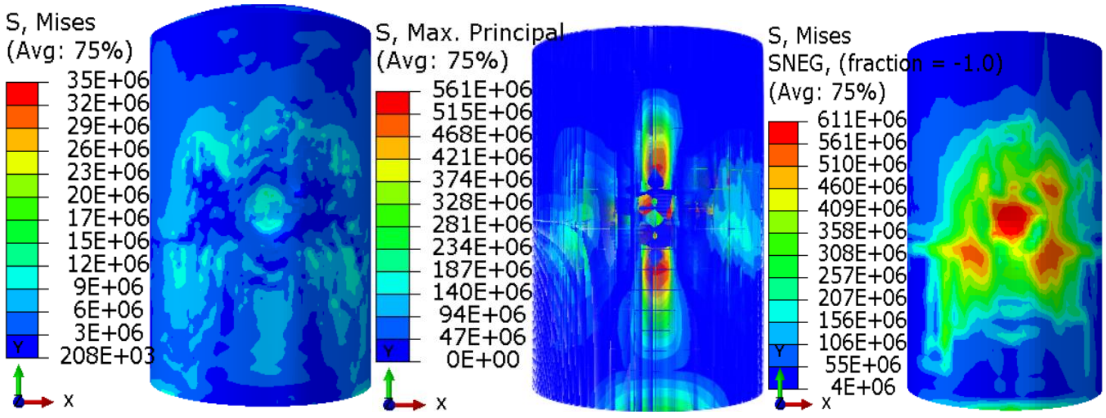

Fig. 5.73 Maximum stress in FBR containment (a) concrete (b) steel rebars (c) inner steel liner

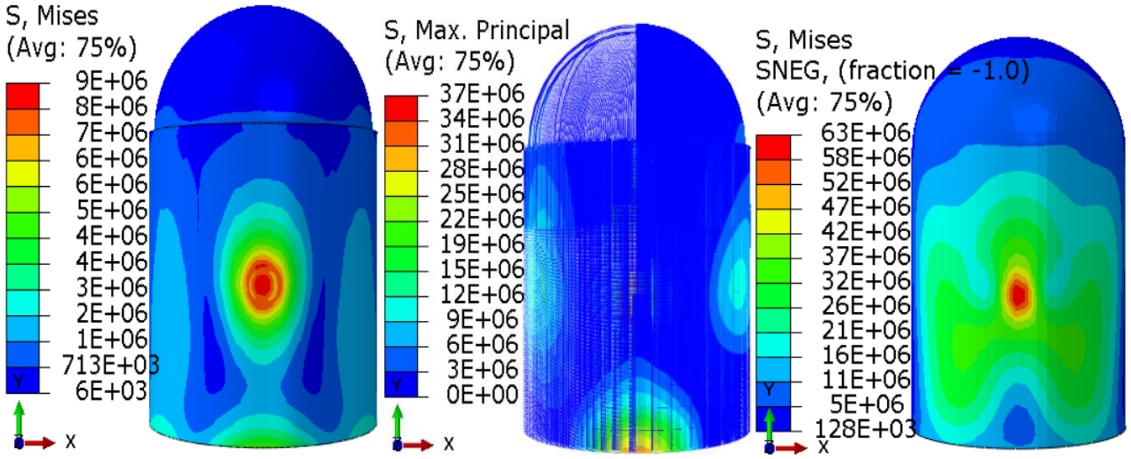

Fig. 5.74 Maximum stress in TMIR containment (a) concrete (b) steel rebars (c) inner steel liner

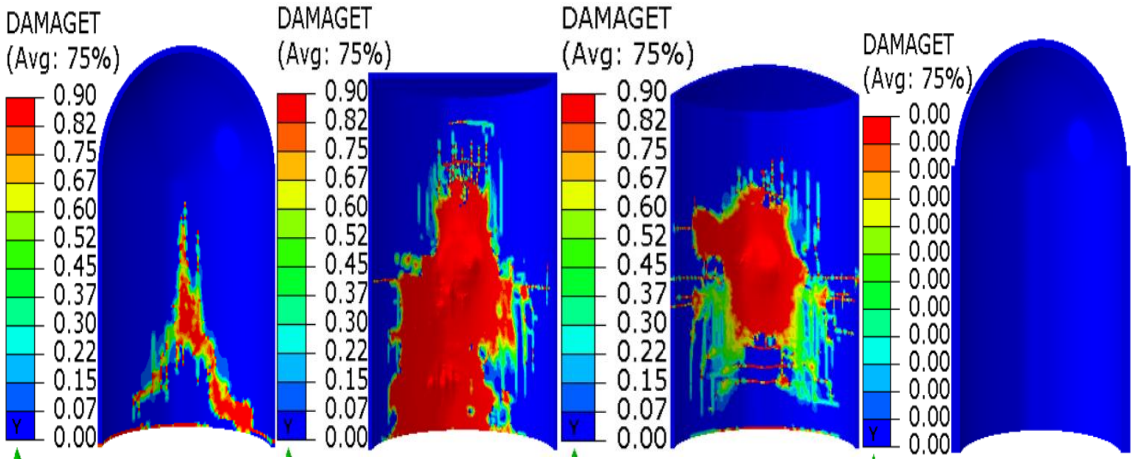

Fig. 5.75 Tension damages in (a) BWR Mark-III (b) CMR (c) FBR (d) TMIR

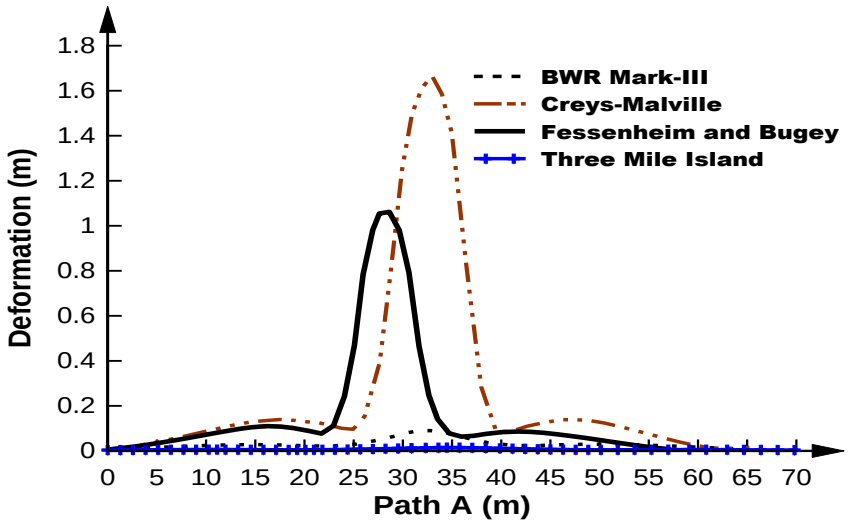

Fig. 5.76 Global deformation in concrete along path A

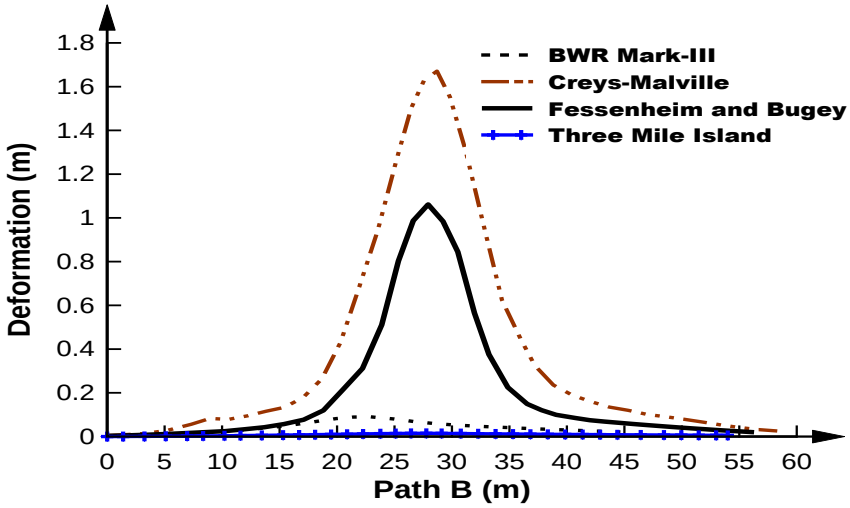

Fig. 5.77 Global deformation in concrete along path B

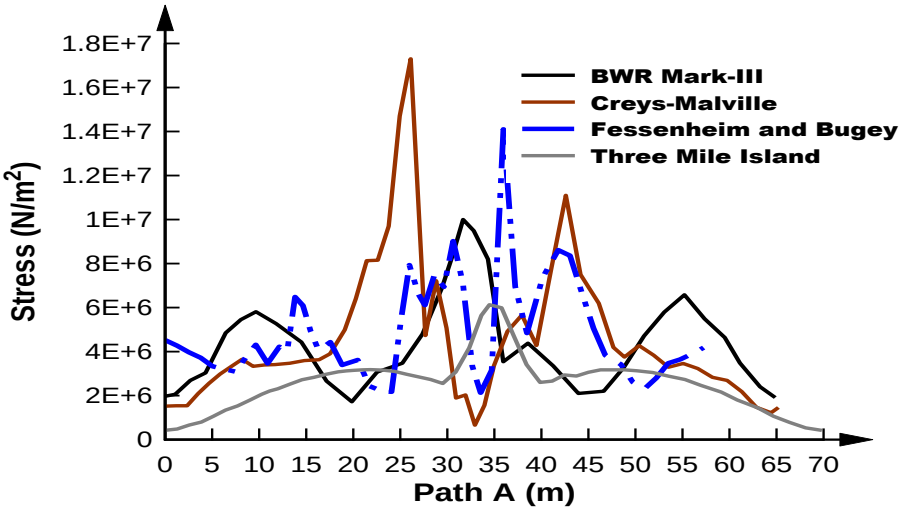

Fig. 5.78 Stress produced in concrete along path A

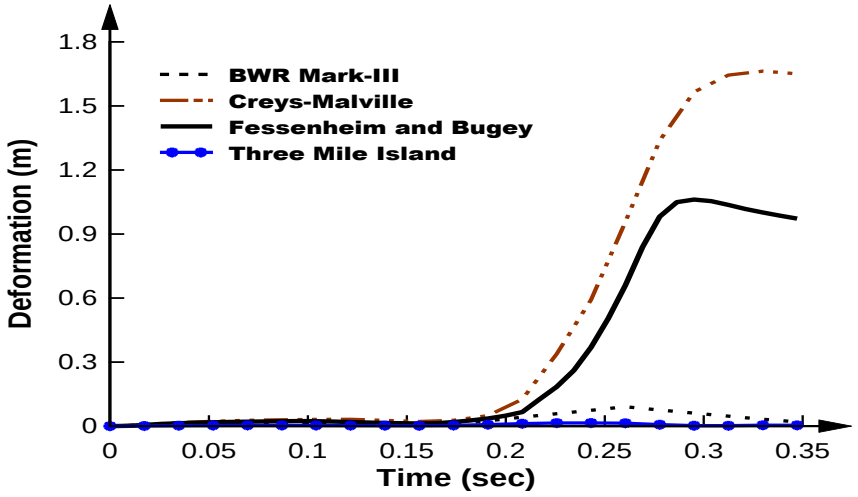

Fig. 5.79 Deformation of an element at impact location in all NPPs

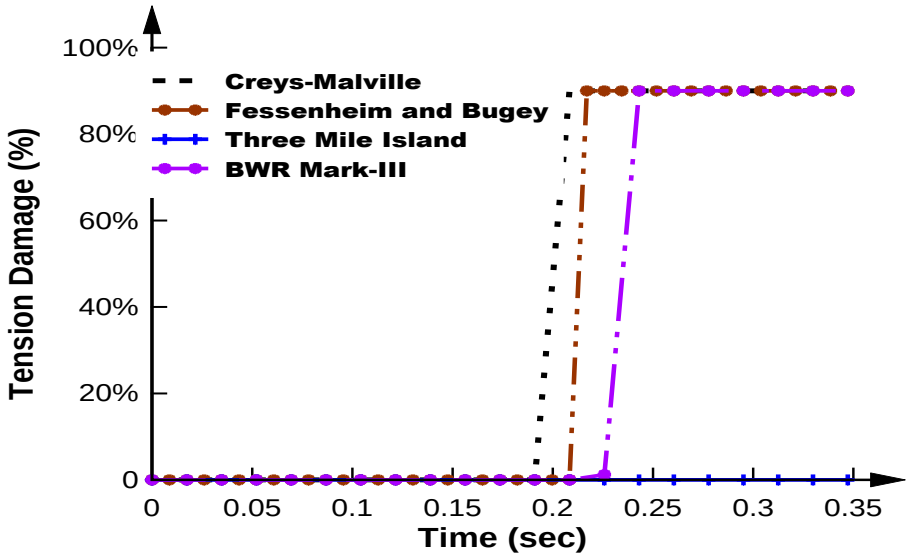

Fig. 5.80 Tension damage of an element at impact location in all NPPs

In the present study, an attempt has been made to find out the most damage prone NPP structure under the impact of Boeing 707-320 aircraft using finite element analysis. The subsequent conclusions are drawn from the analysis:

- The maximum and minimum deformation are observed 2.1m in CMR and 0.015m in TMIR respectively when the impact load is applied at mid-height from the base of containment. Such kind maximum deformation value is found in concrete because the concrete gets damaged.
- The maximum tension damages are observed at impact location in CMR due to less thickness of containment.
- The minimum tension damage is observed in TMIR due to more thickness of containment.
- After some time of impact, the elements experienced plastic strain and get damaged.

- The elements experienced plastic strain and damage when the wings of aircraft come in contact with NPP containment. This results in maximum deformation and stress.
- The damage due to the considering aircrafts over the containment structure is not a global failure.
- Finally, it may conclude that the CMR is more damage prone NPP containment.

5.7. MOST DAMAGING AIRCRAFT ON NPP CONTAINMENT

In this study, total four types of aircraft have been taken to find out the most devasting aircraft on BWR mark-III and TMIR containment wall. The four types of aircraft are Boeing 707-320, Boeing 767-300, Phantom F4 and Airbus A320 aircraft.

5.7.1 Most damaging aircraft on BWR Mark-III containment

The impact location for all the aircraft is considered at 23m height from the base of containment structure in the present study. This height has been taken because it is the most vulnerable location of BWR containment wall. The average area approach is used to apply the load via the reaction-time curves. The Explicit impact analysis is performed for simulation of model and the deformation and damage are measured for different aircrafts. The maximum deformations of 0.168m for Boeing 767-300, 0.251m for Phantom F4, 0.091m for Boeing 707-320 and 0.039m for Airbus A320 are observed which has been shown in Fig. 5.81-5.84. The aircraft Boing 767-400 has the maximum damaging potential and Airbus A320 has the minimum damaging potential as shown in Fig. 5.81 and Fig. 5.84 respectively. The deformation is high but the damage is not

maximum for Phantom F4 fighter jet because it has maximum impact velocity but minimum in wing's span (less area of impact). Due to the larger wing's span in Boeing 767-400, this aircraft is responsible for more damage in concrete. When the deformation variation of an element in impact location has been drawn for every aircraft throughout the total time of impact, it has been also observed Phantom F4 provides large deformation (Fig. 5.85) and it is a local phenomenon. When the stress profile has been plotted for an element in impact location, the maximum stress is found for Phantom F4 (Fig. 5.86). When the reaction variation for an element (located at the base of containment) has been plotted, the maximum reaction is found for Boeing 767-400 (Fig. 5.87). From Fig. 5.88 it may be concluded that after sometime of impact, the plastic strain also initiated in the element. The deformation and stress behaviour (global behaviour) on containment along path A (along half periphery) and along path B (along height) has been shown in Fig. 5.89, 5.90, 5.91. From these plots it is observed that the Boeing 767-400 is the responsible for maximum deformation and maximum stress. As the base of containment is fixed so deformation is zero but some deformation is found at the junction between cylinder and dome (Fig. 5.90).

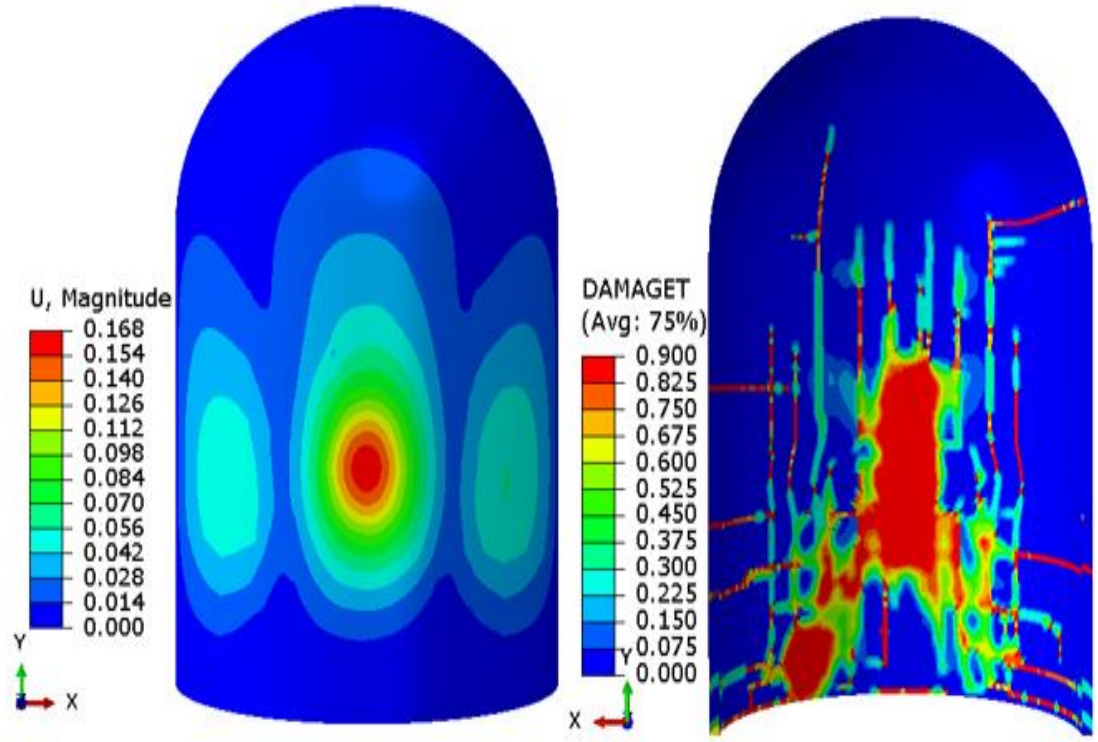

Fig. 5.81 Maximum deformation and tension damages in containment for Boeing 767-400

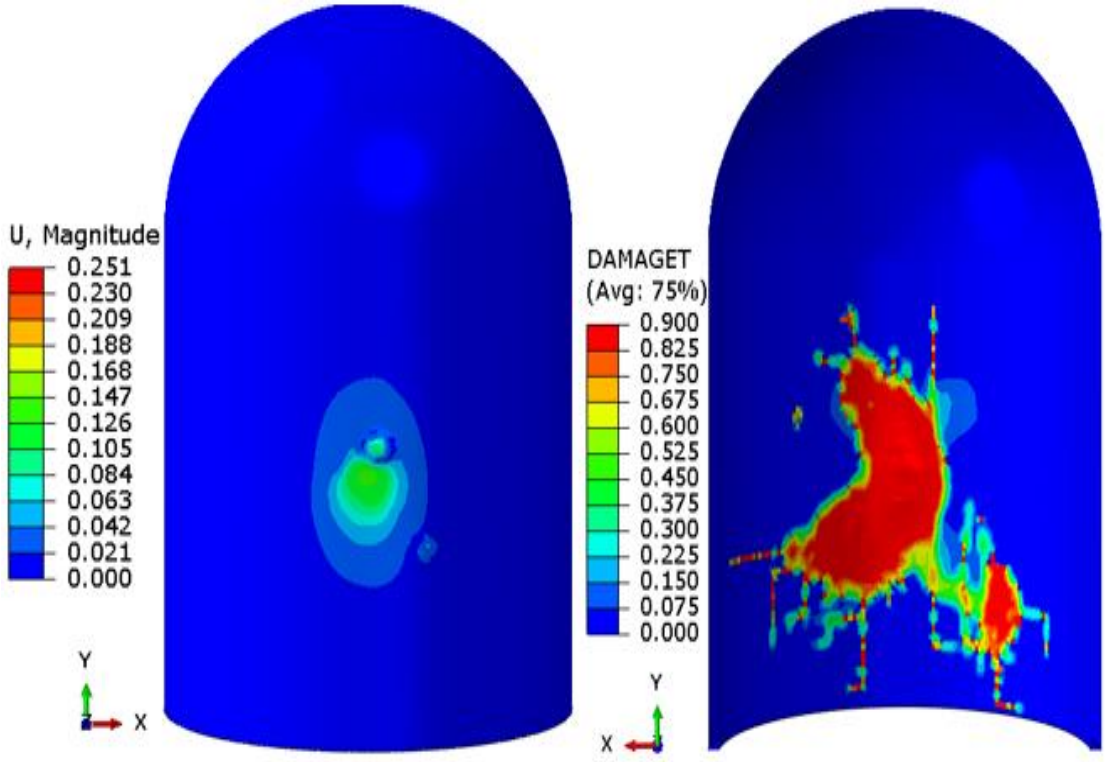

Fig. 5.82 Maximum deformation and tension damages in containment for Phantom F4

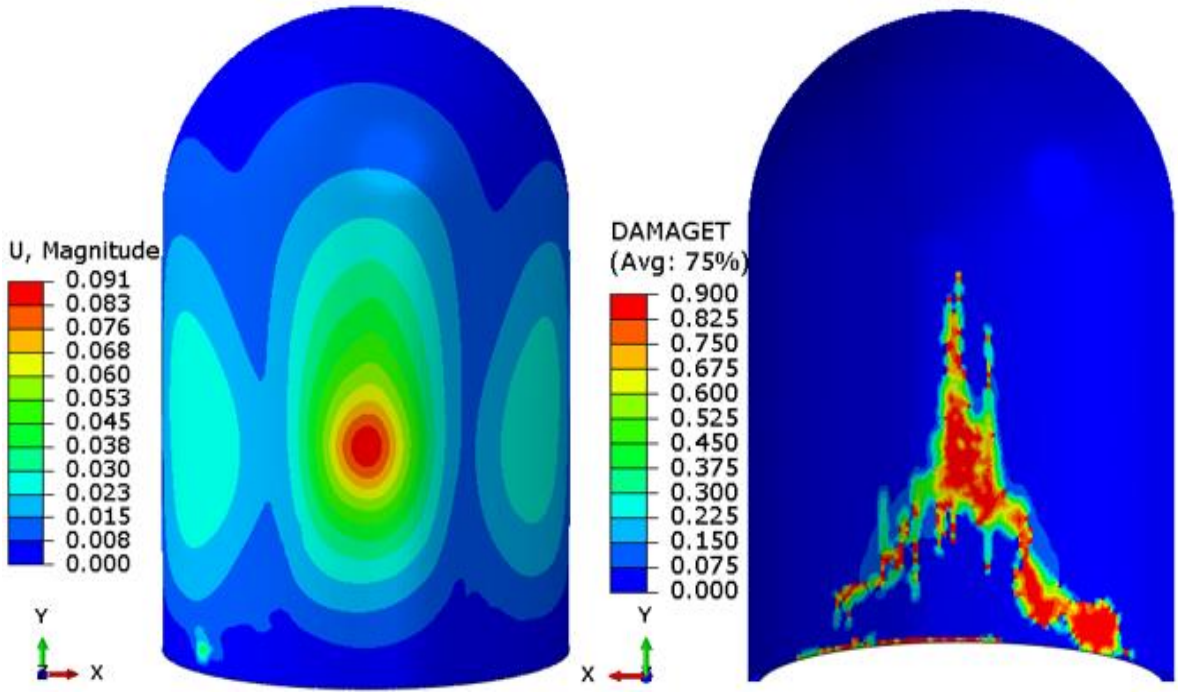

Fig. 5.83 Maximum deformation and tension damages in containment for Boeing 707-320

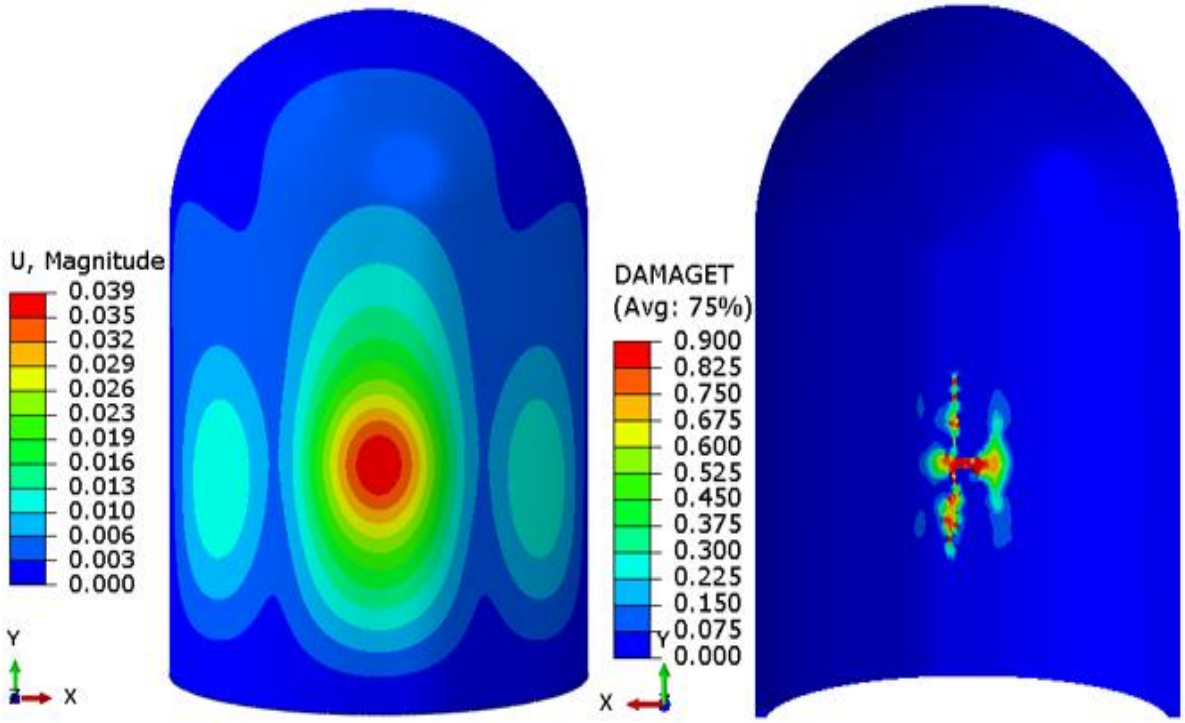

Fig. 5.84 Maximum deformation and tension damages in containment for Airbus A320

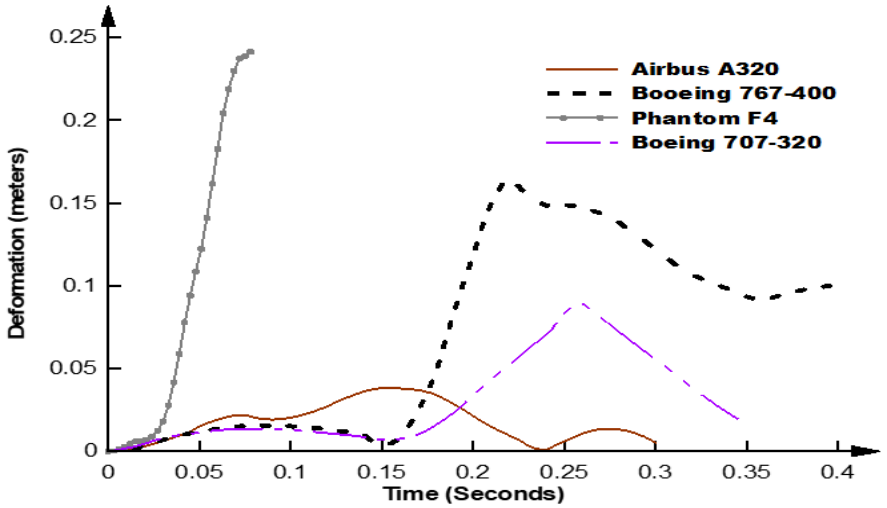

Fig. 5.85 Deformation of an element at impact location for different aircrafts

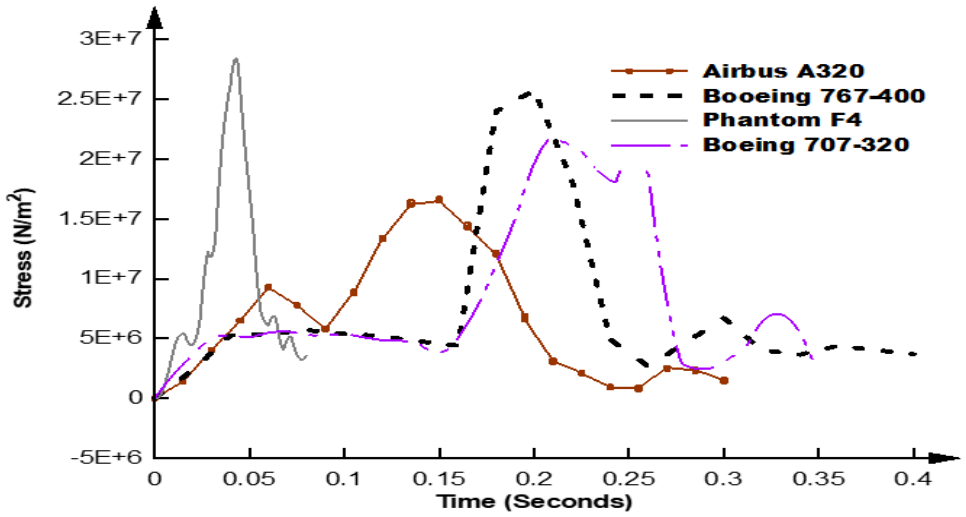

Fig. 5.86 Stress of an element at impact location for different aircrafts

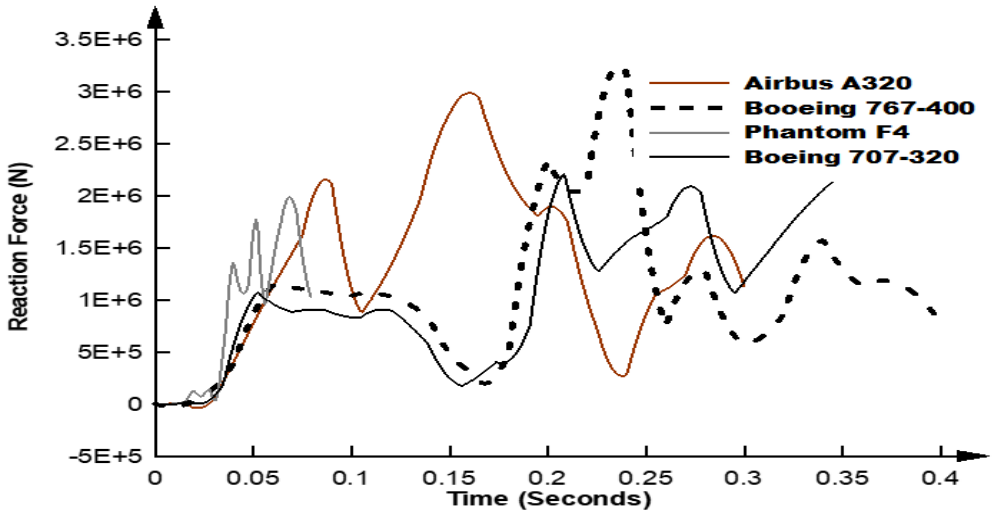

Fig. 5.87 Reaction force at the base of containment produced by different aircrafts

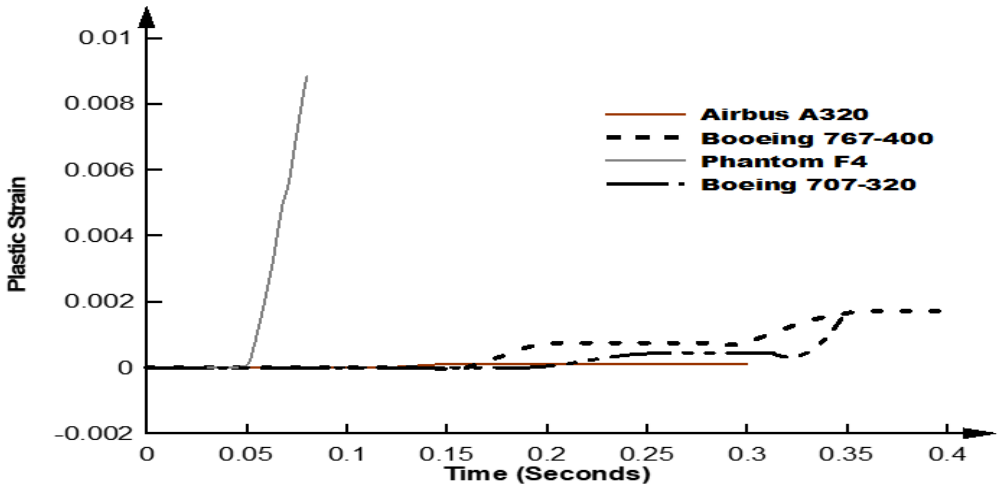

Fig. 5.88 Plastic strain of an element at impact location for different aircrafts

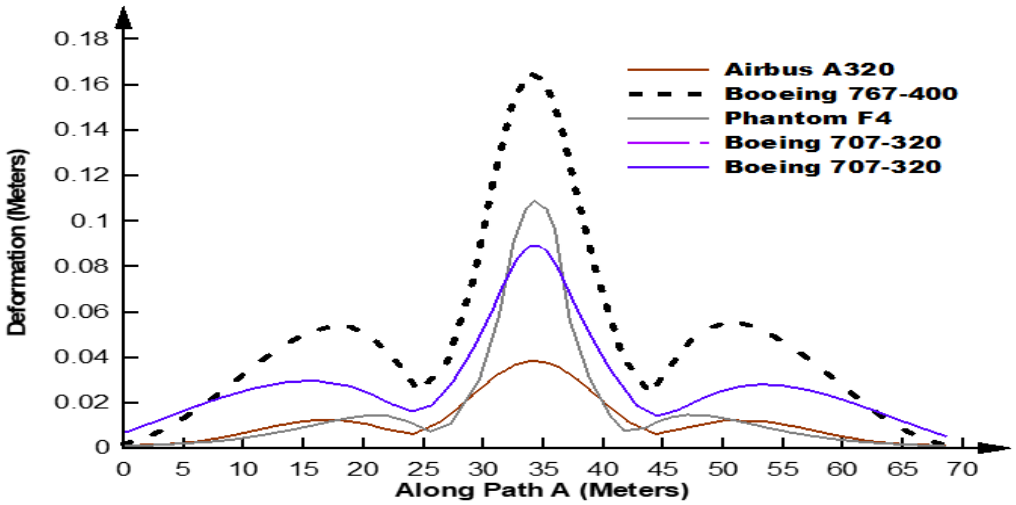

Fig. 5.89 Global deformation in concrete along path A

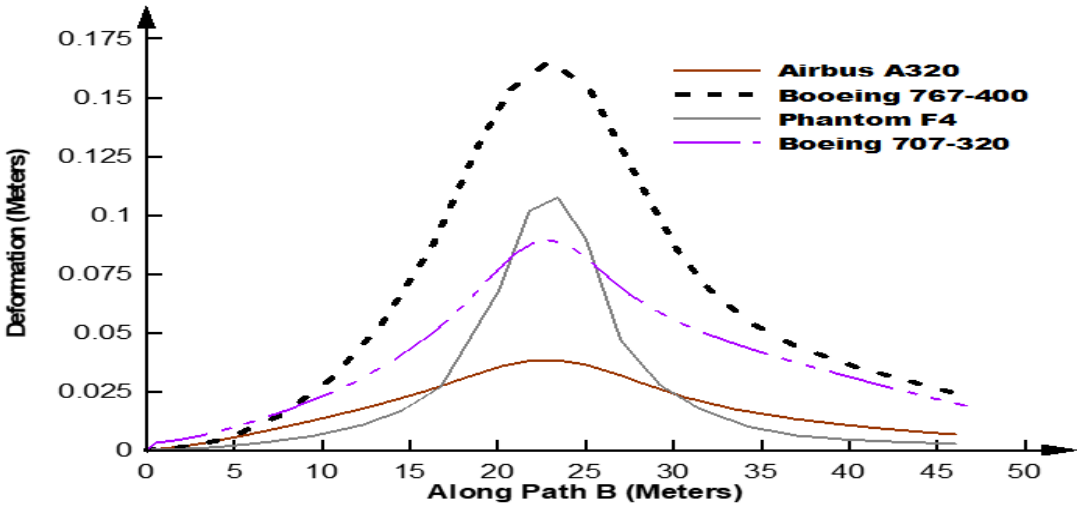

Fig. 5.90 Global deformation in concrete along path B

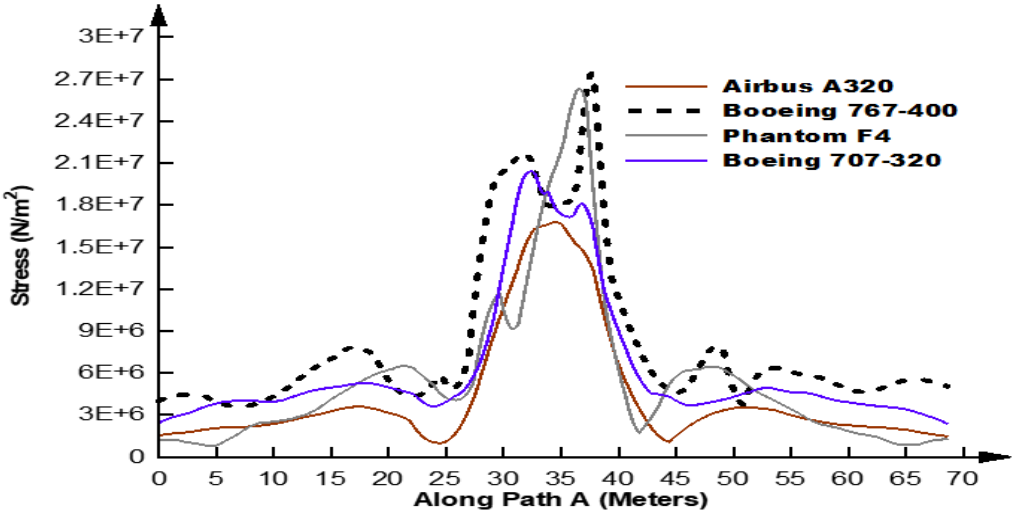

Fig. 5.91 Stress produced in concrete along path A

In this study, an attempt has been made to find out the most damaging aircraft on NPP structure (BWR Mark-III) under different aircraft crash (Boeing 707-320, 767-400, Phantom F4 and Airbus A320) using finite element analysis. The subsequent conclusions are drawn from the analysis:

- The maximum and minimum deformation are observed 0.251m for PhantomF4 and 0.039m for Airbus A320 respectively when the impact load is applied at 23m height from the base of containment.
- The maximum tension damage is observed at impact location for Boeing 767-400 due to more impact area.
- The minimum tension damage is observed at impact location for Airbus A320 due to less impact force.
- When the wings of aircraft come in contact with NPP containment, the deformation and stress are maximum.
- After some time of impact, the elements experienced plastic strain and get damaged.

- The damage due to considering aircrafts over the containment structure is not a global failure.
- Finally, it is concluded that the Boeing 767-400 aircraft has more damaging potential among the all considering aircrafts.

5.7.2 Most damaging aircraft on Three Mile Island containment

The impact location for all the aircrafts is considered at 27.25m height from the base of containment structure in the present study. This height has been taken because maximum deformation is observed in this location that means it is the most critical location of NPP containment wall. The average area approach is used to apply the load via the reaction-time curves. The Explicit impact analysis is performed for simulation of model and the deformation and damage are measured for different aircrafts. The deformation contours of concrete, steel reinforcement and inner steel liner for TMIR containment wall are shown in Fig. 5.92-5.95. Thereafter the stress contours of concrete, steel reinforcement and inner steel liner are shown in Fig. 5.96-5.99. The maximum deformation of 0.041m in concrete, 0.041m in steel rebars and 0.040m in steel liner are observed under the impact of Boeing 767-400 aircraft (Fig. 5.92). The minimum deformation of 0.011m in concrete, 0.011m in steel rebars and 0.011m in steel liner are also noticed for the impact of Airbus A320 aircraft (Fig. 5.92). The maximum stress of 98.8 MPa in concrete, 203.8 MPa in steel rebars and 302.7 MPa in steel liner are observed for the impact of Boeing 767-400 aircraft (Fig. 5.96). The minimum stress of 6.7MPa in concrete, 25.5MPa in steel rebars and 44.7MPa in steel liner are found for the impact of Airbus A320 aircraft (Fig. 5.99). The aircraft Boing 767-400 has the more damaging potential, Phantom F4 has the less damaging potential but Boeing 707-320 and Airbus

A320 has no damaging potential on TMIR containment wall which shown in Fig. 9.100. Due to the larger wing's span in Boeing 767-400, this aircraft is responsible for more damage in concrete while the smaller wing's span in Phantom F4 makes less damage in concrete. The deformation and stress behaviour (global behaviour) on TMIR containment wall along path A (along half periphery) and along path B (along height) has been shown in Fig. 5.101-5.104. From these plots it is observed that the Boeing 767-400 is the responsible for maximum deformation and maximum stress. As the base of containment is fixed so deformation is zero but some deformation is found at the junction between cylinder and dome (Fig. 5.102). When the graph of deformation of an element in impact location has been plotted for every aircraft throughout the total impact time, it is also observed Boeing 767-400 is responsible for large deformation (Fig. 5.105) but this is a local phenomenon. When the stress profile has been plotted for an element in impact location, the maximum stress is found for Boeing 767-400 (Fig. 5.106). From Fig. 5.107 it may be concluded that the tension damage starts in structural elements at different time because every aircraft has different impulse time. For Boeing 767-400 impact, the tension damage started at 0.18 sec whereas for Phantom F4 the tension damage started at 0.03 sec. When a single element has been taken in impact location for deformation and stress plotting with time so it is also found that the maximum deformation occurs when wings come in contact with the object and all the plots of deformation and stress for every aircraft is similar to the force-time history curves (Fig. 5.105 and 5.106). In the previous study, the BWR containment wall get damaged under the impact of Boeing 707-320 and Airbus A320 aircraft but TMIR wall has no damage under these aircraft because TMIR containment wall has more thickness compare to BWR containment wall.

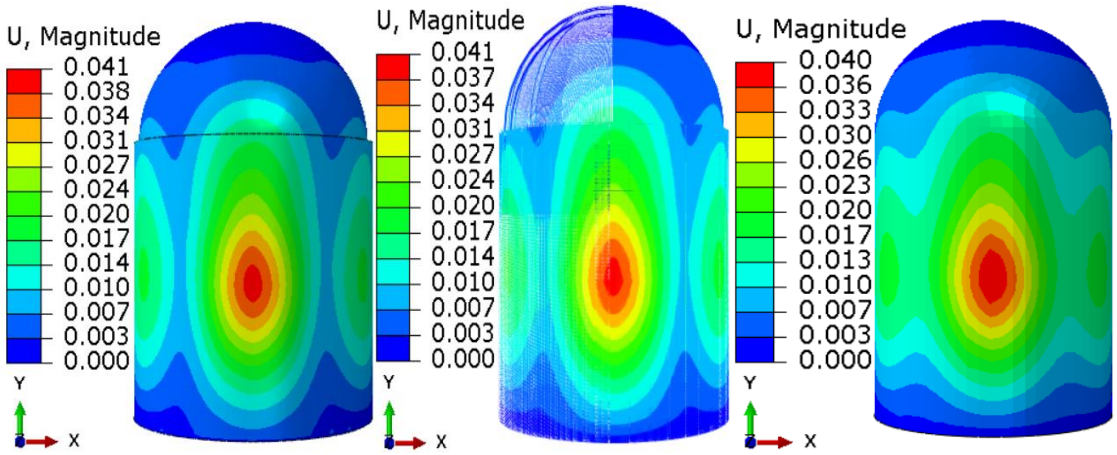

Fig. 5.92 Maximum deformation in concrete, Steel rebars and steel liner for Boeing 767-400

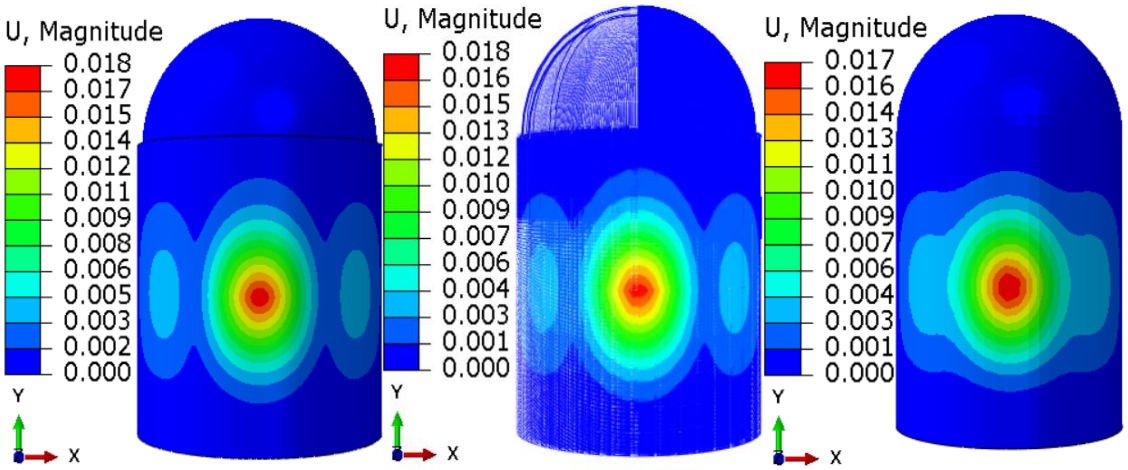

Fig. 5.93 Maximum deformation in concrete, Steel rebars and steel liner for Phantom F4

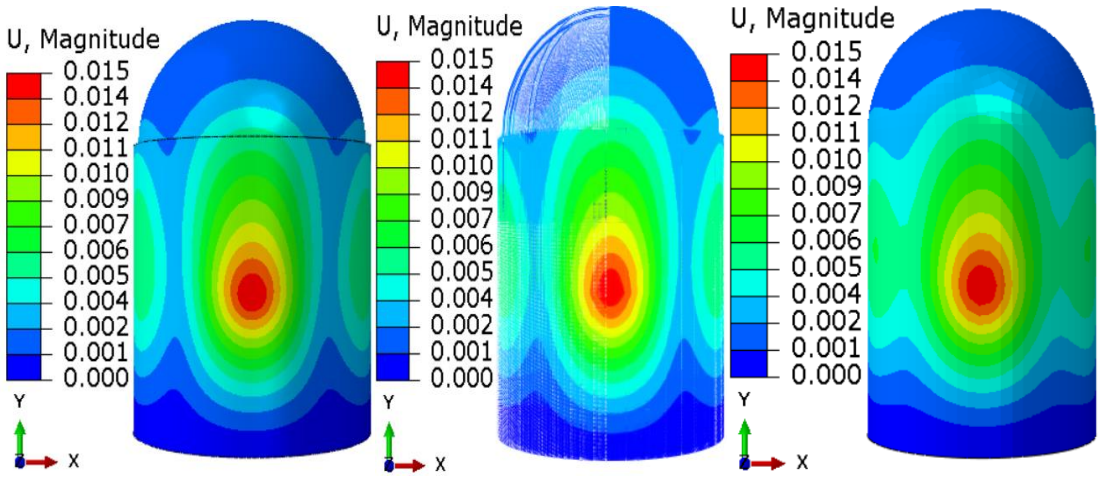

Fig. 5.94 Maximum deformation in concrete, Steel rebars and steel liner for Boeing 707-320

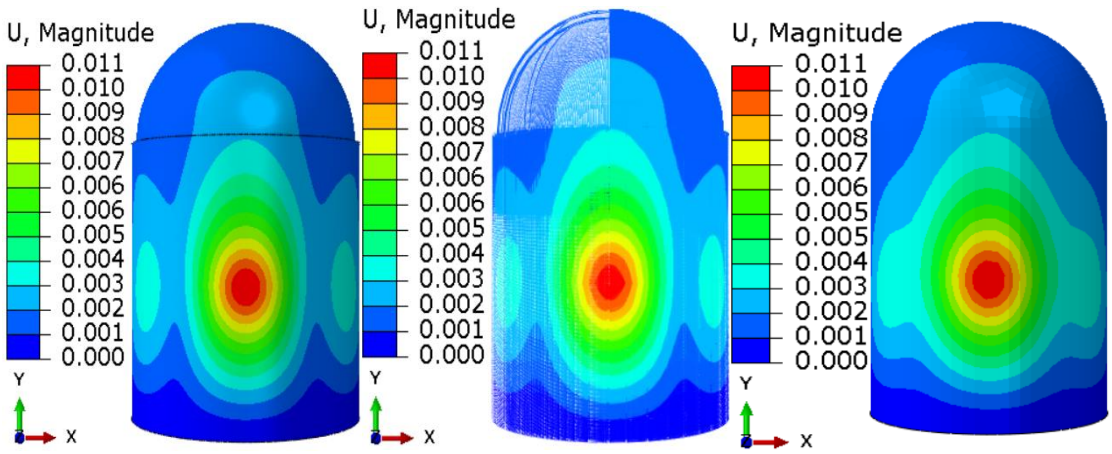

Fig. 5.95 Maximum deformation in concrete, Steel rebars and steel liner for Airbus A320

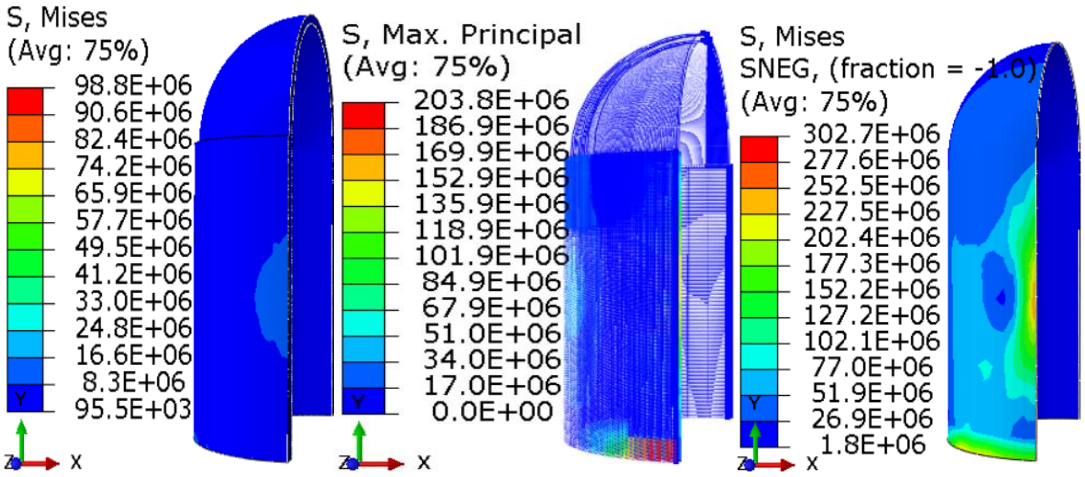

Fig. 5.96 Maximum stress in concrete, Steel rebars and steel liner for Boeing 767-400

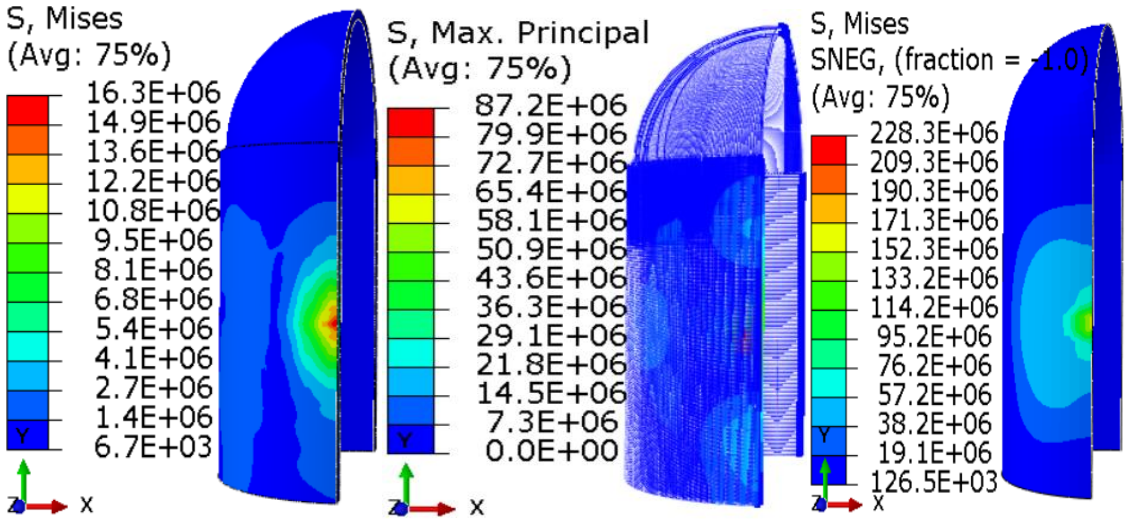

Fig. 5.97 Maximum stress in concrete, Steel rebars and steel liner for Phantom F4

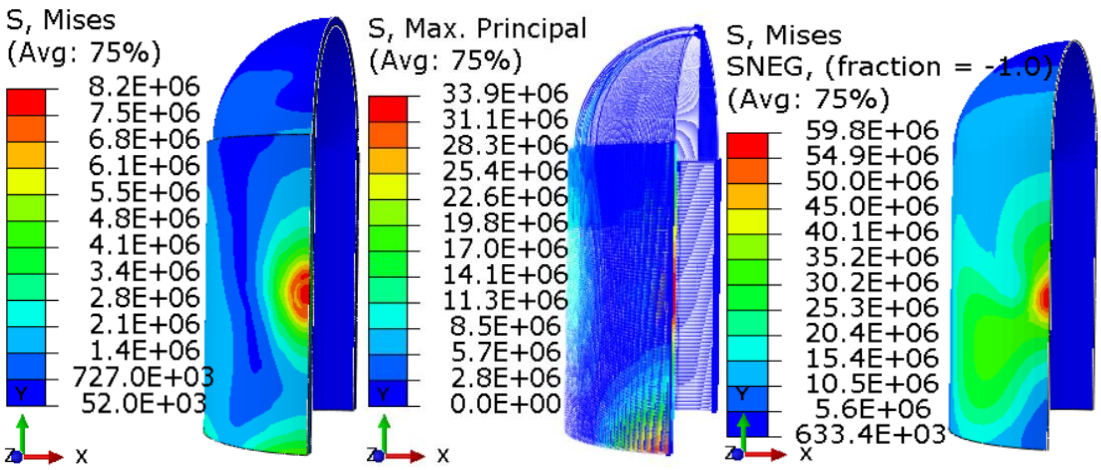

Fig. 5.98 Maximum stress in concrete, Steel rebars and steel liner for Boeing 707-320

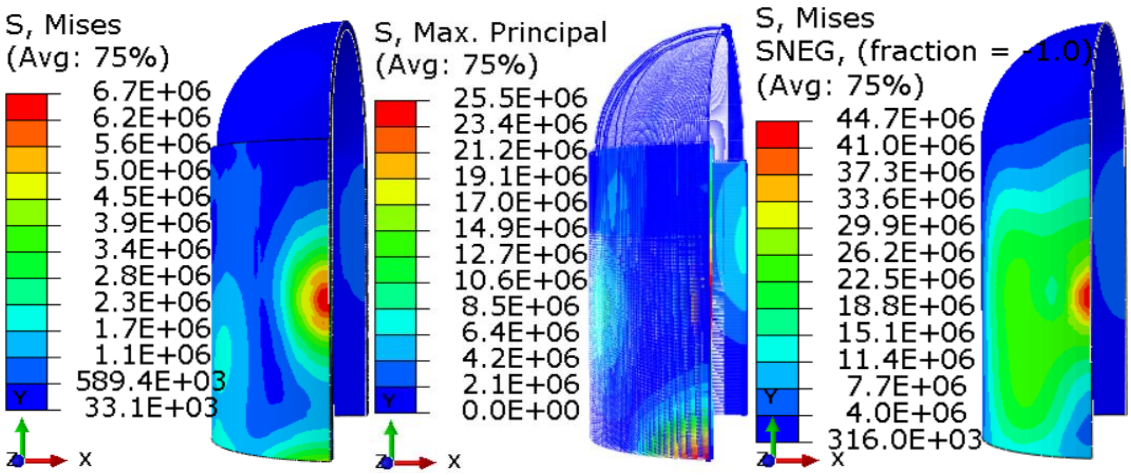

Fig. 5.99 Maximum stress in concrete, Steel rebars and steel liner for Airbus A320

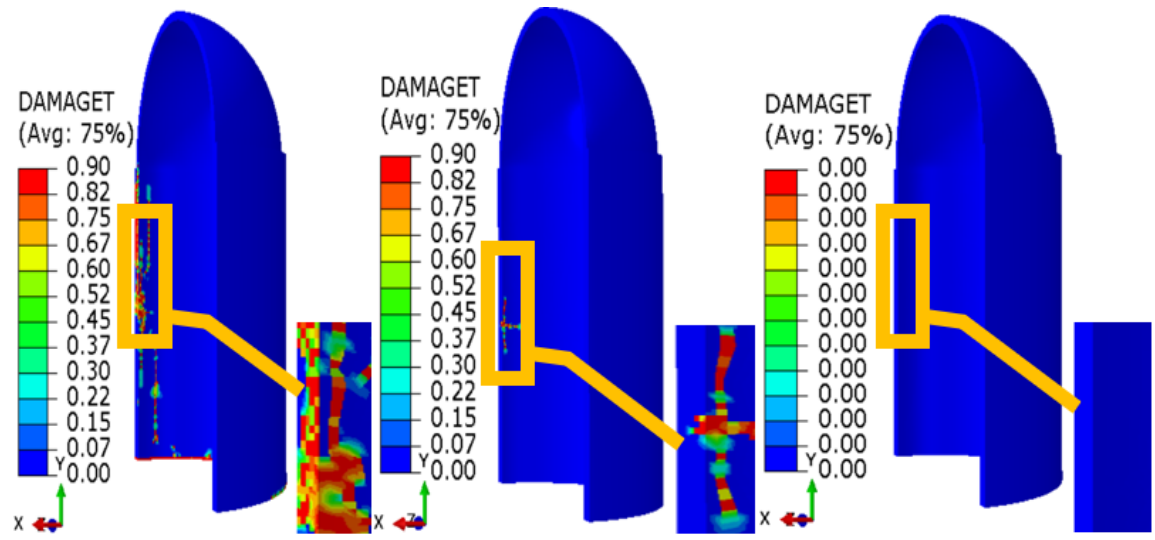

Fig. 5.100 Tension damages in concrete of containment for (a) Boeing 767-400 (b) Phantom F4 (c) Boeing 707-320 and Airbus A320

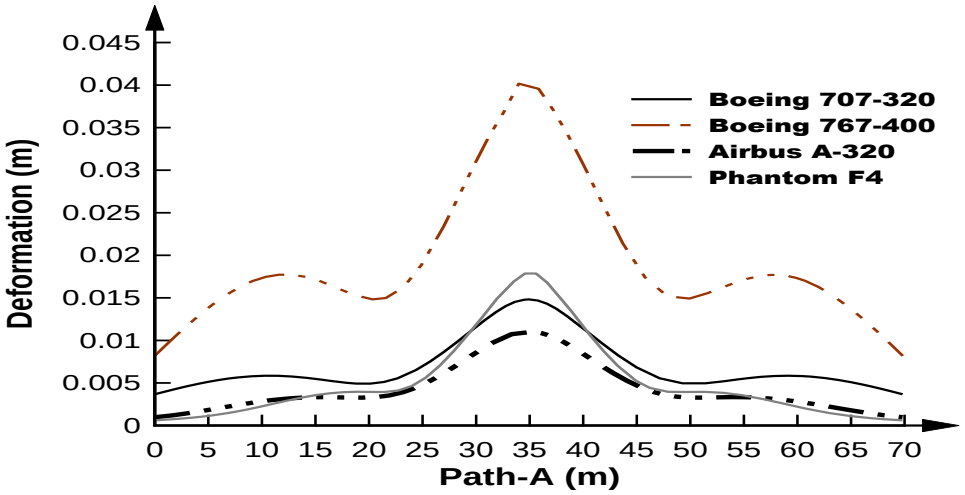

Fig. 5.101 Global deformation in concrete along path A

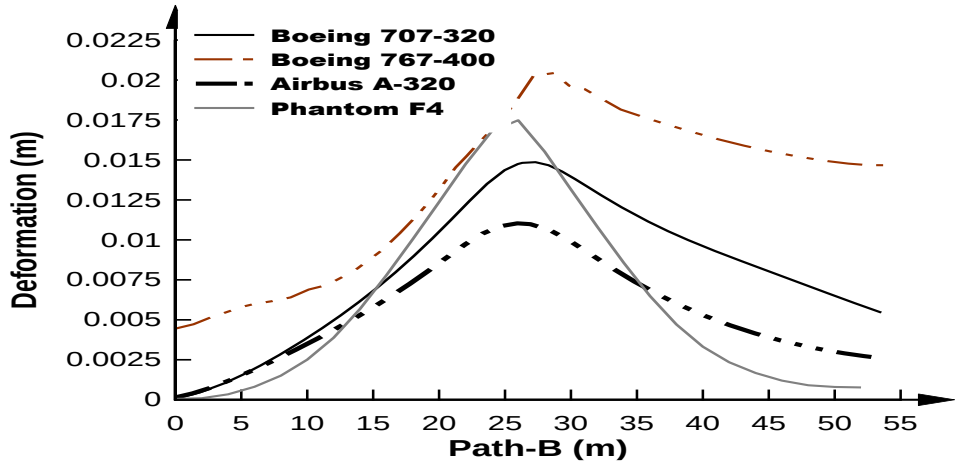

Fig. 5.102 Global deformation in concrete along path B

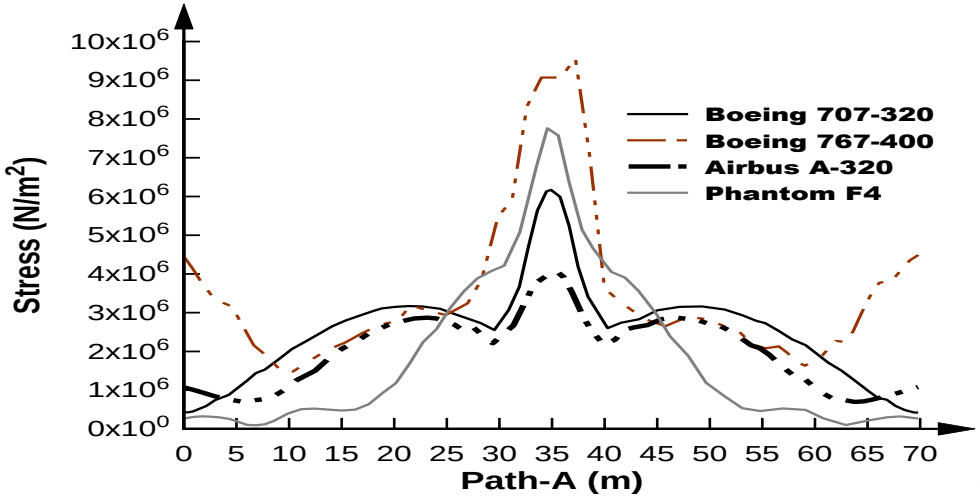

9+

Fig. 5.103 Stress produced in concrete along path A

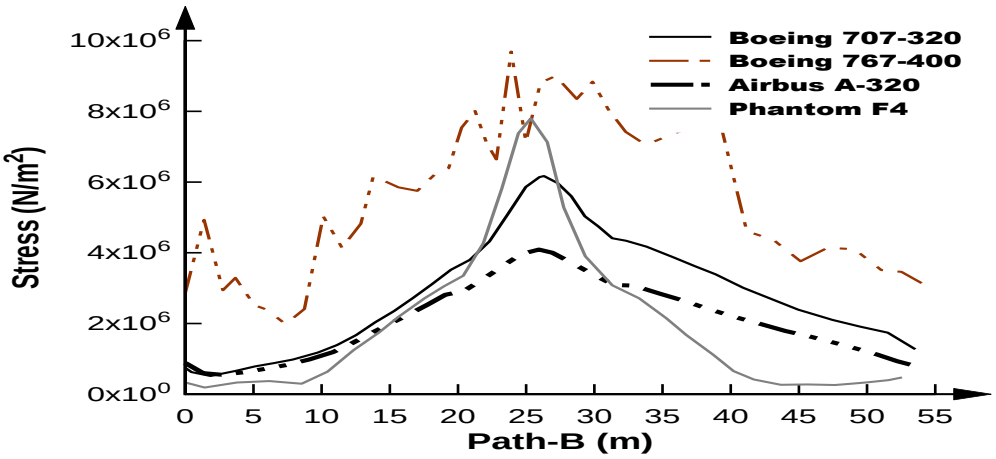

Fig. 5.104 Stress produced in concrete along path B

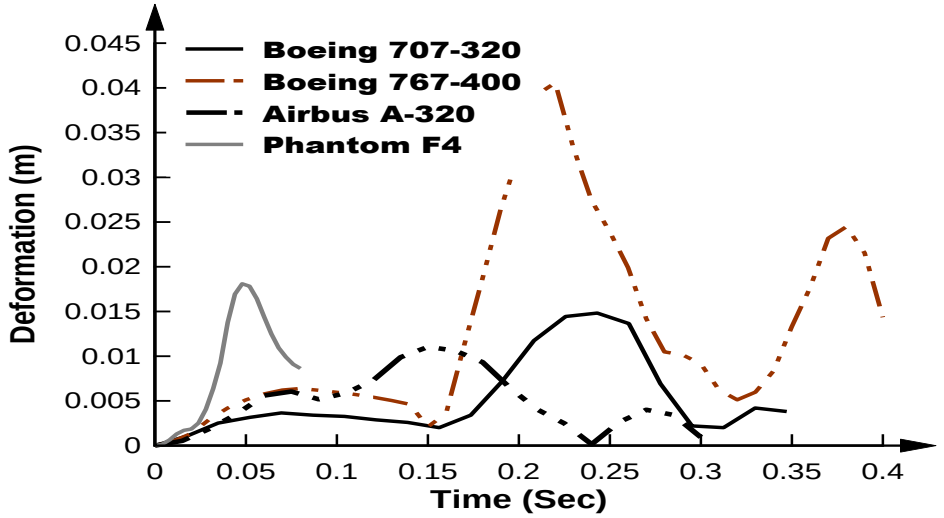

Fig. 5.105 Deformation of an element at impact location for different aircraft

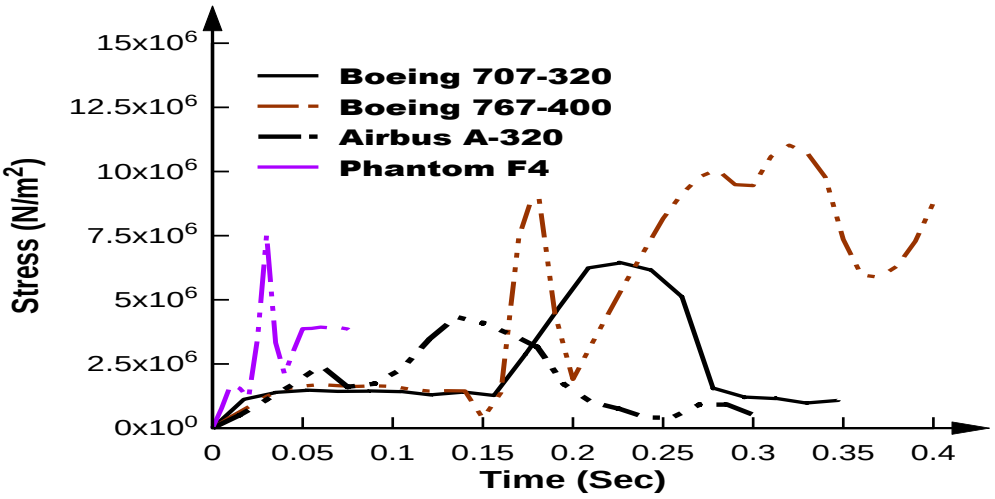

Fig. 5.106 Stress of an element at impact location for different aircraft

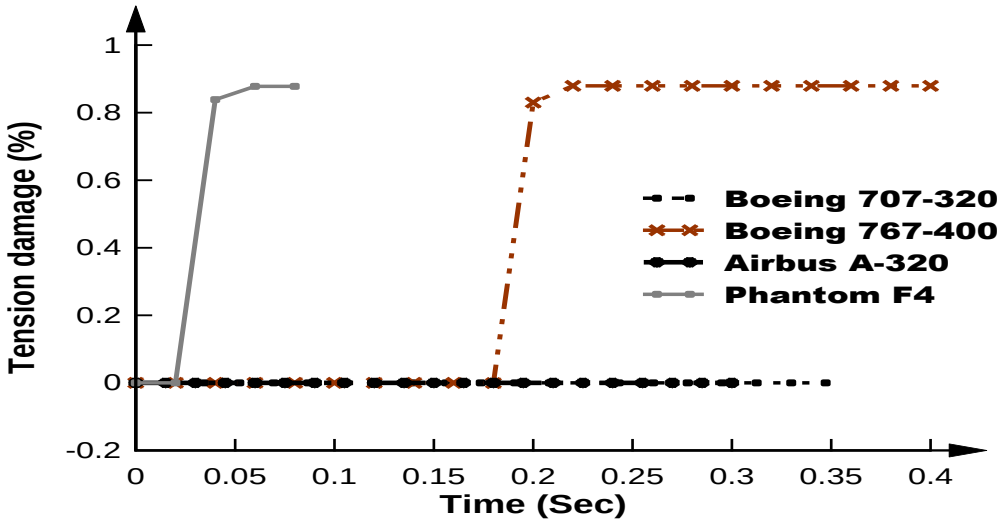

Fig. 5.107 Tension damage of an element at impact location for different aircraft

In this study, an attempt is made to find out the most damaging aircraft on NPP structure (Three Mile Island) for different aircraft crash (Boeing 767-400, 707-320, Phantom F4 and Airbus A320) using finite element analysis. The subsequent conclusions are drawn from the analysis:

- The maximum and minimum deformation are observed 0.041m for Boeing 767-400 and 0.011m for Airbus A320 respectively when the impact load is applied at 27.25m height from the base of containment.
- The maximum tension damages are observed at impact location for Boeing 767-400 due to more impact area.
- The minimum tension damage (zero damage) is observed at impact location under the impact of Airbus A320 and Boeing 707-320 aircraft and it due to less impact force.
- When the wings of aircraft come in contact with NPP containment, the deformation and stress get maximum.
- After some time of impact, the elements experienced plastic strain and get damaged.

- When the wings of aircraft come in contact with NPP containment, the elements experienced plastic strain and damage. In this circumstance, the maximum deformation and stress is occurred.
- The damage due to considering aircrafts over the containment structure is not a global failure.
- Finally, it may be concluded that the Boeing 767-400 aircraft has more damaging potential compared to other aircrafts.

5.8 CRITICAL IMPACT LOCATION

In the previous research, it was concluded that the mid height of BWR containment is most vulnerable location under aircraft crash. In the present study, a BWR containment wall has been considered to find out the most vulnerable location. The impact load of Boeing 707-320 aircraft is applied at different location i.e., location-A (at height 10m), location-B (at height 23m), location-C (at height 24m), location-D (at height 35m), location-E (at height 46m), location-F (at height 55m) and location-G (at height 67m), Fig. 5.108.

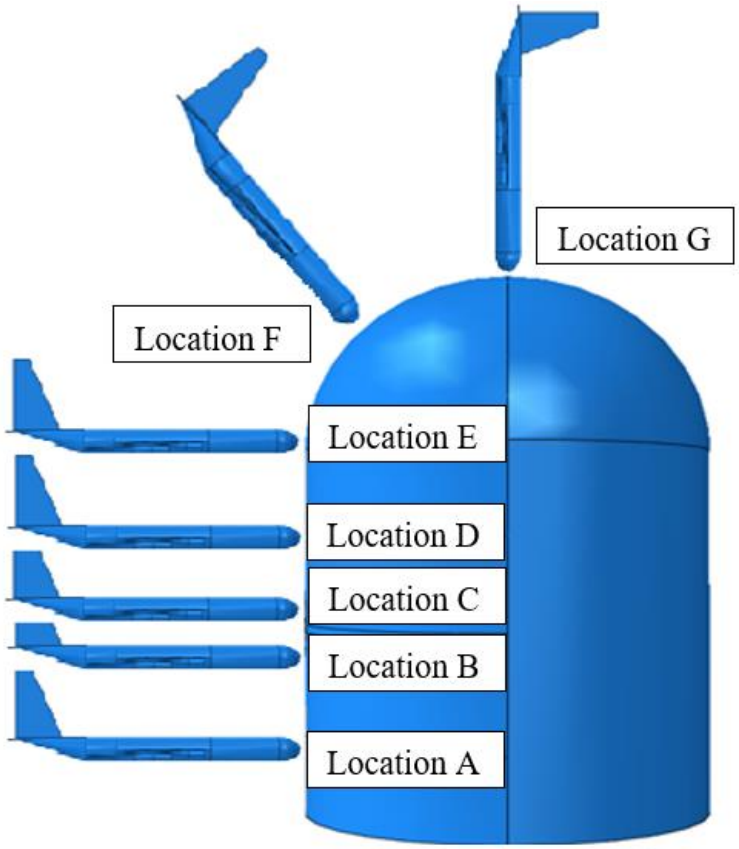

Fig. 5.108 NPP containment with different impact location

In this study, the average area approach is used to apply the impact load using the reaction force time curve. The Explicit impact analysis is performed up to 0.3472sec. The deformations and damages in concrete body for the different impact location has been shown in Fig. 5.109-5.115. The maximum deformation is found 0.087m in concrete when the aircraft impact is applied at location C which has been shown in Fig. 5.111. and when the impact load is applied at in any other locations, the deformation and damages are not much higher (Fig. 5.109-5.115). It is clearly observed that the damages in concrete start at time 0.1736sec and at the end of analysis, the damages are maximum at time 0.3472sec. The maximum damages occurs when the impact is at location C (Fig. 5.111). Here the damages are due the tensile cracking not due to compression cracking. At initial stage, the damage is only found at the middle of the model but at the end, the damage has been noticed at the fixed end of the model. This is due to the fixed end moments and reactions. Fig. 5.116 is showing the reaction variation for a single element (at base) for different impact locations. It is observed that the maximum reaction occurs at bottom when impact is applied at location A (near the base) and in this case maximum damage is found at the base of containment (Fig. 5.116). When a single element has been taken in impact location for deformations and stresses plotting, it has been observed that the maximum deformation and stress occurs for location C (Fig. 5.117, 5.118). When the damages are found in concrete, the plastic strain generated in concrete also and its value is increased with increase in time (Fig. 5.119). For every impact location concrete get damaged under Boeing 707-320 aircraft. From the impact analysis it is clearly observed that the maximum deformation at location E is 37mm in the present analysis and the deformation is almost same (36.3mm) in the literature of Abbas et al. (1996) for the validation point of view.

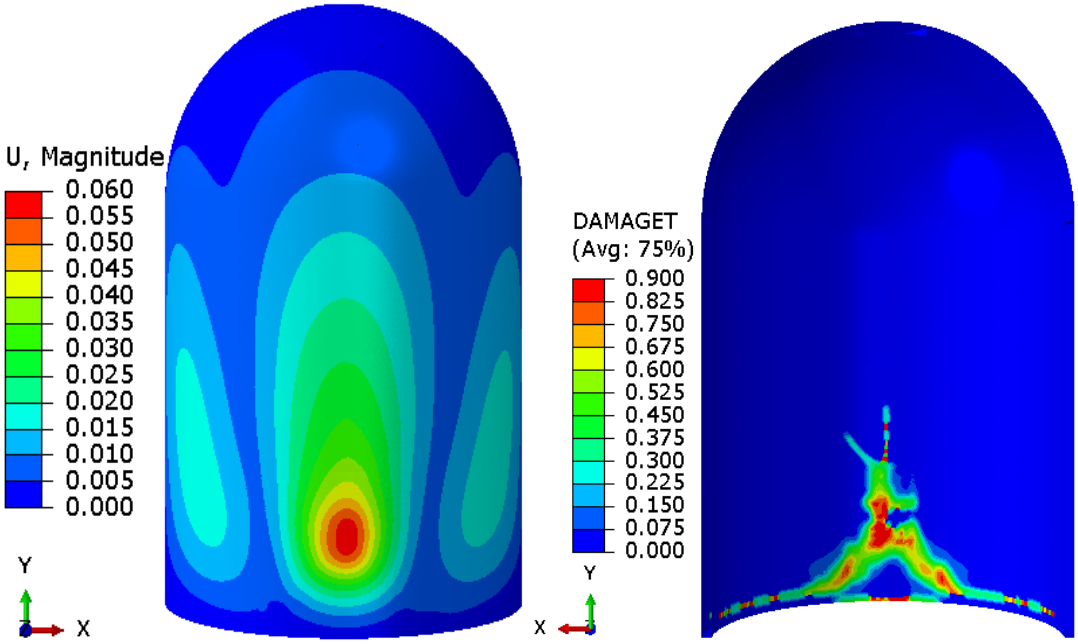

Fig. 5.109 Deformation and tension damages for location A

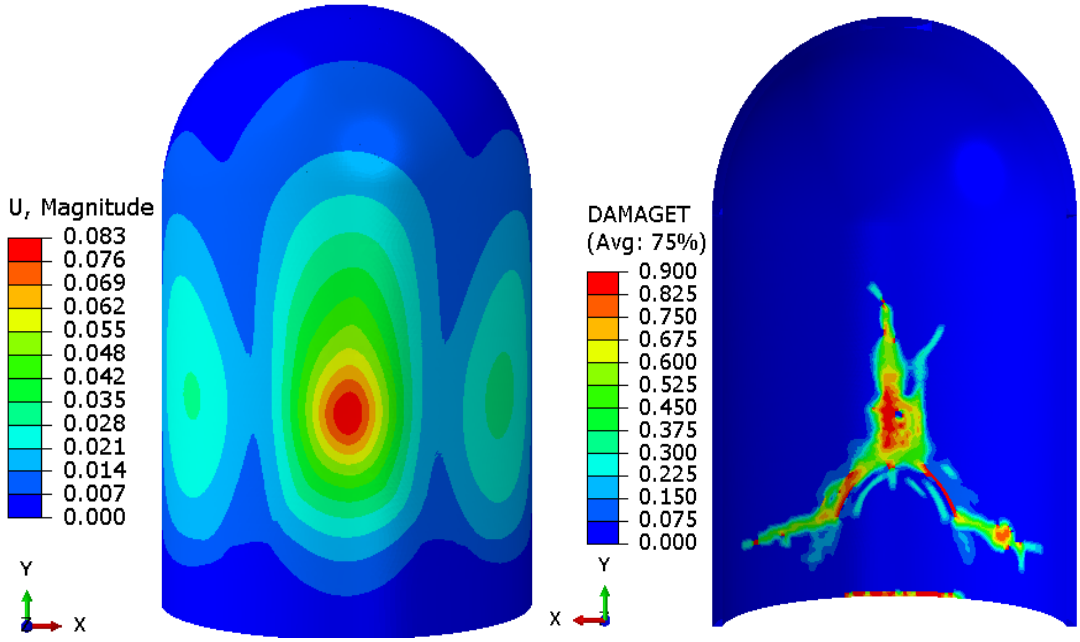

Fig. 5.110 Deformation and tension damages for location B

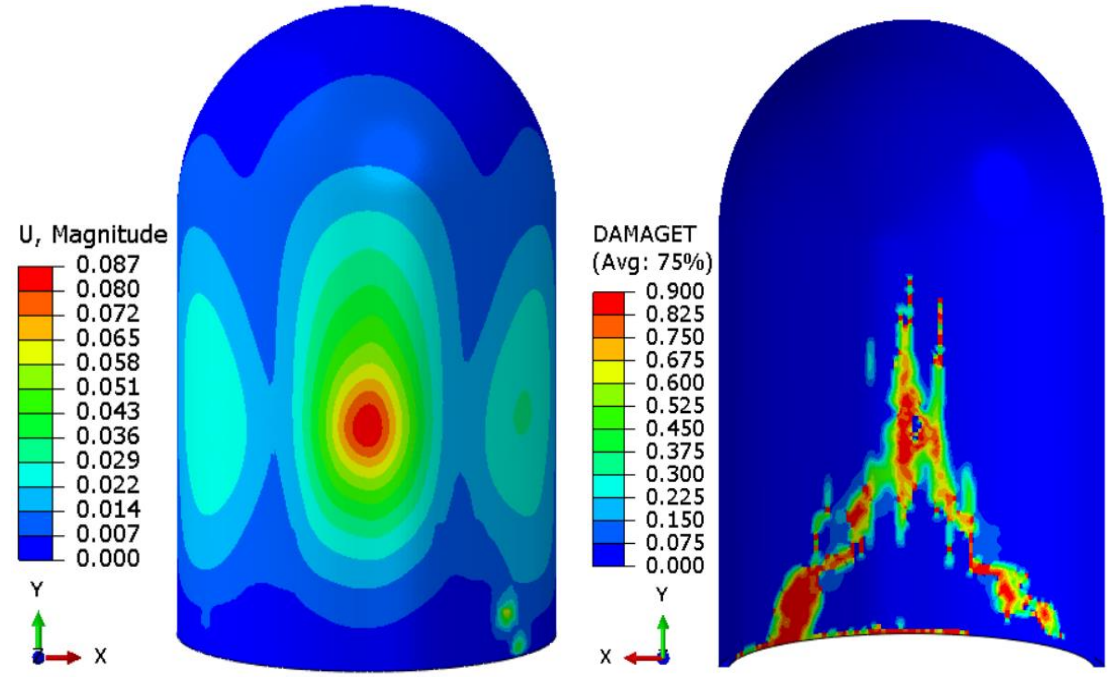

Fig. 5.111 Deformation and tension damages for location C

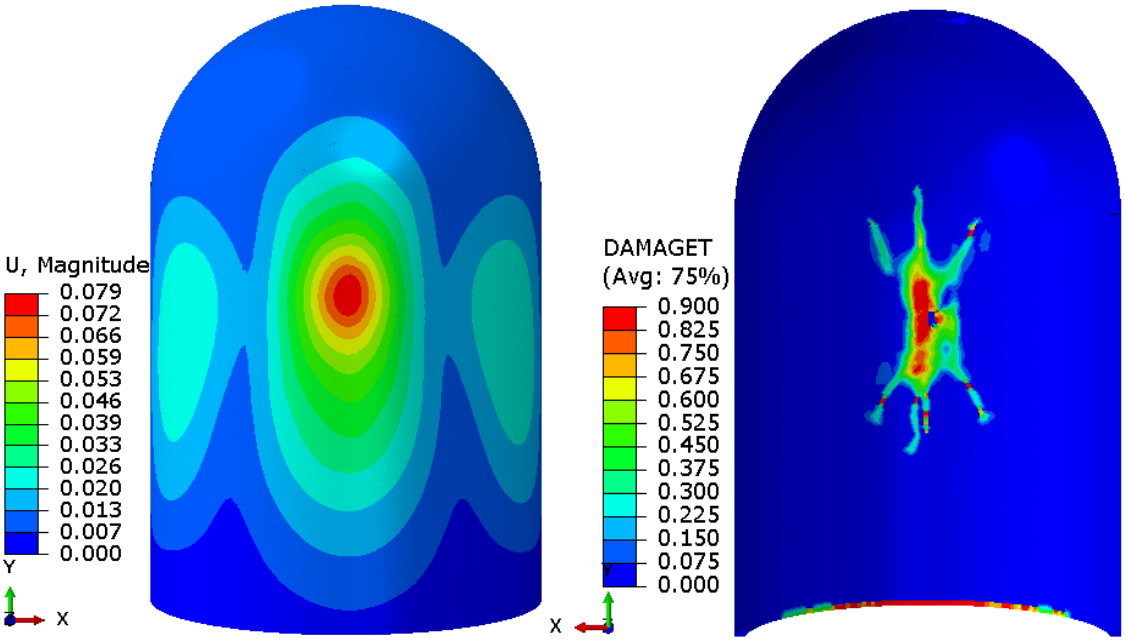

Fig. 5.112 Deformation and tension damages for location D

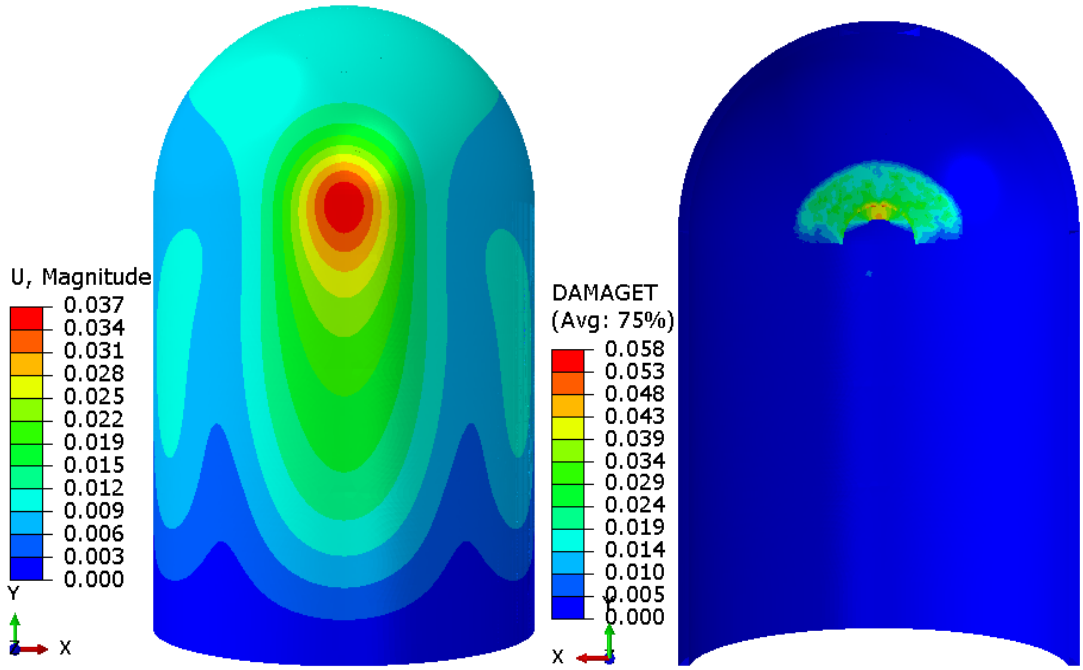

Fig. 5.113 Deformation and tension damages for location E

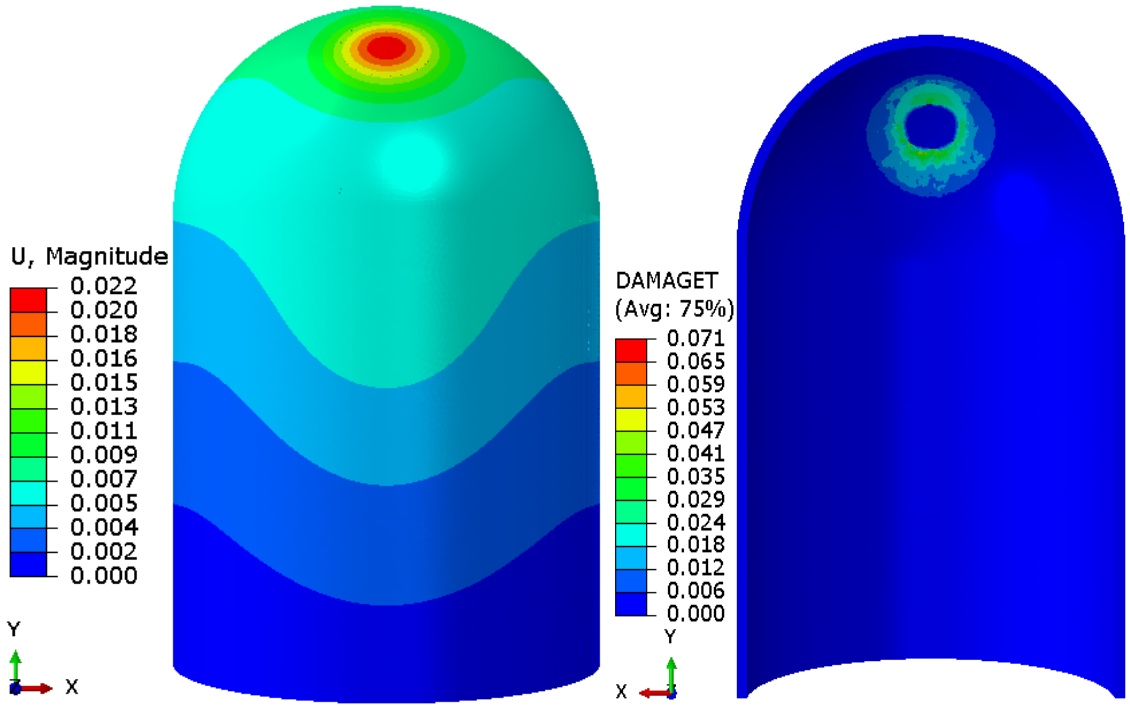

Fig. 5.114 Deformation and tension damages for location F

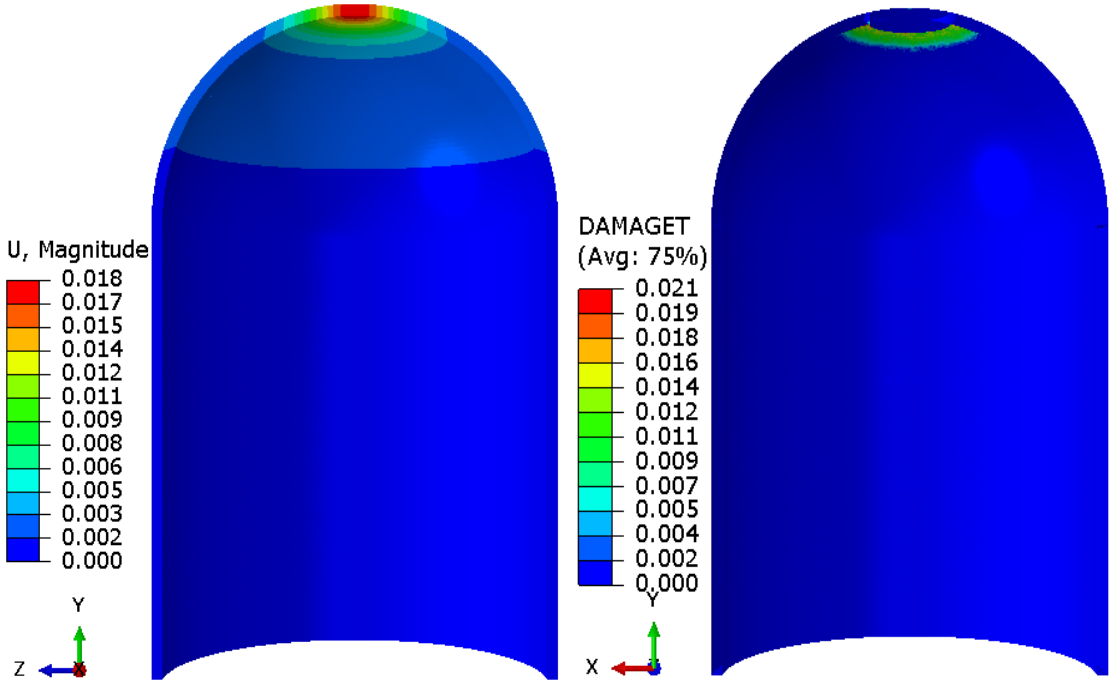

Fig. 5.115 Deformation and tension damages for location G

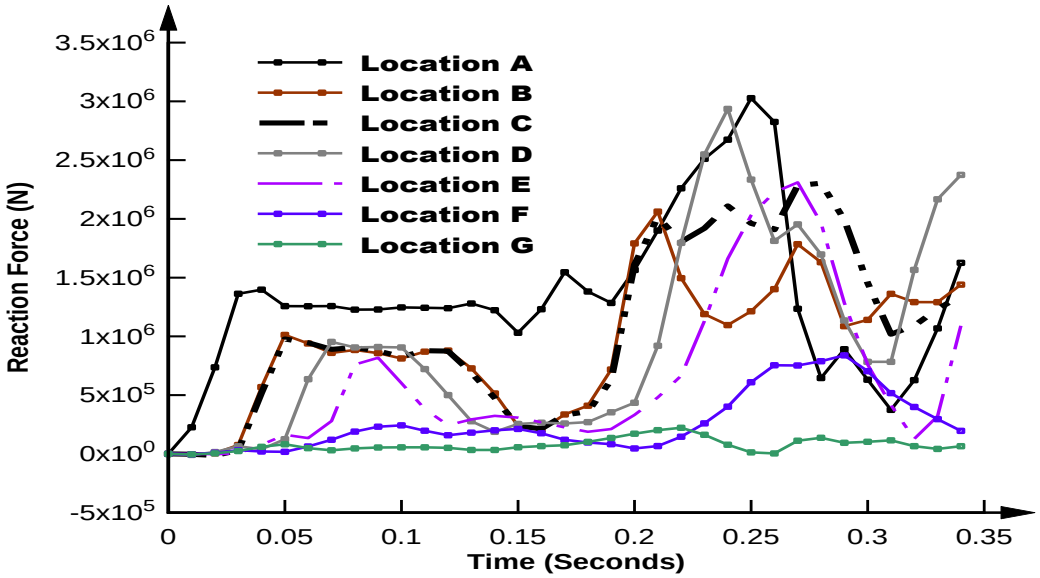

Fig. 5.116 Reaction force at the base of containment for different impact location

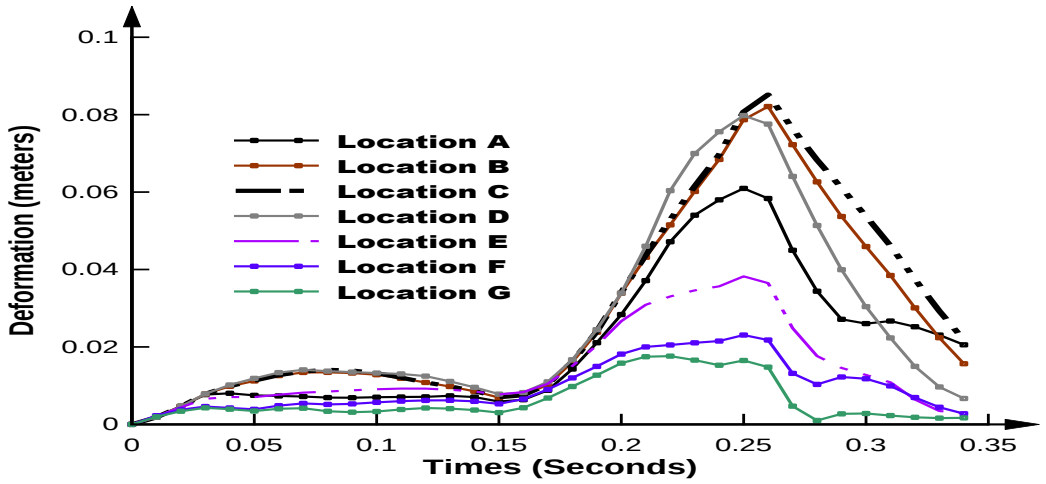

Fig. 5.117 Deformation of an element at impact location for different impact case

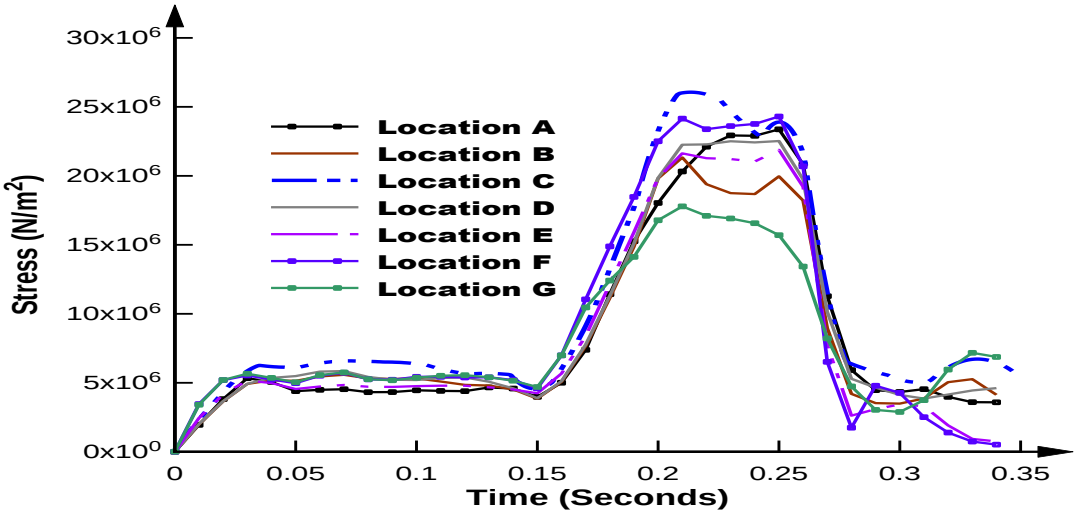

Fig. 5.118 Stress of an element at impact location for different impact case

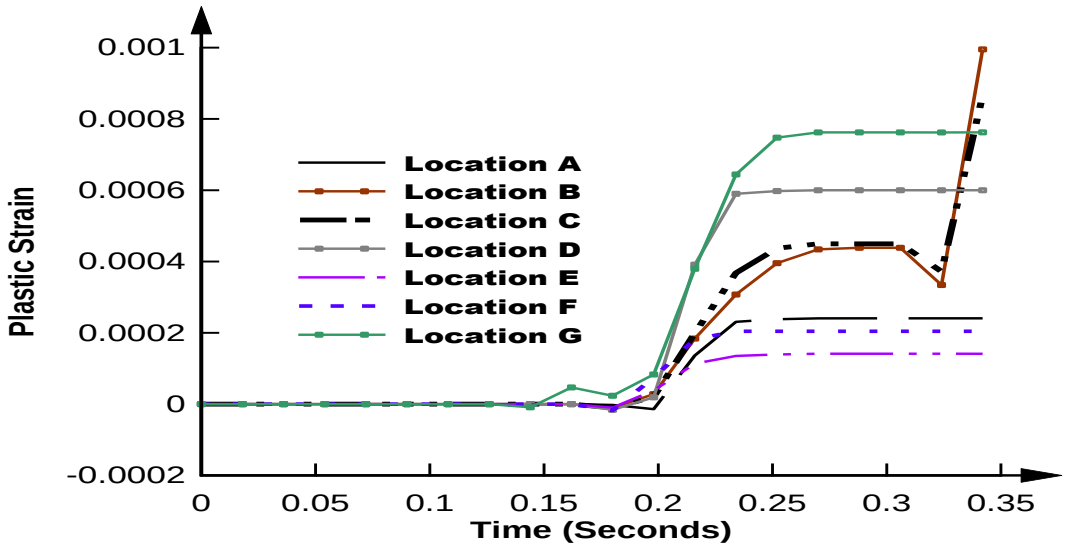

Fig. 5.119 Plastic strain of an element at impact location for different impact case

In this study, an attempt has been made to find out the most vulnerable location of NPP structure for Boeing 707-320 aircraft crash using finite element analysis. The following conclusions are drawn from the analysis:

- The maximum deformation is observed 0.087m when the impact load is applied on location C (24m height from the base of containment).
- The maximum tension damages are observed at impact location C.
- When the impact load is near the base of containment, the damages are also observed at the base because of additional reaction forces.
- At around 0.19 sec, the elements experienced plastic strain and get damaged.
- The damage due to Boeing 707-320 aircraft over the containment structure is not a global failure.
- The impact of B707-320 on NPP containment cause local damage and global failure was not observed in any case.
- Maximum observed deformation and damage at location C makes it the most critical location in BWR containment wall.

5.9 RESPONSE OF CONTAINMENT UNDER DIFFERENT STRAIN RATES

The strain rate is an important parameter to describe the behavior of material under high impact loading. The effect of strain rate has been studied in order to determine its influence on the response of the containment. Here Boeing 707-320 aircraft has been considered to apply impact load on the BWR outer containment wall. The loading of the aircraft has been assigned through the reaction-time response curve.

In the present study, total four types of strain rate have been considered i.e., zero strain rate, 290 s^{-1}, 620 s^{-1}, and varying strain rate. Two paths are selected to plot the deformation variation with different strain rate (Fig. 5.120). Some elements at the inner

face of concrete body have been taken for stress and damage plotting (Fig. 5.121). The deformation variation along path A and along path B has been shown in Fig. 5.122 and 5.123 respectively. Form these plot it can be concluded that the maximum deformation is found at zero strain rate and value is similar at 620 s^{-1} and varying strain rate. Fig. 5.124 is showing the elemental stress variation with different strain rate. The stress pattern for every element is almost similar for 620 s^{-1} and varying strain rate (Fig. 5.124). The tension damage at some selective nodes in concrete body have been shown in Fig. 5.125. The tension damage pattern is almost same for 620 s^{-1} and varying strain rate (Fig. 5.125).

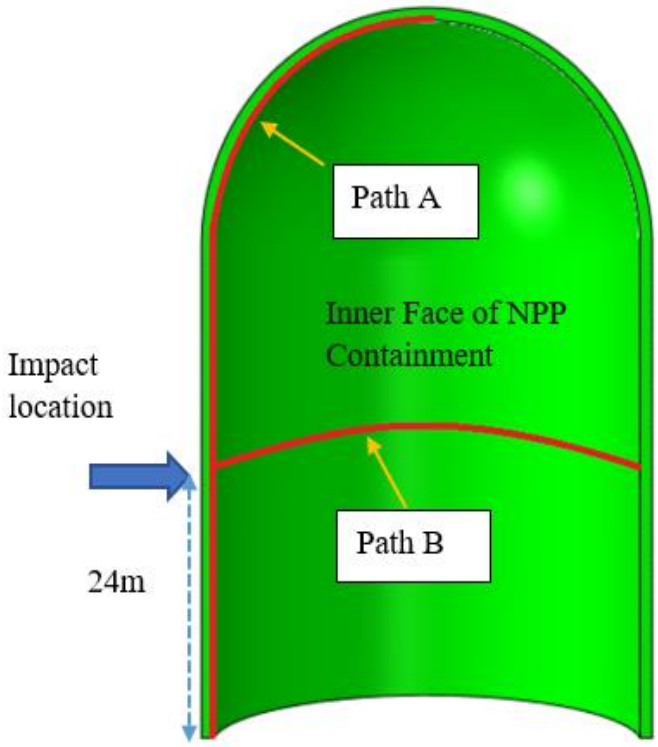

Fig. 5.120 BWR containment with path A and path B

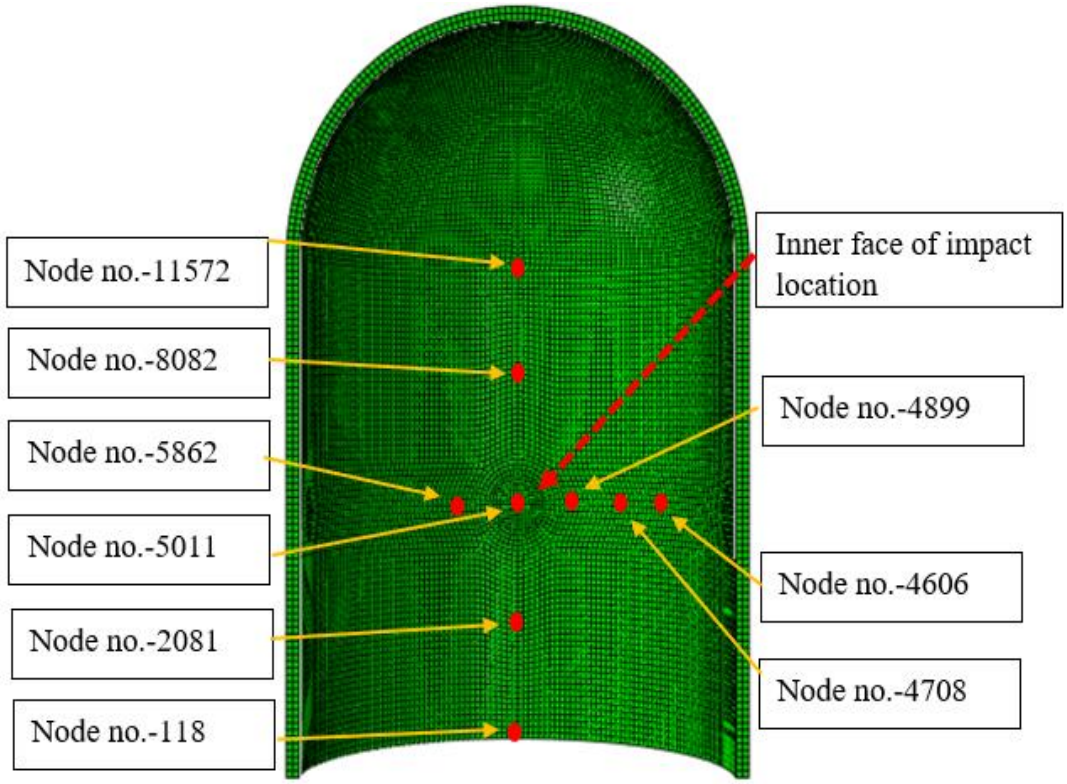

Fig. 5.121 The selective nodes in concrete body at inner face

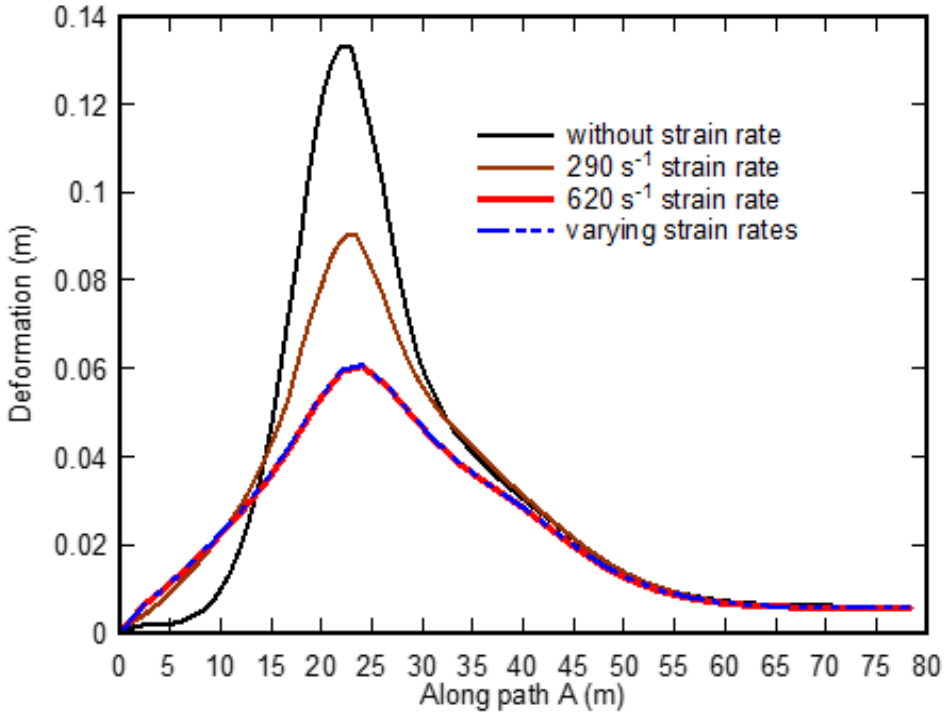

Fig. 5.122 Deformation variation along path A with different strain rates

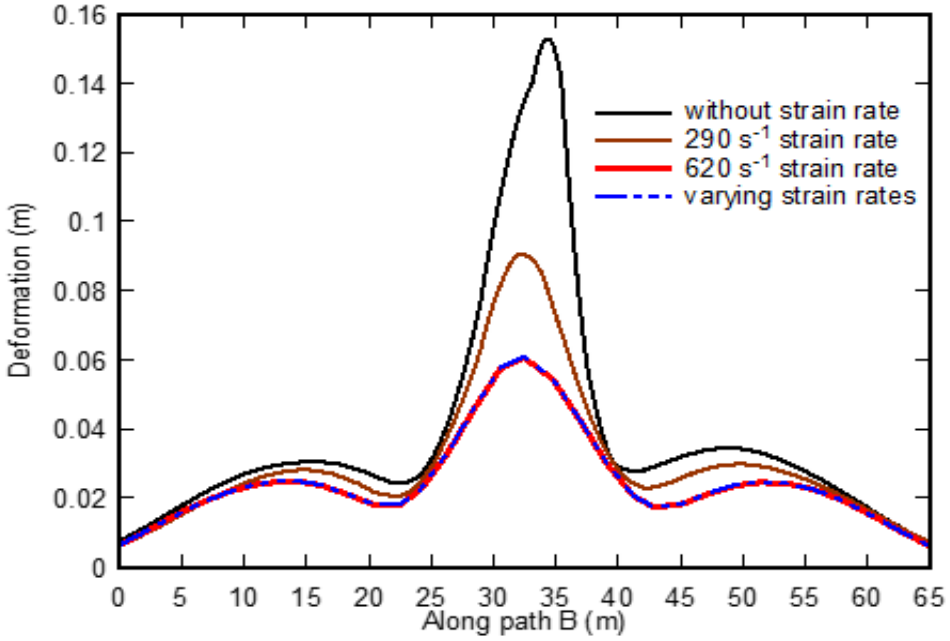

Fig. 5.123 Deformation variation along path B with different strain rates

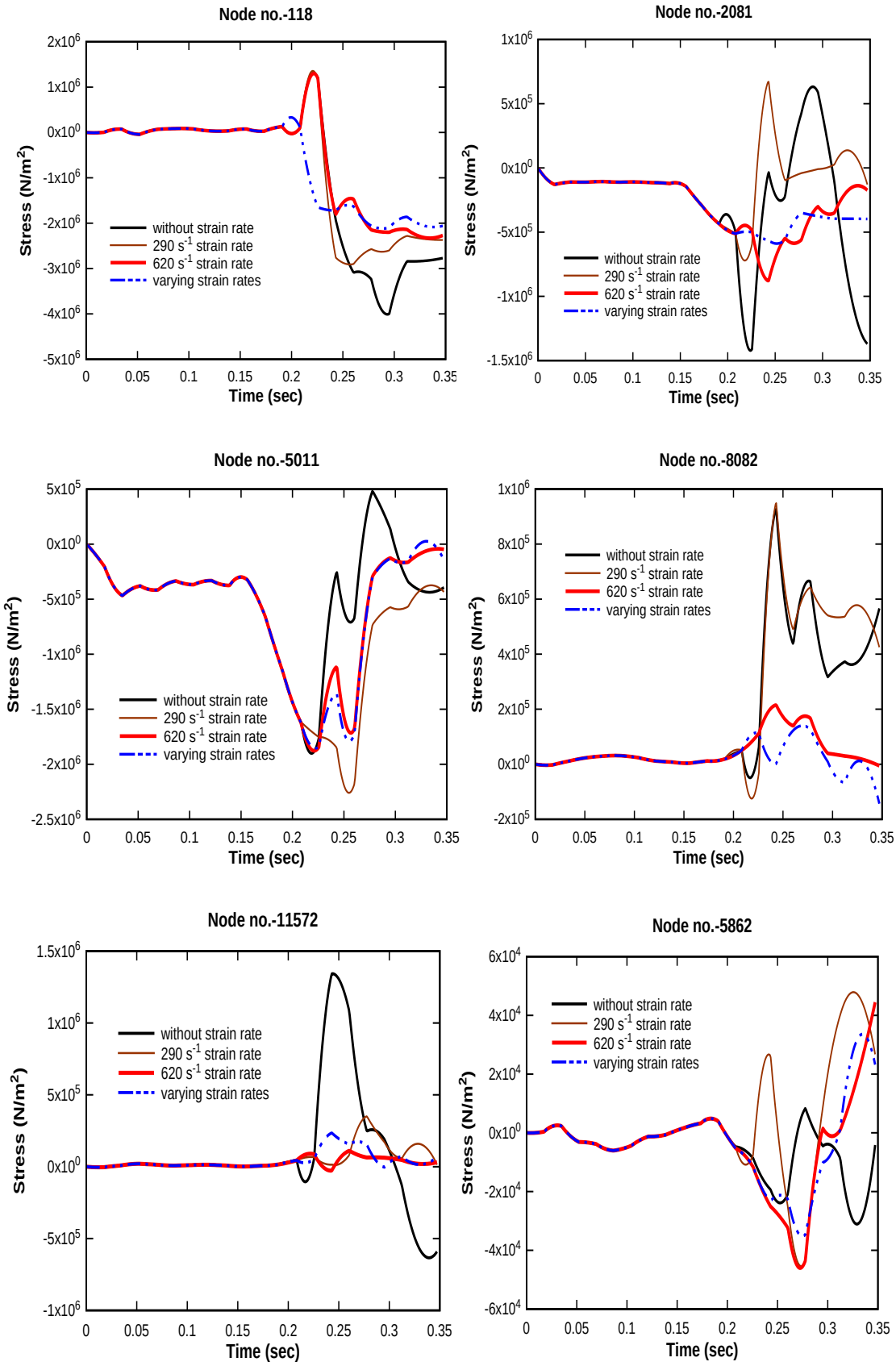

Fig. 5.124 Stress variation in selective elements with different strain rate

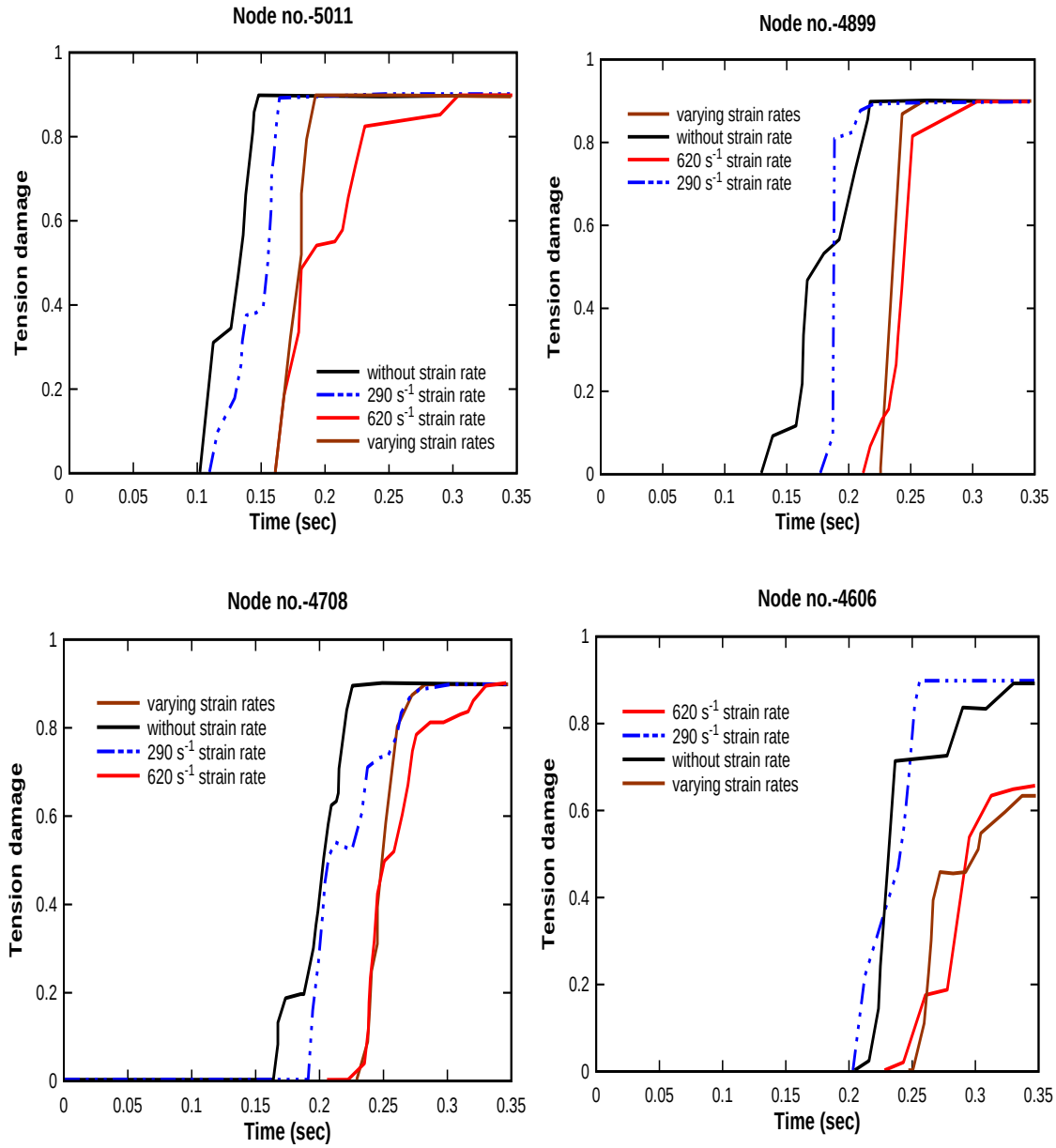

Fig. 5.125 Tension damages in selective elements with different strain rate

In this study, an effort has been made to find out the most appropriate value of strain rate. The material model has been analyzed considering zero, 290, 620 and varying strain rates. The deformation response is found maximum at zero strain rate whereas in case of 620 and varying strain rate, the deformation is almost same. As the velocity of aircraft impact load is very high, strain rate is an important parameter which must be

carefully incorporated to model the material behavior of the containment. It can be concluded that the stain rate 620 should be considered.

5.10 PARAMETRIC STUDY OF CONTAINMENT RESPONSE

The response of NPP containment depends upon many parameters but here five important parameters are considered. In this topic BWR containment and aircraft Boeing 707-320 aircraft is taken. In first case, containment is impacted by aircraft with different angles (0^{o}, 10^{o}, 20^{o}, 30^{o}, 40^{o}, 50^{o}, 60^{o}). If the angle is zero degree then angle between the target and aircraft is 90 degree means impact normal to the target, see Fig. 5.126. If the deformation vs time curve is plotted with various impact angle then it is clear that the zero-degree angle gives maximum deformation (Fig. 5.127). So, the zero-degree angle is most damaging angle for aircraft impact. In second case, containment is impacted by aircraft with different velocities (100, 120, 140, 160, 180, 200 m/sec), Fig. 5.128. If the deformation vs time curve is plotted with various impact velocities then it is clear that if the velocity is more, deformation is more which is shown in Fig. 5.129. In third case, different % of reinforcement steel is used in NPP wall (0 to 3%), Fig. 5.130. From the Fig. 5.131 it may conclude that when the ratio is zero deformation is maximum but it can be minimize using more wall thickness. In fourth case, different thickness of NPP wall is considered (0.8m to 3m) in Fig.5.132. When a plot is made for deformation with the various thicknesses then it is observed that more is the thickness less is the deformation from Fig. 5.133. In last case, containment wall with different radius of curvatures is analysed (20m, 30m, 40m, 50m, 60m, 70m, ∞), Fig. 5.134. When the radius of curvature is more deformation is less that can be minimize using more thickness in NPP wall (Fig. 5.135).

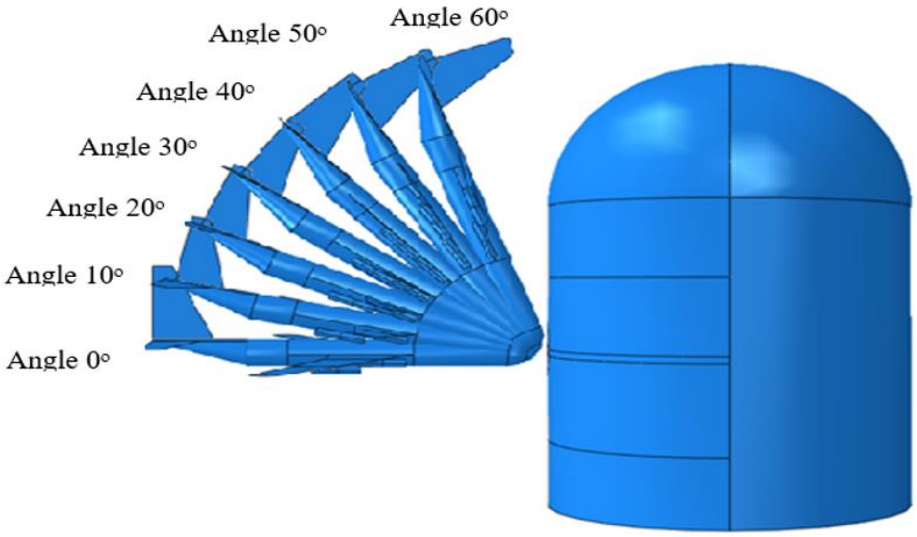

Fig. 5.126 Aircraft impact on NPP containment with various angles

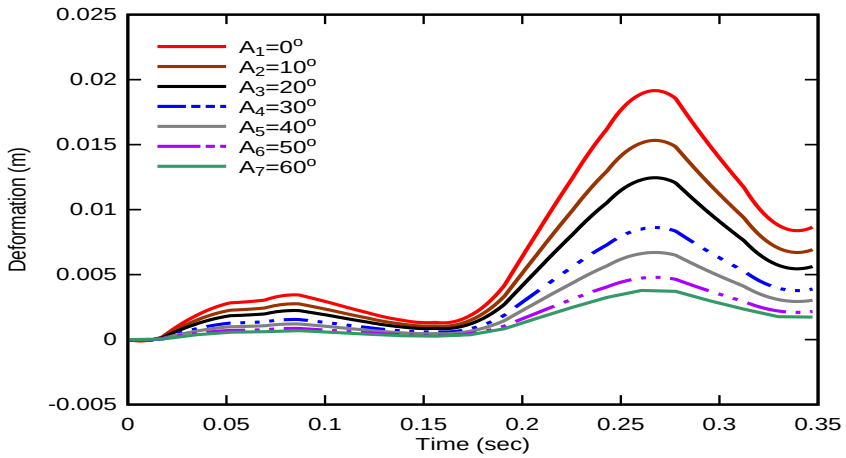

Fig. 5.127 Deformation of an element at impact location with different impact angles

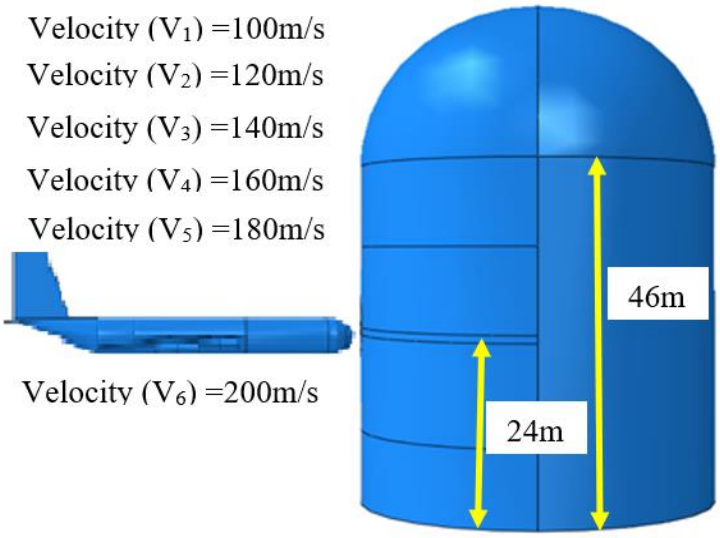

Fig. 5.128 Aircraft impact on NPP containment with various velocities

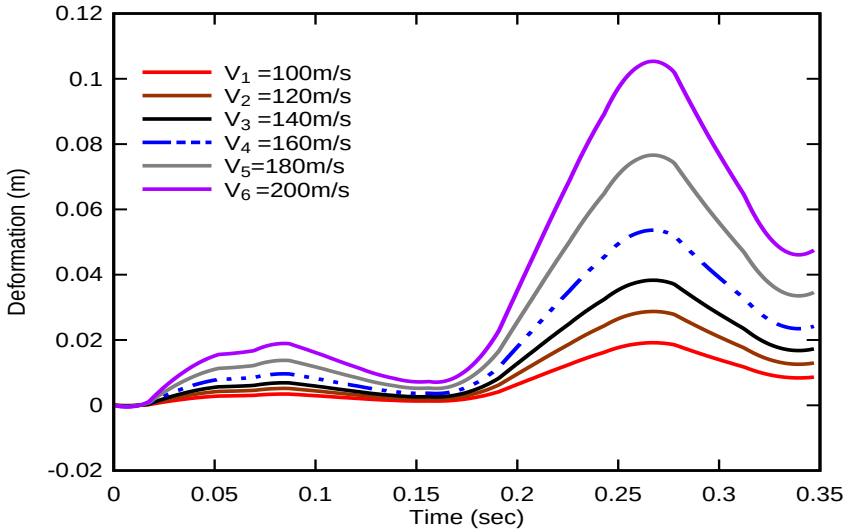

Fig. 5.129 Deformation of an element at impact location with different impact velocities

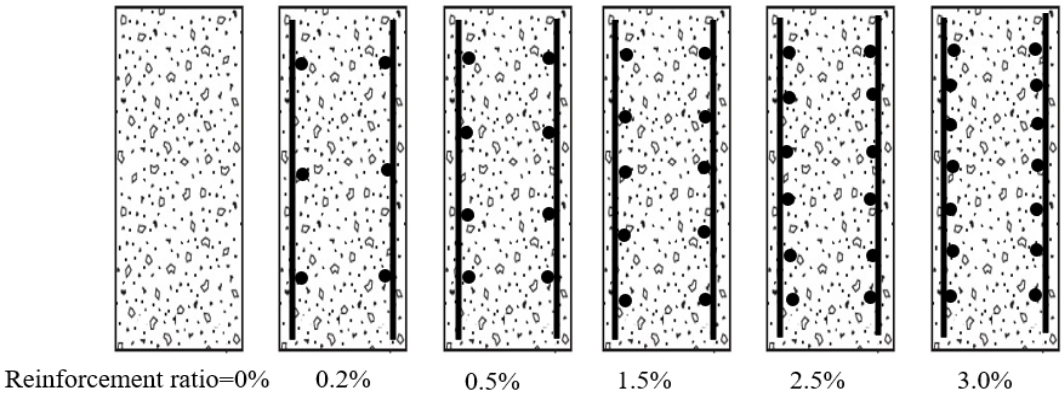

Fig. 5.130 Reinforcement ratio in NPP wall section

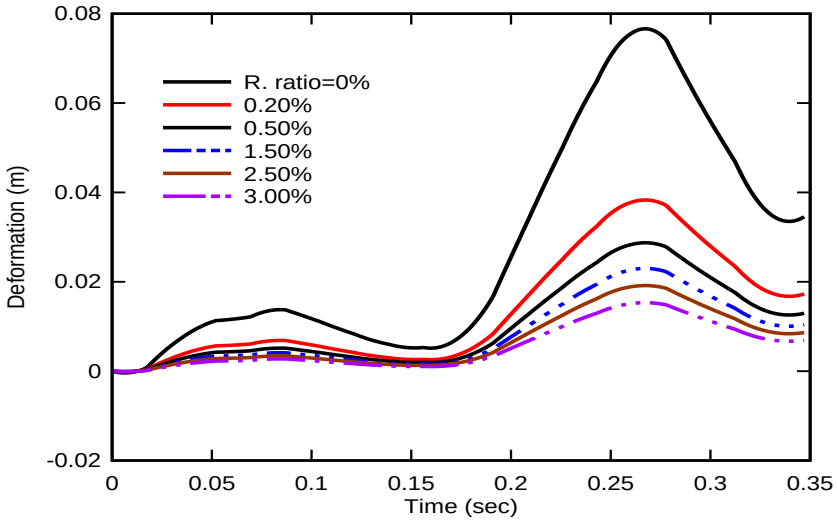

Fig. 5.131 Deformation of an element at impact location with different reinforcement ratio

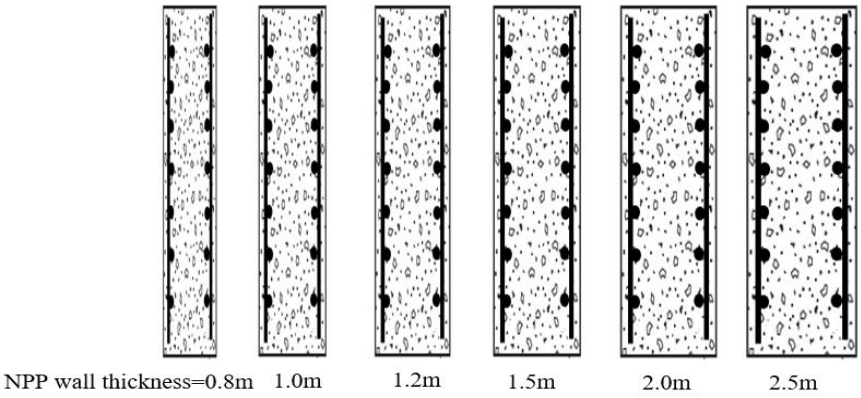

Fig. 5.132 Different NPP wall thicknesses

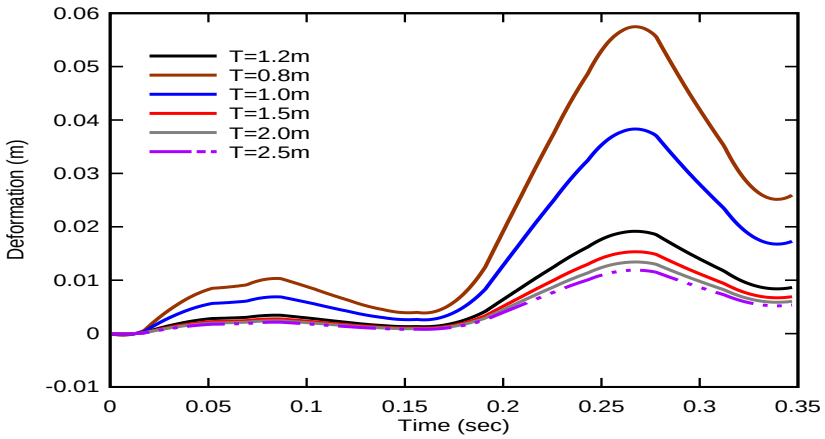

Fig. 5.133 Deformation of an element at impact location with different NPP containment thickness

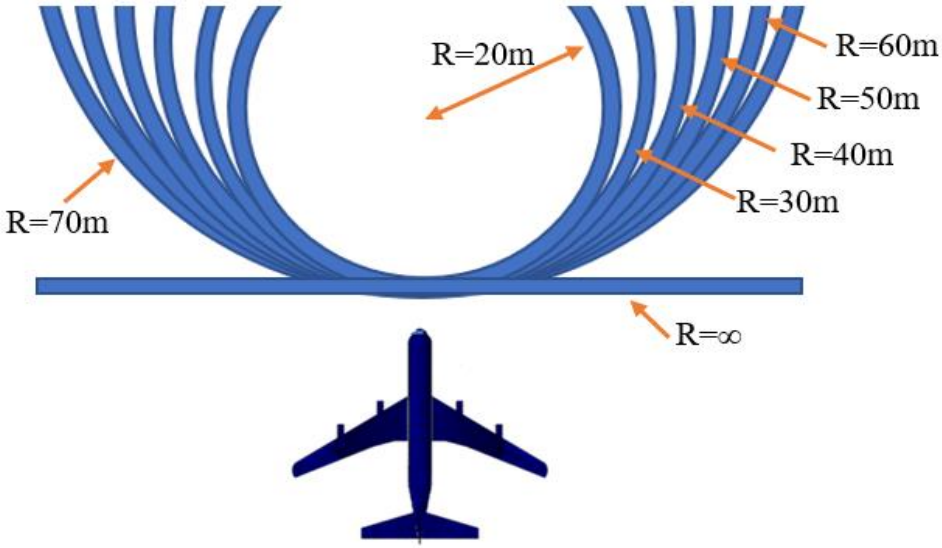

Fig. 5.134 Different radius of curvatures of NPP wall

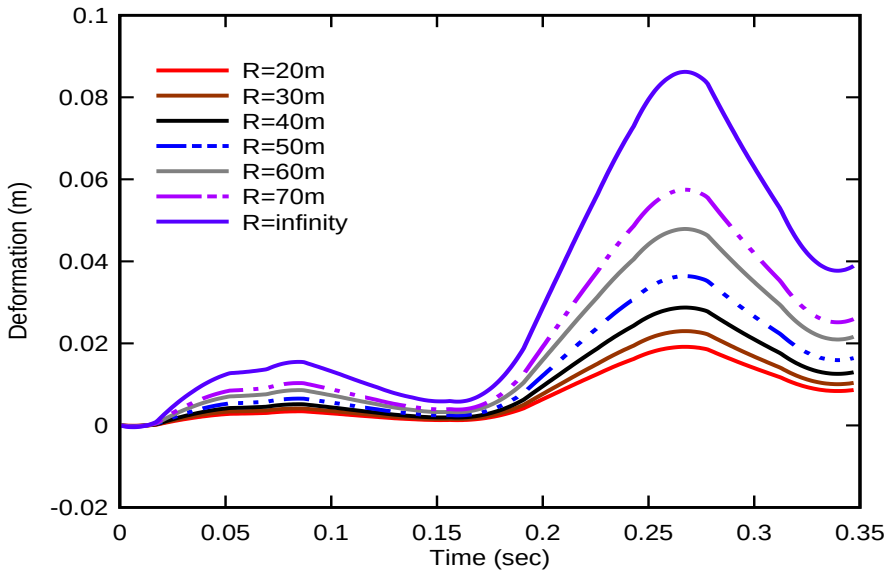

Fig. 5.135 Deformation of an element at impact location with different NPP containment curvatures

5.11 SUMMARY

In this chapter several analyses have been made to get the structural bahaviour of some hypothetical and some real NPP containment wall under the impact of different aircraft. The following conclusions are drawn from this chapter:

- It is observed that the most vulnerable location is just above the mid height of cylindrical portion of the BWR containment and this is different from existing literature.
- It is also found that the Boeing 747-400 has the most damaging potential and the CMR is more affected NPP containment.
- As the velocity of aircraft impact load is very high, strain rate is an important parameter which must be carefully incorporated to model the material behavior of the containment. It can be concluded that the stain rate 620 should be considered.

- It is also observed that the thickness of NPP wall, % of steel reinforcement in wall, radius of curvature of containment, impact angle of aircraft and velocity of aircraft affects the deformation response.